DEVELOPMENT OF CHEMICAL SENSORS EMPLOYING POLYMER MEMBRANES FOR COMBINED SEPARATION AND DETECTION

SUPHASINEE SATEANCHOK

DOCTOR OF PHILOSOPHY

IN CHEMISTRY

GRADUATE SCHOOL

CHIANG MAI UNIVERSITY

MAY 2019

DEVELOPMENT OF CHEMICAL SENSORS EMPLOYING POLYMER MEMBRANES FOR COMBINED SEPARATION AND DETECTION

SUPHASINEE SATEANCHOK

A THESIS SUBMITTED TO CHIANG MAI UNIVERSITY IN PARTIAL FULFILLMENT OF THE REQUIREMENTS FOR THE DEGREE OF DOCTOR OF PHILOSOPHY IN CHEMISTRY

GRADUATE SCHOOL, CHIANG MAI UNIVERSITY

MAY 2019

DEVELOPMENT OF CHEMICAL SENSORS EMPLOYING POLYMER MEMBRANES FOR COMBINED SEPARATION AND DETECTION

SUPHASINEE SATEANCHOK

THIS THESIS HAS BEEN APPROVED TO BE A PARTIAL FULFILLMENT OF THE REQUIREMENTS FOR THE DEGREE OF DOCTOR OF PHILOSOPHY IN CHEMISTRY

Examination Committee:

.....Chairman
(Assoc. Prof. Dr. Prasak Thavornyutikarn)

.....Member
(Prof. Dr. Kate Grudpan)

.....Member
(Asst. Prof. Dr. Sunanta Wangkarn)

.....Member
(Asst. Prof. Dr. Chalermpong Saenjum)

.....Member
(Prof. Dr. Eric Bakker)

.....Member
(Assoc. Prof. Dr. Piyarat Nimmanpipug)

.....Member
(Asst. Prof. Dr. Tinakorn Kanyancc)

Advisory Committee:

.....Advisor
(Prof. Dr. Kate Grudpan)

.....Co-advisor
(Asst. Prof. Dr. Sunanta Wangkarn)

.....Co-advisor
(Asst. Prof. Dr. Chalermpong Saenjum)

28 May 2019

ACKNOWLEDEMENT

I sincerely thank my supervisor, Prof. Dr. Kate Grudpan, for continuous encouragement and valuable guidance and direction throughout my study, leading to the completion of the dissertation. I also sincerely thank all the co-supervisors, the officially appointed co-supervisors in the program, Asst. Prof. Dr. Sunanta Wangkarn and Asst. Prof. Dr. Chalermpong Saenjum, and the oversea co-supervisor, Prof. Dr. Eric Bakker who gave me opportunity as a visiting student in his research group. I have learnt a lot from his advice in both academic and social activities during one year.

I would like to acknowledge the Science Achievement Scholarship of Thailand (SAST) for the great opportunities via the scholarship during my Ph.D. study. Addition support by the Swiss National Science Foundation (SNSF) and the University of Geneva, Switzerland is greatly appreciated. Acknowledgements are also due to the Center of Excellence for Innovation in Analytical Science and Technology (I-ANALY-S-T) and the Department of Chemistry, Faculty of Science, Chiang Mai University. The authors would like to take this opportunity to thank Asst. Prof. Chartchai khanongnuch and his group (Faculty of Agro-Industry, Chiang Mai University) for the appreciated assistance with the preparation of bio-cellulose membrane and the valuable advice. I also would like to express my thankfulness to PIP International company for their kindness and support on these membrane materials in this work.

I thank Assoc. Prof. Dr. Prasak Thavornyutikarn, Assoc. Prof. Dr. Piyarat Nimmanpipug, and Asst. Prof. Dr. Tinakorn Kanyanee, who are the thesis examination committee members.

I would like to take this opportunity to thank my beloved friends and all colleagues of the I-ANALY-S-T group for sharing their truthful, friendship, support and splendid moment sharing throughout my study. The same are also due to the people in Bakker's group.

Importantly, I dedicate this thesis to my parents for their patience, truly love and understanding as the way I am. I would like to thank many people whose names are not mentioned here.

Suphasinee Sateanchok

หัวข้อดุษฎีนิพนธ์	การพัฒนาเซ็นเซอร์ทางเคมีที่ใช้เมมเบรนพอลิเมอร์ เพื่อการแยกและตรวจวัดแบบรวมกัน
ผู้เขียน	นางสาวสุภาศินีย์ เสถียรโชค
ปริญญา	ปรัชญาดุษฎีบัณฑิต (เคมี)
คณะกรรมการที่ปรึกษา	ศ. ดร. เกตุ กรุดพันธ์ อาจารย์ที่ปรึกษาหลัก ผศ. ดร. สุนันทา วังกานต์ อาจารย์ที่ปรึกษาร่วม ผศ. ดร. เฉลิมพงษ์ แสนจุ้ม อาจารย์ที่ปรึกษาร่วม

บทคัดย่อ

การพัฒนาเซ็นเซอร์ทางเคมีได้เพิ่มขึ้นอย่างต่อเนื่อง ในช่วงหลายทศวรรษที่ผ่านมา ดังนั้นจึงสร้างเซ็นเซอร์ที่มีประสิทธิภาพอาศัยวัสดุเมมเบรนเพื่อการแยกสารและการตรวจวัดสารเข้าด้วยกัน เมมเบรนที่สนใจประกอบด้วยเซลลูโลสจากแบคทีเรีย, เซลลูโลสจากพืช และเยื่อสังเคราะห์ทางเคมีในรูปแบบของแพลตฟอร์มที่ลดขนาดลง วัสดุเมมเบรนที่แตกต่างกันถูกนำมาใช้เป็นช่องทางการไหลสำหรับสารละลายอย่างง่ายโดยไม่ต้องมีการสร้างที่ซับซ้อน

เซ็นเซอร์ทางเคมีที่พัฒนาขึ้นโดยการใช้เมมเบรนถูกนำมาทดสอบโดยปฏิกิริยาเคมีบางประเภทเพื่อตัวอย่างด้านสิ่งแวดล้อมและสุขภาพ เมมเบรนที่สร้างจากแบคทีเรียถูกนำมาใช้สำหรับตัวบงชี้ต้นแบบบางตัวได้แก่ พีเอช และกลูโคส โดยการวิเคราะห์ค่าพีเอช ขึ้นอยู่กับการวัดสีด้วยรีเอเจนต์อินดิเคเตอร์ ทั้งที่เป็นธรรมชาติและมีจำหน่าย ส่วนของการทดสอบกลูโคสมุ่งเน้นไปที่กระบวนการของเอนไซม์กลูโคสออกซิเดสและฮอร์ราดิชเปอร์ออกซิเดส ซึ่งอาศัยสารตั้งต้นที่จำเพาะ ในการวัดค่าพีเอชมาตรฐานสามารถทำได้ในช่วง 4-8 ขณะที่กราฟมาตรฐานสำหรับการวิเคราะห์กลูโคสคือ $y = 6.8205x + 2.2506$, $R^2 = 0.9897$ ในช่วงความเข้มข้นกลูโคส 0-10 mM สำหรับการประยุกต์ใช้ตัวอย่างจริงได้ทำการศึกษาเกี่ยวกับอาหารเพื่อสุขภาพและเหงื่อเทียม

เมมเบรนจากพืชธรรมชาติทั้งเส้นด้ายและกระดาษถูกนำพัฒนาขึ้นเพื่อสร้างเครื่องมือวิเคราะห์ทางเคมีสำหรับการวิเคราะห์โลหะหนัก ได้แก่ แคดเมียม, คอปเปอร์, โคบอลต์ และสารต้านอนุมูลอิสระ (โพลีฟีนอล) ซึ่งการตรวจหาไอออนของโลหะมักใช้รีเอเจนต์ (4-(ไพริดิล-2-อะโซ)-เรซอร์ซิ

นอล (พีเออาร์)) ส่วนปฏิกิริยาเคมีสำหรับการหาปริมาณโพลีฟีนอลรวมและความสามารถในการต้านอนุมูลอิสระนั้นได้ใช้วิธีโฟลิน-ไซโอแคลทู และดีพีพีเอชเรดิคอล กราฟมาตรฐานของปริมาณฟีนอลิกได้ถูกสร้างขึ้นในช่วง 0-100 ppm โดยมีการประยุกต์ใช้กับตัวอย่างจริงที่เป็นชาเขียวจากหลายพื้นที่ในการวิเคราะห์คุณสมบัติต้านอนุมูลอิสระ

เมมเบรนแลกเปลี่ยนไอออน (โพลิเมอร์สังเคราะห์ทางเคมี) ได้รับการพัฒนาเพื่อสร้างเซ็นเซอร์ที่หาปริมาณฟอสเฟตในน้ำทะเล การตรวจหาฟอสเฟตนั้นสัมพันธ์กับวิธีวัดค่าสีโมลิบดีนัมบลูและวิธีทางไฟฟ้าจากสารเชิงซ้อน พบว่ากราฟมาตรฐานฟอสเฟตที่ได้มีความเป็นเส้นตรงในช่วงความเข้มข้น 0.1-10 μM ซึ่งประสบความสำเร็จสำหรับงานทางด้านสิ่งแวดล้อม

เซ็นเซอร์ที่ใช้เมมเบรนเหล่านี้สามารถทำการวิเคราะห์แบบลดขนาดด้วยประโยชน์ในการใช้งานได้หลากหลายประกอบด้วย การวิเคราะห์ที่ง่าย, ไม่ต้องปรับสภาพตัวอย่าง, ลดปริมาณสารละลาย, และต้นทุนต่ำ ซึ่งเป็นอีกทางเลือกหนึ่งสำหรับการวิเคราะห์ในสถานที่จริง

Dissertation Title	Development of Chemical Sensors Employing Polymer Membranes for Combined Separation and Detection
Author	Miss Suphasinee Sateanchok
Degree	Doctor of Philosophy (Chemistry)
Advisory Committee	Prof. Dr. Kate Grudpan — Advisor Asst. Prof. Dr. Sunanta Wangkarn — Co-advisor Asst. Prof. Dr. Chalermpong Saenjum — Co-advisor

Abstract

The development of chemical sensor has increased gradually over the past several decades. In this approach, the effective sensors employing membranes have been fabricated in order to combine separation and detection parts. The proposed membranes include bacteria-produced cellulose, plant-cellulose, and chemical synthetic membrane in terms of the downscaling platform. Different membrane materials were especially used as the individual channel without the sophisticated fabrication, responsible for the simple passive delivery of the solution.

The proposed chemical sensors employing membranes were assessed by some chemical reactions respect to the environmental and health related samples. The bacteria-produced cellulose membrane was demonstrated for some model markers namely pH and glucose determination. The pH analysis was based on a colorimetric measurement by indicator reagents (natural and commercial ones). The glucose assay was focused on an enzymatic process (glucose oxidase and horseradish peroxidase) with a special substrate. The standard pH benchmark was obtained in the range of 4-8, while a glucose calibration was $y = 6.8205x + 2.2506$, $R^2 = 0.9897$ in the range of 0-10 mM glucose. The real samples application was studied involving healthy foods and artificial sweat, aiming to a wearable sensor.

The natural plant membranes, the cotton thread and paper materials, were offered for chemical analyses including heavy metals (Cd, Cu and Co), and antioxidant

(polyphenol) determination. The metal ions assay was commonly used with a chromogenic reagent (4-(pyridyl-2-azo)-resorcinol (PAR)). The chemistries for the antioxidant assay were based on Folin-Ciocalteu and diphenylpicryhydrazyl (DPPH) for the total polyphenol and antioxidant capacity, respectively. A calibration curve of the total phenolic quantity was plotted in the range of 0-100 ppm. Real applications were demonstrated for green tea samples from different places were analyzed for antioxidant capacity

An ion-exchange membrane (chemical synthetic polymer) was developed for the in-line determination of phosphate in seawater. The phosphate evaluation involves the colorimetric molybdenum blue means and the electroactive complex method. A linear calibration graph in the range of 0.1–10 µM phosphate was achieved, which is sufficiently attractive for environmental field.

These chemical sensors employing polymeric membranes achieved miniaturized analysis with various advantages including the easy operation, negligence of sample pretreatment, solution reduction, and cost-effectiveness, which is an alternative way for the on-site analysis.

CONTENTS

LIST OF TABLES

LIST OF FIGURES

Page

LIST OF ABBREVIATIONS, SYMBOLS AND UNITS

PC	Plant cellulose
BC	Bacterial cellulose
GOD	Glucose oxidase
TMB	Tetramethylbenzidine
HRP	Horseradish peroxidase
BP	Butterfly pea reagent
MB	Molybdenum blue
GAE	Gallic acid equivalents value
IC_{50}	Inhibition concentration at 50 percent
PAR	4-(pyridyl-2-azo)-resorcinol
DPPH	2,2-diphenyl-1-picrylhydrazy
SD	Standard deviation
RSD	Relative standard deviation
LOD	Limit of detection
RGB	Red Green Blue
AE	Auxiliary electrode
RE	Reference electrode
WE	Working electrode
CV	Cyclic voltammetry
SWV	Square wave voltammetry

ข้อความแห่งการริเริ่ม

1) งานวิจัยนี้มีวัตถุประสงค์เพื่อพัฒนาเซ็นเซอร์ทางเคมีที่ใช้เยื่อเมมเบรนพอลิเมอร์สำหรับการแยกและตรวจวัดภายในอุปกรณ์ขนาดเล็กชิ้นเดียว แพลตฟอร์มเมมเบรนที่หลากหลายถูกประดิษฐ์ขึ้นได้แก่ ไบโอเซลลูโลส (แบคทีเรีย), เซลลูโลสจากพืชและโพลิเมอร์สังเคราะห์

2) เซ็นเซอร์ทางเคมีที่ใช้เมมเบรนที่ผลิตจากแบคทีเรียสามารถนำมาใช้สำหรับการวิเคราะห์ทางเคมีสัมพันธ์กับตัวบงชี้บางตัวได้แก่ พีเอชและระดับน้ำตาล คุณสมบัติหลักของวิธีนี้คือเซ็นเซอร์ต้นทุนต่ำและใช้งานได้ดี (ความสามารถในการดูดซับสูง, ความเป็นพิษต่ำ, เมมเบรนที่มีความยืดหยุ่น, ขนาดเล็กและลดการใช้สารละลายตัวอย่าง) มีแนวโน้มที่จะทำตัวเป็นเซ็นเซอร์ที่ใช้ได้กับผิวหนัง

3) การวิเคราะห์ทางเคมีผ่านการไหลแบบไมโครฟลูอิดิกโดยอาศัยเมมแบรนจากพืชธรรมชาติ (เส้นด้ายและวัสดุกระดาษ) เพื่อใช้สำหรับการวิเคราะห์โลหะหนัก และสารต้านอนุมูลอิสระ (โพลีฟีนอล) งานวิจัยนี้ได้สร้างแนวคิดใหม่ที่มีความเป็นไปได้สำหรับเคมีวิเคราะห์สีเขียวและสำหรับการทดสอบตัวอย่างบริเวณพื้นที่จริงโดยเฉพาะอย่างยิ่งในพื้นที่ห่างไกล

4) ระบบการไหลโดยผ่านเมมเบรนแลกเปลี่ยนไอออน (พอลิเมอร์สังเคราะห์ทางเคมี) สามารถพัฒนาขึ้นมาเพื่อหาปริมาณฟอสเฟตในน้ำทะเล สิ่งสำคัญของวิธีการนี้คือหลักการส่งผ่านรีเอเจนต์เข้าไปในระบบโดยใช้เมมเบรนที่ง่าย เมื่อเทียบกับวิธีการที่ต้องอาศัยการเติมสารละลายผ่านเครื่องมือที่ยุ่งยาก

5) การใช้เมมเบรนแลกเปลี่ยนไอออนควบคู่ไปกับการตรวจวัดทางเคมีไฟฟ้ามีความเหมาะสมสำหรับการวัดสารเชิงซ้อนฟอสโฟโมลิบเดตในน้ำทะเล การตรวจวัดได้ใช้ขั้วไฟฟ้าแบบไหลเพื่อให้ปริมาณตัวอย่างที่ใช้ลดลง, เป็นอุปกรณ์ขนาดเล็ก, พกพาได้, และใช้พลังงานต่ำซึ่งสามารถเชื่อมต่อกับระบบไมโครฟลูอิดิกได้

STATEMENTS OF ORIGINALITY

1. This research aimed to develop chemical sensors employing polymeric membranes for separation and detection within one small device. The diverse membrane platforms were fabricated including bio-cellulose (bacteria), plant cellulose, and synthetic polymer systems.

2. Bacteria-produced membrane was demonstrated as chemical sensor for some important markers including pH and glucose determination. The main feature of this approach is low-cost and quite functional sensor (high adsorption capacity, low toxicity, flexible membrane, small size, and sample solution reduce), promising to behaved as a wearable sensor with human skin.

3. Natural plant membrane (cotton thread and paper materials) was presented via self-microfluidic behaviors for chemical analysis including heavy metals, and antioxidant (polyphenol) determination. This work has established a new concept in possibility of green analytical chemistry and possible for at site assay, especially being useful in some remote areas.

4. Ion-exchange membrane (chemical synthetic polymer) in terms of in-line flow system was successfully developed for the determination of phosphate in seawater. The key advantage of this approach is a simpler, more integrated membrane-based reagent delivery principle, compared to established approaches that rely on the complex addition of solution.

5. Ion-exchange membrane coupled with electrochemical detection was properly demonstrated for measuring an electroactive phosphomolybdate complex in seawater. Cross-flow electrode detection was used to receive the minimized sample volume demonstrating a small, portable equipment and receiving low power consumption interfaced with microfluidic module.

CHAPTER 1

Introduction

1.1 The membranes from natural and chemical synthetic resources

A membrane is defined as a selective barrier, allowing some particles to pass through such as ions, molecules, and small particles. The structures of membranes can be neutral or charged [1]. They have been a separator in some chemical techniques, especially chromatography, and electrochemical sensors [2,3]. It can be generally classified into natural and chemical synthetic membranes. Cellulose materials have been realized and chosen as a membrane for microfluidic sensors without external forces. They are a common structure in various materials, mostly in plants (paper and cotton thread). However, it is also produced by a variety of microorganisms such as bacteria, algae and fungi, derived from a fermentation process (bio-cellulose). Another approach of a down scaling sensor with membrane is focused on the thin layer polymeric membrane via ion selective behavior. The determination of an ionic activity is proportional to the membrane potential [4]. Most chemical synthetic membranes are made of polymer structure, generally meant for separation purposes in the laboratory or industry [5].

1.2 Chemical sensors employing the separation and detection part

By the International Union of Pure and Applied Chemistry (IUPAC), a chemical sensor is defined as a device that transforms the chemical information into the analytical useful signal. The information can be a concentration of the specific component or total composition of analysis. A chemical sensor involves two basic units, namely, receptor and transducer. The receptor part deals with transforming the chemical information into a form of energy. The transducer part involves converting the transformed energy based on chemical information of the sample into a useful analytical signal. The transducer does not then show selectivity. Apart from these mentioned above (two basic units), a sensor should include the separator, for example, a polymer membrane [6]. The chemical sensing

development has grown steadily over the past several decades by the diversity of chemical measurements such as thermal, electrochemical, mass, magnetic and optical sensors. The sensors may be categorized based on their physical and mechanical properties [6,7]. The ideal chemical sensor is an inexpensive, portable, and foolproof device that responds with the good selectivity to the analyte of interest [8]. There have been various aspects of developments for such the ideal chemical sensor. Some recent trends of sensor development have been driven by miniaturization (downscaling sensors). Due to reducing the size of an assay by decreasing the amount of substance and power consumption, it results in the lower costs, short time and waste reduction. According to small sensors, a microfluidic flow has been of much interest. It relates to the manipulation of fluids, in microliter scales, which has been applied in several fields such as biology, medicine, pharmacy and agriculture [9].

From the long history, the fabrication of new chemical sensors is substantial and has increased steadily in various material designs. The range of sensor applications was from sophisticated industrial processes to common consumer products. In the beginning, temperature sensitivity in diverse materials was presented in the early 1800s. In 1860, *Siemens* exhibited a temperature sensor with a copper resistor. After that, the silicon material was used to create a new method for transducing the electrical signal processed by a computer. Modern sensors encompass many opportunities for introducing new materials for effectiveness [10]. The recognition of a low cost and simpler gadget, the downscaling sensor has been highlighted, which microfluidic device is very appealing because of the manipulation of fluid in small volumes, or known as a micro total analysis system (μTAS) [11,12]. First of all, microfluidic sensors started in the 1990s from a silicon and glass platform (lap on chip), then PDMS (Polydimethylsiloxane) was instead fabricated because of high prices and inflexibility from the previous material [13]. Recently, many polymer membranes were selected for creating the microfluidic sensor.

The separation behavior on the cellulose membrane, one of the polymer sheets, is significantly focused by some chemical researches [14,15]. For instance, a blood grouping system by the cotton natural materials based on the principle of antigen and antibody binding was presented. Separation of the red blood cells (RBCs) from the whole blood by the antibody principles considered the changing of colors. The blood group of ABO and Rh samples could be isolated using 2 μL for 1 minute without any preparation

of the blood clot. Colorimetric and electrochemical detections were mostly found in cellulose based sensors. For examples, using multiple colorimetric indicators for paper based devices were presented. The principle of this device was based on the oxidation of indicators by hydrogen peroxide produced by oxidase enzymes for each analyte. Different indicators generated the several colors of analyte products. This approach was successfully applied to the determination of glucose, lactate, and uric acid [16]. After that, the study of micro-fluid flow systems has appeared. Dipping cotton in the protein solution with different concentrations illustrated the variation of different blue intensity related to increasing a concentration of the solution [17]. Another colorimetry on the cellulose membrane was presented by cotton thread-based analytical devices for semiquantitative analysis. This paper described the simple quantitative analysis methods for a chemical sensor. Using a ruler measured the indicators color length which was changed on the thread. The system was made from cotton and polyester using multi-thread lines on the polymer film as a capillary flow system. In the result, the reaction between the reagent and different sample concentrations could be presented according to the length of the different colors on the yarn. The application to biological tests was available including protein and nitrite in the marine samples [18]. Electrochemical detection is also used for the lab on cellulose such as the rapid screening of Au(III) in industrial waste. Screen-printed electrode using carbon ink was placed on the cellulose paper [19].

Apart from the cellulose based membranes as previously mentioned, chemical synthetic polymer membranes is a valuable part usually combined with electrochemical detection based on potentiometric and coulometric methods. For separation step of a polymeric membrane, selective chemical receptors in this membrane often used a lipophilic or ionophore as an ion exchanger [4]. Recently, the low-cost thin layer coulometric microfluidic device with a calcium selective membrane (porous polypropylene) was illustrated [20]. This device can be fabricated outside the common laboratory facilities regardless of external equipment. Calcium determination in the range of 10-100 μM in the mineral water was applied to compare with atomic absorption spectroscopy in a good agreement. A polymeric membrane ion-selective electrode for the assay of enzymes and their inhibitors was reported. Applications of this approach included the detection of both free and labeled enzymes and some bio-analytes. Substrate ions are consumed by a reaction of the enzyme in solution or immobilized on the

membrane surface offering a rapid and continuous sensor [21]. Thin layer coulometric determination of nitrate in fresh waters was studied. A nitrate ion-selective electrode (ISE) employing a permeable tubular membrane comprising a nitrate ionophore was supported on porous polypropylene, detected in the range of 10–100 M [22].

This work is then aimed to develop chemical sensors employing polymeric membranes for separation and detection that are situated within one small device.

1.3 Downscaling chemical analysis leading to green chemical sensors

Downscaling analysis system has been introduced since the serious risks for operators and the environmental damage was occurred due to toxic reagents and the waste products from normal chemical experiments [23]. The reduction of solution was concerned via automation machines, flow-based method, novel green chemical system, and downsizing techniques [24,25]. The early stage of downscaling via flow-based techniques was originated by Ruzicka and Hansen with the high efficiency in various routine methods [26]. These can be illustrated into green chemical sensors in various application such as the lab on chip, paper based sensors and thread diagnostic system [17, 27-32]. The functional advantages of these systems include portability, easy operation, less waste consumption, and low-cost device, applying to analytical monitoring, especially in limited areas.

1.4 Colorimetric and electrochemical techniques

Colorimetric techniques within this research are based on spectrophotometry, a general technique involving a quantitative measurement of the light intensity in terms of the spectrum [33,34], and the color processing (RGB value). This latter is associated with three primary colors from a digital image; red (R), green (G) and blue (B) shown in Figure 1.1 [35], evaluated in the range of 0 to 255 by means of ImageJ and Adobe Photoshop. A mobile phone camera, a popular and portable device, was chosen to capture the digital images. Generally, image sensors were chosen to detect the reflected light from the target products including charge-coupled devices (CCD) and complementary metal oxide semiconductors (CMOS) [36]. The relation between RGB intensity and sample quantitation can be used in diverse chemical analysis such as chromium, iron, methanol, glucose determination [37-43].

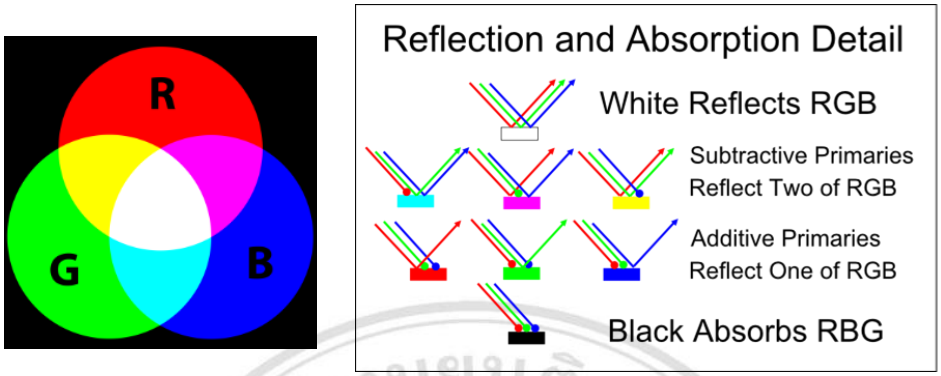

Figure 1.1: RGB color reflection

Electrochemical techniques of this experiment are also discussed in potentiometry, cyclic voltammetry, and square wave voltammetry. Potentiometry, zero-current technique, is based on the potential across the membrane of the indicator electrode. It normally consists of two parts including ion-selective part (indicator electrode) and reference electrode which their different potential is measured under zero current (Figure 1.2). This different potential is described by the Nernst equation (eq.1) where a_i is the activity of analyte ion, R is the universal gas constant, T the absolute temperature, F the Faraday constant, z_i the charge of the primary ion, and K is an experimentally determined constant potential value. According to the existence of interfering ions, the potential is measured by Nicolsky equation (eq.2), where a_i and a_j are the activities of the primary and interfering ions respectively, z_i is the charge of ion i, K_{ij}^{pot} is the potentiometric selectivity coefficient that illustrating the selectivity of analyte ion over interfering ion [44]. The separate solution method (SSM) is clarified as the two potentials along with the two ion activities are chosen to measure the selectivity coefficient [45].

$$E = K + \frac{RT}{z_i F} \ln a_i \quad (eq.1)$$

$$E = K + \frac{s}{z_i} \log \left(a_i + \sum_{j \neq i} K_{i,j}^{pot} \, a_j^{z_i/z_j} \right) \quad (eq.2)$$

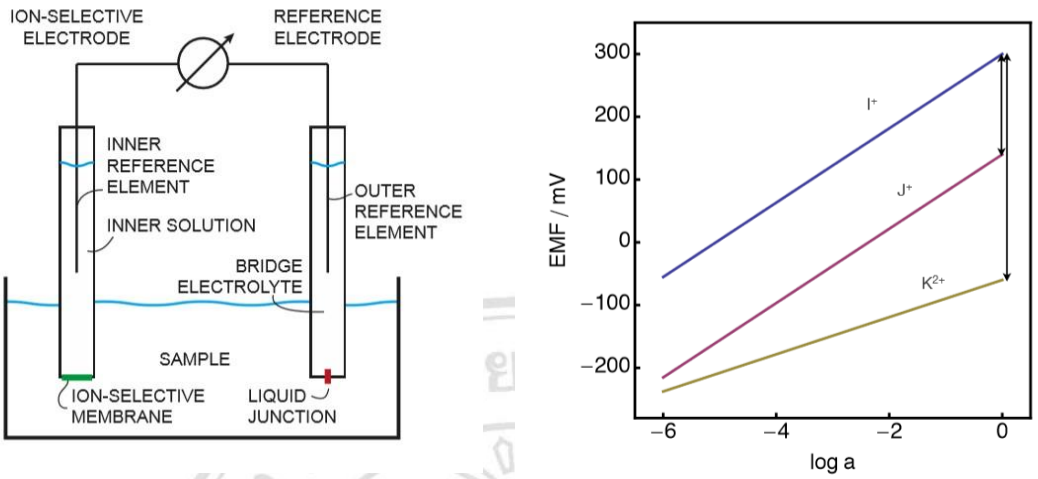

Figure 1.2: Electrochemical cell with ion-selective electrode for potentiometry (left), the potentials of the separately measured calibration curves (right) [44]

Voltammetry is based on the measurements of current resulting from redox reaction in a function of the potential applied to the electrochemical cell. This technique allows to identify and quantify a large number of compounds such as cations, anions, organic compounds. Cyclic voltammetry (CV) is a useful method for identification of electroactive species during oxidation and reduction step. In this technique, the potential of a working electrode is linearly scanned by a triangular potential waveform. The resulting current is obtained and then plotted with potential as cyclic voltammogram as shown in Figure 1.3. The position of the cathodic peak current (I_{pc}, forward scan) is shifted to cathodic potentials (E_{pc}) relative to the anodic peak current (I_{pa}, backward scan). This technique allows the measurement of the curves I = f (E). Additionally, If the electrochemical reaction is controlled by diffusion, the peak height is related to the square root of the scan rate [44, 46].

Square wave voltammetry (SWV), one of the most popular techniques for the quantitative analysis, provides good speed and high sensitivity. A square wave pulse of the constant amplitude is covered on a staircase waveform, which their potential increases corresponding to oxidation and reduction waves. The net current is measured from the difference between the forward and reverse pulses at the end illustrated in Figure 1.4. Since the net signal is measured under the almost complete rejection of the capacitive

current, square wave voltammetry provides better sensitivity than cyclic voltammetry or simple step techniques, resulting in the detection limits as low as 10^{-8} M. The peak height is relative to the concentration of the electroactive species. This fast technique exhibits bell-shaped response curves that the different current is calculated from forward and reverse currents [44, 47].

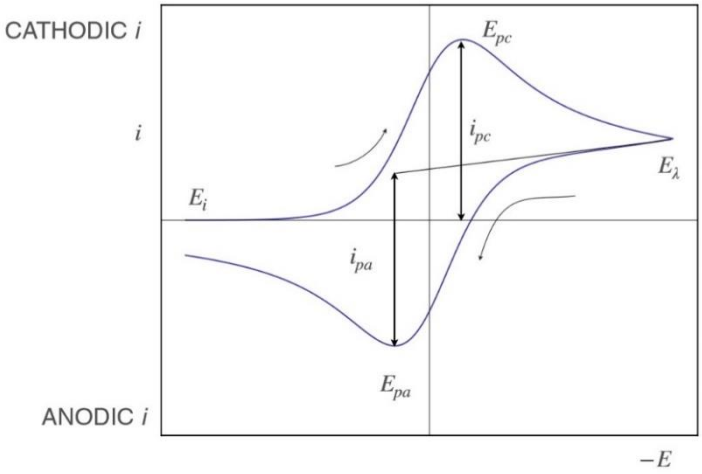

Figure 1.3: Cyclic voltammogram for a reversible electrode [44]

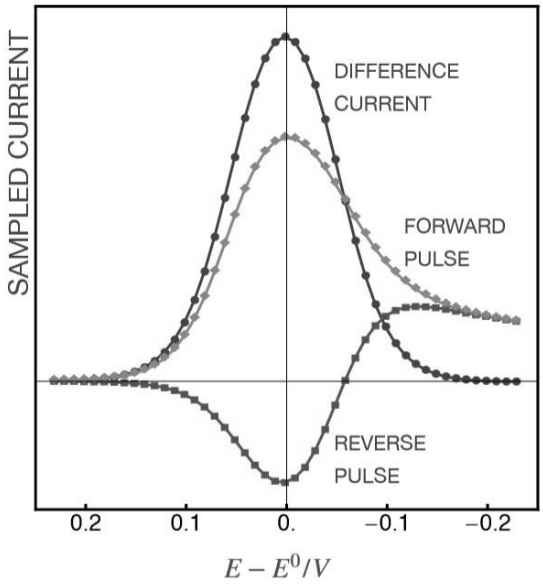

Figure 1.4: Mathematical simulation of the current calculated from the forward and reverse sampled currents, providing the bell-shaped square wave voltammetry [44]

1.5 Research objective

To develop chemical sensors via both separation and detection/measurement steps in the same device, by employing polymer membranes for environmental and health related samples.

CHAPTER 2

Chemicals, materials, instruments and devices

2.1 Chemicals

All are analytical grade, otherwise stated.

1. Potassium chloride (KCl), ≥99.5% w/w, Merck, Germany
2. Sodium hydroxide (NaOH), ≥98% w/w, Sigma-Aldrich, Germany
3. Monopotassium phosphate (KH_2PO_4), ≥99.5% w/w, Merck, Germany
4. p-anisidine, ≥99% w/w, Sigma-Aldrich, Germany
5. 3,3′,5,5′-Tetramethylbenzidine (TMB), ≥99% w/w, Sigma-Aldrich, Germany
6. D-glucose, ≥99.5% w/w, Sigma-Aldrich, Germany
7. Glucose oxidase (GOD) from *Aspergillus niger*, Sigma-Aldrich, Germany
8. Horseradish peroxidase (HRP), Sigma-Aldrich, Germany
9. L-histidine monohydrochloride hydrate ($C_6H_9N_3O_2$), Himedia Laboratories
10. Sodium chloride (NaCl), ≥99% w/w, Sigma-Aldrich, Germany
11. Sodium dihydrogen phosphate dihydrate ($Na_2HPO_4.2H_2O$), Sigma-Aldrich, Germany
12. Sodium dodecyl sulfate (SDS), 98% w/w, Sigma-Aldrich, Germany
13. Copper (II) sulfate pentahydrate ($CuSO_4.5H_2O$), ≥99% w/w, Merck, Germany
14. Cadmium (II) acetate ($Cd(COOCH_3)_2$), ≥99% w/w, Sigma-Aldrich, Germany
15. Cobalt (II) chloride ($CoCl_2$), ≥97% w/w, Sigma-Aldrich, Germany
16. 4-(pyridyl-2-azo)-resorcinol (PAR), ≥96% w/w, Sigma-Aldrich, Germany
17. Gallic acid, $(HO)_3C_6H_2CO_2H•H_2O$, ≥98% w/w, Sigma Aldrich, Germany
18. L-ascorbic acid, $C_6H_8O_6$, ≥99% w/w, Fisher Scientific, UK
19. Folin- Ciocalteu reagent, Merck, Germany
20. 2,2-diphenyl-1-picrylhydrazy reagent (DPPH: $C_{18}H_{12}N_5O_6$), ≥95% w/w Sigma-Aldrich, Germany

21. Sodium molybdate dihydrate ($Na_2MoO_4.2H_2O$), ≥99.5% w/w, Sigma Aldrich, Germany
22. Ammonium molybdate tetrahydrate ($(NH_4)_6Mo_7O_{24}\cdot 4H_2O$), ≥99% w/w, Sigma Aldrich, Germany
23. L-ascorbic acid ($C_6H_8O_6$), ≥99% w/w, Fisher Scientific, UK
24. Potassium antimonyl tartrate trihydrate ($C_8H_4K_2O_{12}Sb_2\cdot 3H_2O$), ≥99% w/w, Sigma Aldrich, Germany
25. Sodium phosphate monobasic (NaH_2PO_4), ≥99% w/w, Sigma Aldrich, Germany
26. Sodium hexafluorosilicate (Na_2SiF6), ≥99% w/w, Sigma Aldrich, Germany
27. Hydrochloric acid (HCl), 37%v/v, ACS grade, Sigma-Aldrich, Germany
28. Sulfuric acid (H_2SO_4), 96%v/v, ACS grade, Sigma-Aldrich, Germany
29. Ethanol (C_2H_5OH), ≥96% v/v, laboratory reagent, Sigma-Aldrich, Germany
30. Universal pH solution (4.0-10.0), Merck, Germany
31. The artificial seawater sample from NEPTUNEA SA (Aquarium shop in Confignon)
32. The real seawater samples were from Arcachon Bay (France) and Genoa Station, Italy. All collected samples were immediately stored in a cold box and finally in a fridge at 4 ^{o}C, pH around 8.
33. Cotton thread, Chom Thong, Chiang Mai, Thailand

2.2 Instruments, devices and materials

1. Micro well-plate with 96 wells or 24 wells, Sigma Aldrich, Germany
2. UV/Vis spectrophotometer UV-1800, Shimadzu, Japan
3. UV/Vis spectrophotometer Lambda 35, Perkin Elmer, USA
4. Scanning electron microscope, SEM, JEOL, Japan
5. Micropipett, Eppendorf, Germany
6. Light controlling box (7 in.×10 in.×7 in.)
7. Mobile phone camera, Apple Inc., all pictures were captured with the flash-off
8. Plastic material (Polyethylene)
9. Small vials
10. Micropipette

11. Potentiostat/galvanostat PGSTAT 128N (Metrohm Autolab, Utrecht, Netherlands) controlled by Nova 1.11 software
12. Peristaltic pump (Model ISM935c, Clattbrug, Switzerland
13. Two-position selector and switching valves, VICI® (Valco Instruments Company Inc.), USA
14. Silicone rubbers (Angst + Pfister), APSOparts®, Germany
15. Cation-exchange membrane FKL-PK-130 (thickness 110-140 μm) and anion-exchange membranes FAPQ-375-PP (thicknesses 70-80 μm), Fumatech®, FuMA-Tech GmbH, Germany

2.3 The preparation of solutions and membrane

2.3.1 The bio-cellulose membrane production

The essential components to synthesize the BC membrane included coconut juice 1.0 L (the main nutrient source), sugar (50 g), vinegar (10 ml), ethanol (150 ml), ammonium phosphate (1 g), the starter *Acetobacter xylinum* (100 ml, 10% of coconut juice). Other gadgets were based on the cotton tissue, pots, and bottles (round bottom type).

2.3.2 pH determination

Standard pH buffers in the range of 4-9 were prepared by 0.1 M potassium hydrogen phthalate (KHP) adjusted with hydrochloric, 0.1 M monopotassium phosphate (KH_2PO_4) adjusted with NaOH. pH reagent was divided into two types involving the natural and commercial sources (the universal pH solution (4.0-10.0)). Firstly, the dried butterfly pea flower, an organic herbal tea (Chiangmai tea), was extracted by soaking in DI water (1g: 20 ml) about 10 min.

2.3.3 Glucose determination

Standard glucose was prepared by D-glucose for a stock solution (1,000 mg/L) dissolving in deionized water. Mix reagents in reaction1 (Figure 3.1A) included 0.1 M p-anisidine (Aldrich), 0.005 M Fe^{2+} in H_2SO_4 0.005 M, and 0.5 M acetate buffer pH 4. Mix reagent in reaction3 (Figure 3.1C) include 2.5 M TMB (substrate), 0.1 M phosphate citrate buffer pH 5.0. The essential enzymes were glucose oxidase (GOD) and horseradish peroxidase (HRP).

2.3.4 Health related samples

Six samples (1-6) were based on healthy and normal food involving sample 1: normal beverage, sample 2: healthy beverage, sample 3: low calorie sugar, sample 4: sugar substitute1 for the weight control and diabetics uses, sample 5: sugar substitute2 for the weight control and diabetics uses, sample 6: daily mate (healthy green tea for diabetics uses).

Other six samples (7-10) were focused on the artificial sweat spiking with the glucose amount. According to the international standard (ISO 105:2013), mimic sweat sample can be obtained by 0.5 g L-histidine monohydrochloride hydrate, 5 g sodium chloride, 2.5 g sodium dihydrogen phosphate dihydrate made up in DI water 1 L.

2.3.5 Comparing the behaviors of materials

Anionic surfactant (sodium dodecyl sulfate (SDS)) prepared for a stock solution (5,000 mg/L) by dissolving 0.5000 g in deionized water and was made up to 100.00 mL volume. A stock methylene blue solution (0.0934% w/v) prepared by dissolving 0.0934 g of the solid in deionized water and made up to 100.00 mL volume.

2.3.5 Heavy metal ions determination

Standard stock solution (100 mg/L) were prepared: copper(II) from $CuSO_4$, cadmium(II) from $Cd(COOCH_3)_2$, and cobalt(II) from $CoCl_2$. The solid of 4-(pyridyl-2-azo)-resorcinol (PAR) reagent was dissolved in water up to 100.00 mL (0.001 mol/L), borate buffer pH 9.2 was prepared by boric acid. All solutions were prepared in deionized water.

2.3.6 Antioxidant determination

Standard gallic acid stock solution (1000 mg/L) was prepared from gallic acid monohydrate. The solution of Folin- Ciocalteu commercial reagent was prepared to 0.02 mol/L. Then, 2, 2-diphenyl-1-picrylhydrazyl reagent (DPPH) was dissolved in ethanol up to 0.06 mmol/L.

2.3.7 Tea sample preparation

0.015x g of tea powder was extracted with 20.00 mL of boiling water at 100 ^{o}C for 10 minutes. Then, the infusions were filtered through filter paper (Whatman^{TM} No.1) and transferred into a volumetric flask (25 mL). Tea samples were freshly prepared.

2.3.8 Colorimetric measurement of phosphate assay

The solution of ammonium molybdate tetrahydrate was prepared by dissolving solid 15 g in 500 mL of water. The sulfuric acid solution was obtained by adding 140 mL of concentrated sulfuric acid in 900 mL of water. Then, ascorbic acid solution was prepared by dissolving 27 g of L-ascorbic acid in 500 mL of water and stored in the freezer. Potassium antimony tartrate solution was prepared by dissolving 0.34 g of solid in 250 mL of water. The mixed reagent for phosphate measurement (Reagent(P)) by mixing the solution via the ratio of molybdate: acid: ascorbic: antimony = 2:5:2:1. For colorimetric detection, the mixed reagent was added to the sample in a volumetric ratio of 1:10.

CHAPTER 3

Chemical sensor employing bacteria-produced cellulose based membrane

Investigating the state of the art accessing to green chemical analysis, the bacteria cellulose material (bio-cellulose) is emphasized to prepare a membrane sensor including a separation and detection part. This proposed sensor is demonstrated to determine pH and glucose quantity in heath related samples. The advantages of this material membrane include its high crystallinity, high degree of polymerization, high water adsorption capacity, and low toxicity. In addition, it is also flexible material that enclosed on others easily such as paper, skin and hydrophilic substance. It is a low cost and pretty functional sensor for further chemical application in terms of wearable sensors.

In this chapter, both important markers including pH and glucose determination were illustrated. The possibility and analytical characteristics of this expected sensor were studies with various factor effects. The real samples were done in terms of healthy foods and artificial sweat.

3.1 Introduction

Cellulose is a common structure in various materials, especially in plants (details in chapter 4). However, it is also synthesized by a variety of microorganisms such as bacteria, algae, and fungi, derived from a fermentation process. The general structure is a linear glucose polymer of β-1,4-glycosidic bond with various polymerizations. The plant cellulose (PC) and bacterial cellulose (BC) have the same chemical structure, but different physical and chemical properties. Cellobiose presents the six hydroxyl groups, which form intra- and intermolecular hydrogen bonds. Multiple cellulose chains form the elementary fibrils that further aggregate into larger microfibrils (5 - 50 nm in diameter and several microns in length). In these microfibrils, the bundles of elongated molecules in which highly crystalline regions alternated with less ordered regions (amorphous) [48].

Plant-based cellulose is a renewable resource that is widely used in multifarious applications such as paper, textiles and construction materials (Chapter4). However, it consists of hemicellulose, lignin, waxy aromatic substances and other impurities that require the additional energy- or chemical- purification processes in order to obtain the pure cellulose. Bio-cellulose (BC), also known as the bacterial cellulose, is a chemically purer form of this cellulose that is synthesized by many micro-organisms in the presence of carbon source and acidic condition. BC exhibits the excellent characteristics than the plant cellulose such as high crystallinity, a high degree of polymerization, good adsorption capacity (over 100 times of its weight), greater tensile strength, stability, and low toxicity. Moreover, bio-cellulose has also a three dimensions property and is resilient for human's skin [49, 50]. So, this can lead to medical application.

Bio-cellulose is produced by various species of bacteria, such as those of the genera *Gluconacetobacter* (formerly *Acetobacter*), *Agrobacterium*, *Aerobacter*, *Achromobacter*, *Azotobacter*, *Rhizobium*, *Sarcina*, and *Salmonella*. However, Acetobacter xylinum is the most important and most efficient bio-cellulose producing a bacterial strain that is capable to produce high levels of polymer from a wide range of carbon and nitrogen sources and the highest yield of BC for industrial applications. It is a gram-negative rod-shaped bacterium that can obtain glucose, sugar, glycerol or other organic substrates and convert them into the pure cellulose. Generally, these bacteria were fermented actively at pH 3 - 7 (pH 4.3 is the most suitable) and 25˚C - 30˚C, using saccharides as a carbon source. Medium supplementation with some nutrients (nitrogen and phosphorus) can also increase the production of bacterial cellulose [48, 51-52]. General BC membrane prepared by the coconut juice medium was often chosen [52,53]. Another one was blended with silver nanoparticles (Ag), or aluminum (Al) to provide the antimicrobial ability [54].

Wearable sensors have been recently fabricated as a tremendous tool for healthcare, security, and environmental fields [55]. Their applications were fairly diverse among the important biomarkers such as chloride, potassium, sodium, glucose, lactate, and pH in perspiration. In the sweat sample, pH is often considered to physiologic health (hydration state). Glucose is also an important marker in the health issue which could diagnose hyperglycemia, and is the essential factor for diabetic patients or people who concern an obese state [56-60].

In this chapter, the important markers were evaluated based on pH and glucose determination. Firstly, the pH measurement using butterfly pea flower, a tropical plant of Asia known as *Clitoria ternatea*, has been commonly used in pharmaceutical and food products [61]. Extracting a butterfly pea is an alternative reagent of acid-base indicator instead of the synthetic chemical reagent [62,63]. Secondly, the glucose concentration was investigated since it is an important marker for diabetes and health diseases. From many literature reviews, they focused on the main mechanism via an enzyme and the substrate compound (Figure 3.1). The reaction by means of glucose oxidase and anisidine substrate was studied to provide the red complex product relating to the glucose quantity [64]. Moreover, horseradish peroxidase was also chosen for the glucose analysis to obtain brown color from the iodine solution [65,66]. Another choice of a mechanism from these enzyme strains was expressed via tetramethylbenzidine (TMB) substrate getting the blue complex [67-69], suitable for this proposed sensor.

(A) D-glucose + H_2O + O_2 $\xrightarrow{GOD}$ D-glucono-1,4-lactone + H_2O_2

H_2O_2 + ρ-anisidine $\xrightarrow{Fe(II)}$ Red color product + H_2O

(B)

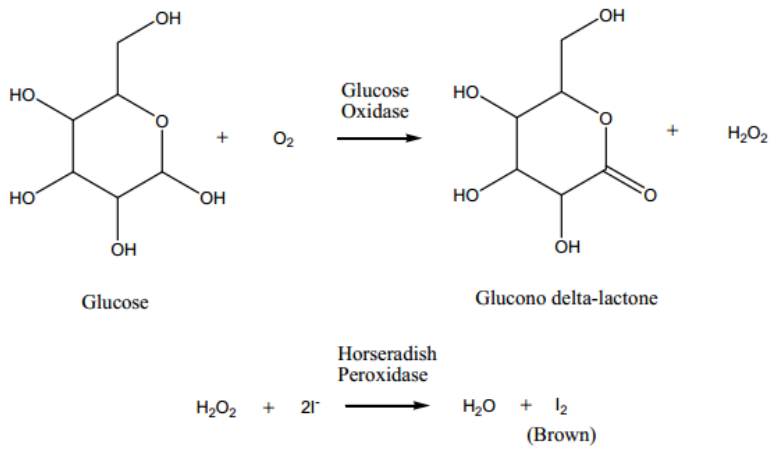

(C)

$$H_2O_{2\ (from\ (B))} + 3,3',5,5'\text{-tetramethylbenzidine (TMB)} \xrightarrow{Horseradish\ peroxidase\ (HRP)} 3,3',5,5'\text{-tetramethylbenzidine cation free radical} \leftrightarrow \text{blue complex}$$

Figure 3.1: The mechanism of glucose determination: (A) GOD and anisidine, (B) GOD with HRP and iodide, (C) GOD with HRP and TMB

3.2 Experimental procedures

3.2.1 The synthetic process of bacteria-cellulose membrane

There are some methods for the BC synthesis process based on the bacteria strain [52, 53]. A. xylinum was used as the acetic acid bacterial strain. The culture medium was prepared with coconut-water and followed by the addition of sugar as the carbon-source and acetic acid as the acidifier. Coconut juice production was excessed from many applications of agro-industries in Southeast Asian countries. Because the residues still contain carbon and nitrogen sources, they could be utilized as a substrate for producing a good quality BC. In addition to carbohydrates and protein substances, coconut water also contains many old minerals needed by Acetobacter xylinum. After sterilization, the medium was inoculated with A. xylinum (5–10%, v/v) and cultivated statically for 3–7 days. The celluloses were collected and rinsed with deionized water several times in order to remove bacteria and nutrients. The wet BC membranes sterilized by an autoclave and compressed to remove the excess water by a compressor. Another medium was cultivating the bacterial with the rice water in an inflatable pool for 10 days.

Additionally, some metal particles were added into this cellulose mask for improving efficiency. A new nanostructure was blended on the BC membrane with Al particle in an aqueous NaOH/urea solution, media containing 0.5% ammonium sulfate, 5.0% sucrose, and 1.0% acetic acid in the coconut water [70]. The BC membranes presented relatively high porosity and flexible membranes combined with the magnetic nanocomposite (iron oxide nanoparticles) functionalized with polyethylene glycol (PEG) [71]. BluRibbon was invented from the combination of two technology platforms: nano-biocellulose technology (Acetobacter xylinum in Thai rice medium) and engineered silver nanotechnology. Silver nanoplates allow a larger amount of the silver ion interact with bacteria and fungi which shows the antimicrobial activities [54].

To prepare our own BC membrane, some ingredients were required. The coconut juice, sugar and nitrogen-containing compounds from a local market, was blended with the brown sugar as a carbon source in a prepared pot and then adding ammonium phosphate into the previous solution. Boiling for 5 min, the pot was taken in the cold-water medium to get a better warm temperature. The vinegar, ethanol and bacterial starter were added into this homogenous solution following the ratio as mentioned above. Cultivating the bacterial solution from the previous procedure in each round-bottom bottle (250 ml), which sterilized by hot water. These bottles were closed and replaced by the tissue at the partial areas of their cap for the good producibility. After incubating in a room temperature environment for 7 days, the bio-cellulose was obtained initially. Produced cellulose membranes were collected by boiling for 5 min and then kept in a freezer at 4 ^{o}C (Figure 3.2-3.4).

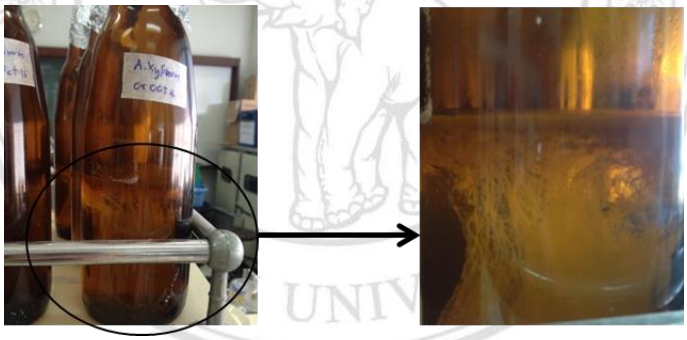

Figure 3.2: Acetobacter xylinum (Starter)

Figure 3.3: Acetobacter xylinum in the nutrient medium

a b c

Figure 3.4: The produced cellulose membrane illustrating from left to right: day 1(a, b), day 3(c)

3.2.2 pH determination via the proposed membrane sensor

To begin the pH assay, the universal reagent or the butterfly pea reagent 10 µl was dropped on a filter paper. After that, buffer samples (100 µl) in the range of pH 4-8 were gradually added into the bio-cellulose membrane and then captured the result by iPhone camera (Figure 3.5). The information was linked to a program of color evaluation (ImageJ).

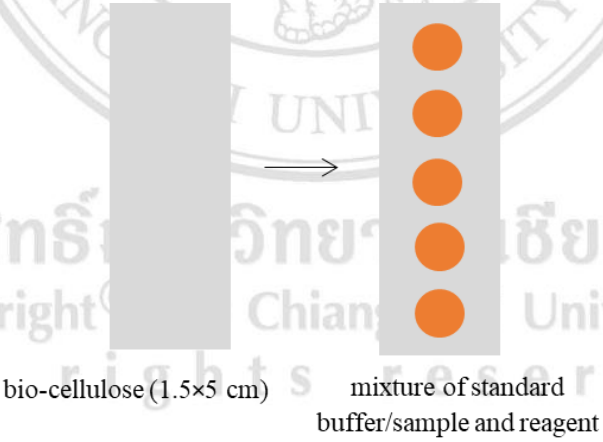

Figure 3.5: A sensor diagram of the bio-cellulose membrane based on pH determination

3.2.3 Glucose determination via the proposed membrane sensor

To initiate a reaction, the ratio of reagent from the chemical part (chapter2) was done, GOD: HRP: buffer: TMB = 10: 10: 40: 250 µl. The mix reagent 10 µl was dropped

on a filter paper and then glucose samples (100 µl) in the range of 0-20 and 0-10 mM were gradually added into the bio-cellulose membrane, captured the result by an iPhone camera (Figure 3.6). The information was linked to a program of color evaluation (ImageJ).

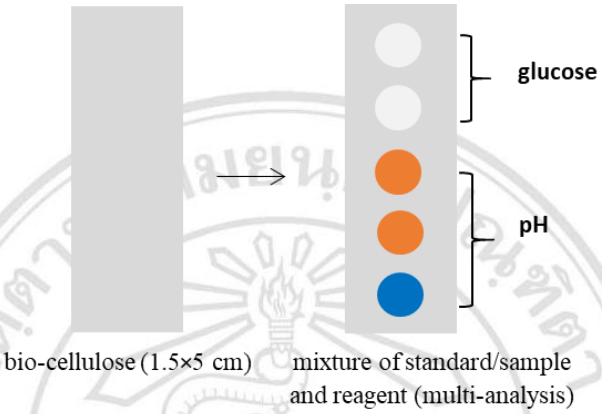

Figure 3.6: A sensor diagram of the bio-cellulose membrane based on multi-analysis

3.3 Results and discussion

3.3.1 The properties of the produced bio-cellulose membrane

3.3.1.1 The physical property

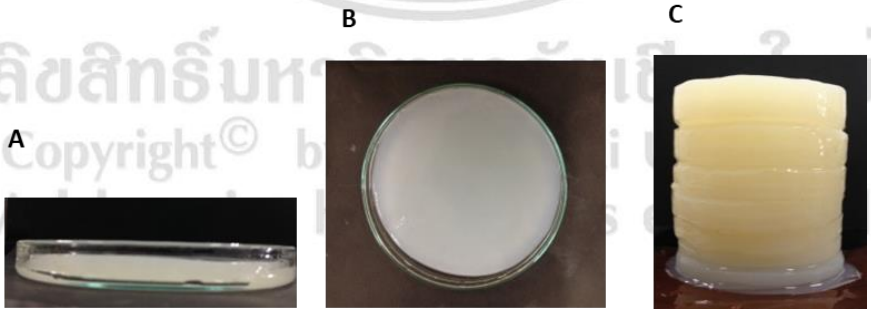

Figure 3.7: The collected cellulose membrane from day 4 in terms of side- and above-capturing (A, B), the accumulated layer membrane from day 2-12 (C)

According to the preparation of the membrane as the experimental procedure (chapter 2.3.1), the proposed bio-cellulose was tough and flexible with the white color (Figure 3.7). Their diameter was around 9 cm based on the size of round bottle

container cultivating bacterial stain. From the above view, the appearance of the membrane was unique and quite homogeneous; however, their thickness was slightly different confirming from the side observation. This unexpected physical property is caused by not being in a static condition through an incubating process and the round bottle container. The average thickness of bio-cellulose membranes was measured by ruler daily presenting in Table 3.1.

Table 3.1: The average thickness of bio-cellulose membranes with the different days

Collecting Days	The membrane thickness [cm]						The example picture (Petri dish: 9×9 cm)
	M1*	M2	M3	M4	M5	Average±SD	
Day 2	0.30	0.40	0.35	0.40	0.45	0.38±0.06	
Day 3	0.60	0.65	0.55	0.52	0.50	0.56±0.06	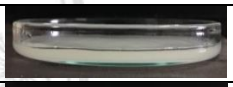
Day 4	0.75	0.70	0.75	-	-	0.73±0.03	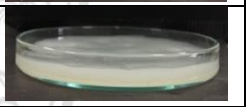
Day 5	0.90	0.95	0.90	-	-	0.92±0.03	
Day 6	0.95	0.95	1.10	-	-	1.00±0.09	
Day 7	1.10	1.00	1.15	-	-	1.08±0.08	
Day 8	1.40	1.60	1.55	-	-	1.52±0.10	
Day 9	1.50	1.50	1.60	-	-	1.53±0.06	
Day 10	1.55	1.60	1.50	-	-	1.55±0.05	
Day 11	1.85	1.80	1.90	-	-	1.85±0.05	
Day 12	2.10	1.90	1.90	-	-	1.97±0.12	

*M: Membrane

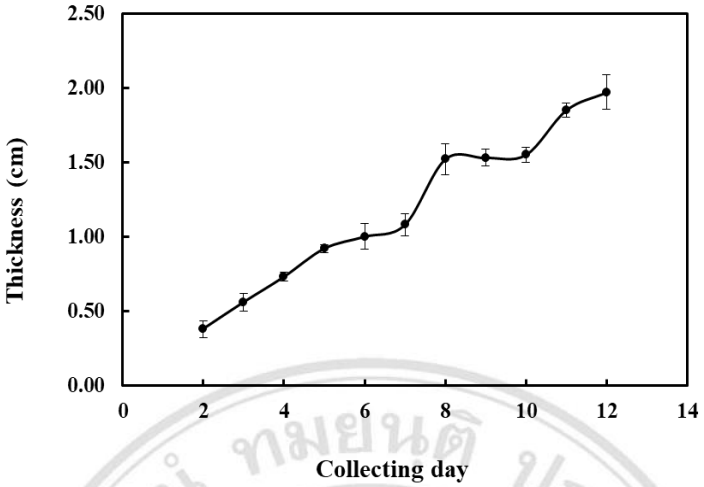

Figure 3.8: The relation graph between the membrane thickness and collecting days

The thickness of the membrane was gradually increased via the incubating day from day 2 to 8 (Figure 3.8), then remained constant among day 8 to 10. After that, it continuously grew until day 12. The range of its thickness was around 0.30 – 2.00 cm. It was observed that the thickness was constant at some periods: days 5-7, days 8-10 and days 11-12.

3.3.1.2 The moisture content ratio: $[W_{wet} - W_{dry}]/W_{wet} \times 100$ [68]

This cellulose sheet has been claimed as a good ability of water absorption in order to maintain the moisture within its structure. In attempt to check this property, our bio-cellulose membranes were cut into the piece of 2 × 2 cm, then heated up to 100 ^{0}C by a mechanical oven (Figure 3.9). It took around 2-5 hours for heating.

Table 3.2: The relation between the weight of membranes and collecting days

Collecting days	Details	The weight of membrane [g]/piece					
		1	2	3	4	5	Average±SD
Day 2	BH*	0.8043	0.7909	0.7656	0.8377	0.6526	-
	AH*	0.0073	0.0075	0.0072	0.0080	0.0063	-
	%moisture	99	99	99	99	99	99±0.02
Day 3 (circle shape)	BH*	1.0561	1.0973	0.9793	1.0968	0.8283	-
	AH*	0.0115	0.0118	0.0099	0.0117	0.0062	-
	%moisture	99	99	99	99	99	99±0.1
Day 3 (square shape)	BH*	1.2191	1.4551	1.4722	1.2543	1.3388	-
	AH*	0.0167	0.0203	0.0218	0.0163	0.0207	-
	%moisture	99	99	99	99	98	99±0.1

Table 3.2 (continued)

Collecting days	Details	The weight of membrane [g]/piece					
		1	2	3	4	5	Average±SD
Day 4	BH*	1.5627	1.5588	1.8632	1.8242	1.8064	-
	AH*	0.0339	0.0303	0.0515	0.0455	0.0402	-
	%moisture	98	98	97	98	98	98±0.3
Day 5	BH*	3.3142	3.3601	3.3572	3.1243	3.1430	-
	AH*	0.1166	0.1203	0.1176	0.1160	0.1154	-
	%moisture	96	96	96	96	96	96±0.1
Day 6	BH*	3.1179	3.3925	3.3574	3.5781	3.0344	-
	AH*	0.1137	0.1154	0.1147	0.1245	0.1104	-
	%moisture	96	97	97	97	96	96±0.1
Day 7	BH*	3.9151	4.3605	3.8731	4.3219	4.4565	-
	AH*	0.1226	0.1278	0.1220	0.1261	0.1263	-
	%moisture	97	97	97	97	97	97±0.1
Day 8	BH*	5.2545	5.5982	5.3961	5.8073	5.7337	-
	AH*	0.1334	0.1362	0.1312	0.1482	0.1423	-
	%moisture	97	98	98	97	98	98±0.1
Day 9	BH*	5.2752	5.2521	5.6628	6.0823	5.2530	-
	AH*	0.1375	0.1309	0.1365	0.1472	0.1325	-
	%moisture	97	98	98	98	97	98±0.1
Day 10	BH*	5.2946	6.3268	5.3705	6.1141	5.9917	-
	AH*	0.1383	0.1414	0.1389	0.1422	0.1448	-
	%moisture	97	98	97	98	98	98±0.2
Day 11	BH*	7.0832	7.7409	6.1348	7.4599	6.1635	-
	AH*	0.1662	0.1661	0.1576	0.1679	0.1526	-
	%moisture	98	98	97	98	98	98±0.2
Day 12	BH*	6.4958	6.8636	6.3635	7.9287	7.6397	-
	AH*	0.1524	0.1586	0.1574	0.1643	0.1648	-
	%moisture	98	98	98	98	98	98±0.2

*BH: Before heating, *AH: After heating

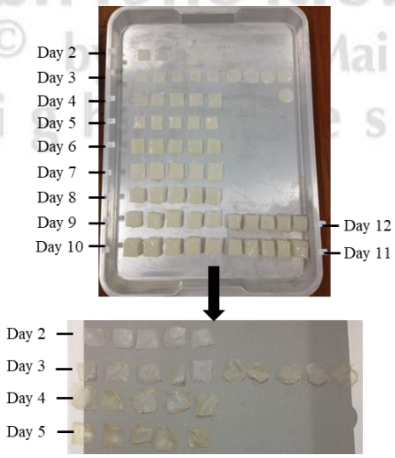

Figure 3.9: The bio-cellulose membrane before- (above) and after- (below) heating

It can be noticed that % moisture contents of the cellulose membranes were calculated in the range of 96-99% (Table 3.2), similarly to the literature review [68], which was not significantly different according to the increasing days. The process of cutting the bio-cellulose membrane into small size, especially thick sheet, was quite difficult that why the thin layer membrane was interesting for further experiment.

3.3.1.3 The absorption ability with blue dye color

Another ability of this membrane is focused on the dye absorption in order to apply in analytical measurement. To clarify this, the cellulose membrane from day3 was chosen to cut into small pieces. After the water had gradually evaporated in proportion to the increasing time (5, 10, 15, 20, 30, 40, 50 min), blue dye (2.0 ppm, 200 µL) was carefully dropped on the cellulose membrane, then eliminating the excess solution.

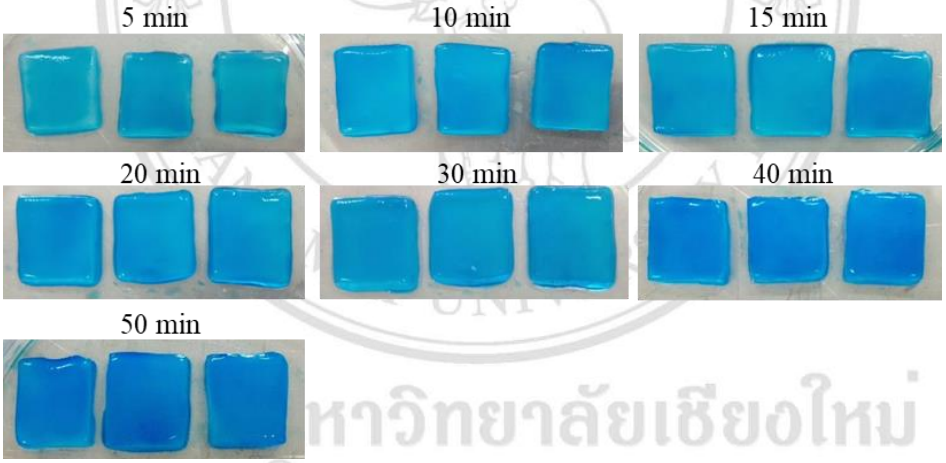

Figure 3.10: The absorption property of membrane (day 3) via blue dye color

It was found that in the first period, the occurred colors on these membranes were slightly rough. After that, this blue solution was passed into each membrane gradually (Figure 3.10). This means the color absorption was affected by the water evaporation resulting in the color consistency. If the thickness of this membrane is selected, the suitable time of water loss will be chosen for the fabrication of the proposed membrane sensors.

3.3.1.4 The moving efficiency

The proposed cellulose membrane was used to compare with a filter paper, a size of 1×7 cm, in terms of flowing red dye. Firstly, a number of filter papers adhering on a plastic sheet were dripped into a vessel containing the red solution 6 ml. It can be concluded via the result that water and the red dye can penetrate along the filter paper in the vertical setting depended on the polarity. Second, bio-cellulose membranes were also cut into the size of 1×7 cm stuck on plastic sheet regardless of using scotch tape. After that, dripping them into the red dye solution in the vessel (Figure 3.11). The results illustrated the difference in behaviors comparing to a filter paper since this dye solution did not flow into the membrane in the vertical setting. This phenomenon can be explained by toughness and strength between materials. However, a red dye solution can flow into this material in a horizontal setting after dropping it. In addition, this cellulose membrane is flexible and adhere properly with other materials such as transparent plastics, filter paper, and skin. Therefore, this membrane material can be used as a channel for the solution flow.

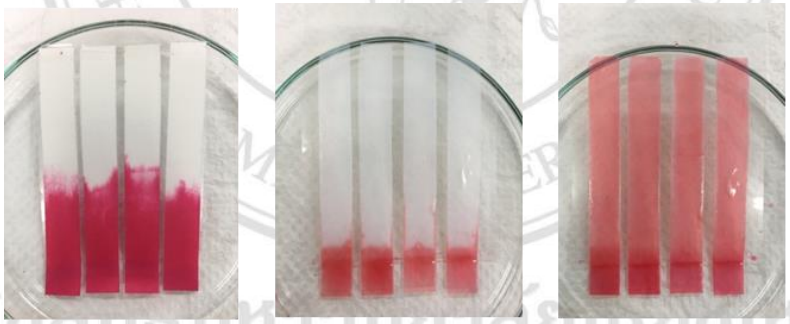

Figure 3.11: The absorption property of membrane (day 3) using blue dye color in a variety of the setting types

3.3.2 The physical property of the commercial cellulose membrane (*PIP* company)

3.3.2.1 The general information

Since our synthetic membrane was difficult to control their thickness and evaporate water, the commercial bio-cellulose sheet has been selected to be a suitable material instead of the old one. This bio-cellulose mask was purchased from PIP

International company, PIP International Co., Ltd: 91/17 Wattananivej 4, Samsen Nok, Huai Khwang, Bangkok 10310 (Figure 3.12-3.13). This membrane has approximately 0.4 mm in thickness, is a white, smooth and highly flexible sheet with pH 7 (Figure 3.14). These appearances are similar to the preliminary results from the synthetic cellulose membrane presented previously, but their thickness homogeneity is better. There is a certificate of natural and innovative material to confirm there were good natural quality.

Figure 3.12: The bio-cellulose sheet from PIP International company

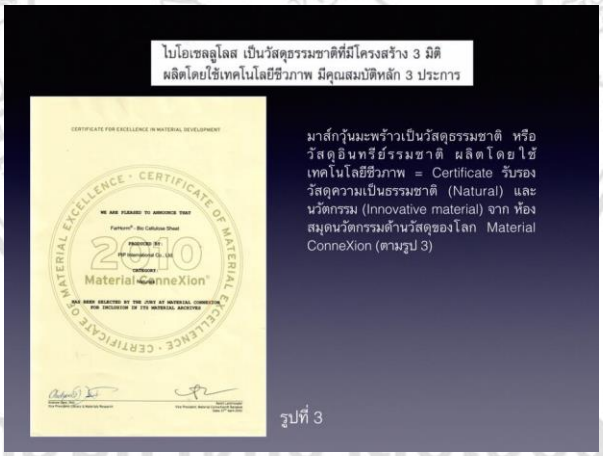

Figure 3.13: The certificate of natural and innovative material (a coconut sheet)

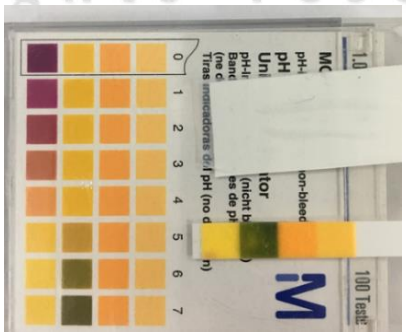

Figure 3.14: pH value of the bio-cellulose sheet

3.3.2.2 Several types of natural membranes

There are four types of natural membranes using for face mask including the face lotion sheet (pulp: A), paper face mask (cotton: B), mask 3D (rayon: C), and this bio-cellulose mask (bacteria: D) as shown in Figure 3.15.

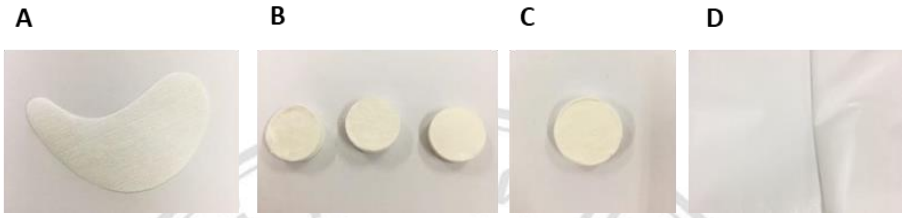

Figure 3.15: The different forms of natural membranes as masks

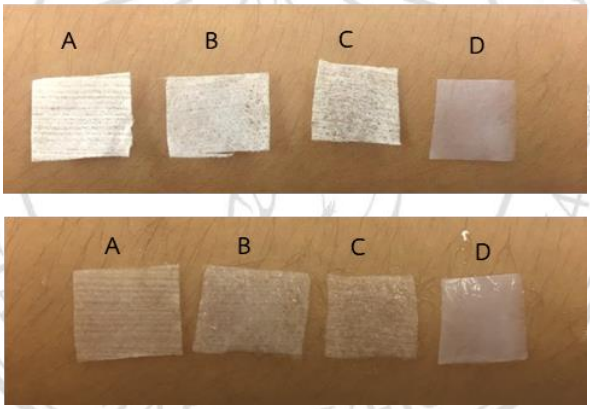

Figure 3.16: The membranes contacting with human skin in the dry condition (above), the wet condition (below)

It is noticed (Figure 3.16) that the flexibility of bacterial fiber was higher than that of natural or synthetic plant fiber (pulp, cotton, rayon). Also, this material can be directly exposed to human skin; therefore, it could be used for chemical analysis with the functional sensor. These properties are related to the inner structure of the membrane as illustrated in Figure 3.17. It can be explained that the bacterial fiber exhibits a delicate and pure structure, compared with the plate fiber, receiving better tensile modulus [72]. In addition, % moisture content ratio from bacterial cellulose was more than that of others (Figure 3.17, Table 3.3).

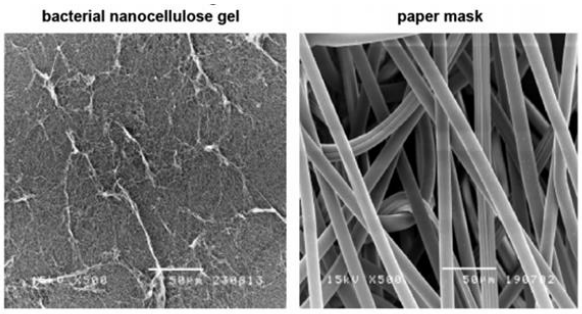

	Tensile modulus (N/mm^2)		Elongation (%)	
	Dry	Wet	Dry	Wet
Silk sericin-releasing bacterial nanocellulose gel	30.84 ± 6.99*	11.23 ± 1.26*	32.89 ± 11.89	67.03 ± 5.72*
Commercial available paper mask	0.86 ± 0.22	0.87 ± 0.05	21.88 ± 8.09	26.9 ± 4.38

*, $p < 0.05$ significant against the value of commercial available paper mask at corresponding condition.

Figure 3.17: The physical appearance of cellulose membranes [73]

Table 3.3: The moisture content ratio of the membrane: %moisture content ratio = (W_{wet} – W_{dry})/ W_{wet} × 100

The mask types	Detail	The weight of membrane [g]/piece					Average±SD
		1	2	3	4	5	
1.1	Wet	0.0589	0.0679	0.0797	0.0660	0.0724	
	Dry	0.0106	0.0106	0.0105	0.0094	0.0098	
	%moisture	82	84	87	86	86	
		6	7	8	9	10	
	Wet	0.0736	0.0749	0.0653	0.0627	0.0504	
	Dry	0.0109	0.0107	0.0093	0.0097	0.0086	$\bar{X}$±SD =
	%moisture	85	86	86	85	83	85±1.53
1.2	Wet	0.0394	0.0538	0.0578	0.0542	0.0534	
	Dry	0.0078	0.0068	0.0080	0.0073	0.0078	
	%moisture	80	87	86	87	85	
		6	7	8	9	10	
	Wet	0.0636	0.0594	0.0546	0.0503	0.0506	
	Dry	0.0090	0.0095	0.0080	0.0080	0.0073	$\bar{X}$±SD =
	%moisture	86	84	85	84	86	85±1.98
1.3	Wet	0.0379	0.0364	0.0419	0.0379	0.0423	
	Dry	0.0057	0.0058	0.0070	0.0068	0.0071	
	%moisture	85	84	83	82	83	
		6	7	8	9	10	
	Wet	0.0456	0.0360	0.0421	0.0504	0.0406	
	Dry	0.0069	0.0067	0.0063	0.0069	0.0063	$\bar{X}$±SD =
	%moisture	85	81	85	86	84	84±1.49
1.4	%moisture (from the previous results (3.3.1.2))						$\bar{X}$±SD = 99±0.2

3.3.2.3 The fabrication of the proposed membrane sensor

These membranes were cut into small pieces as shown in Figure 3.18 which the rectangular shape is the suitable pattern for further experiment. Considering the benefit of this material membrane resulting in the propose of this work, bio-cellulose was chosen to absorb the sample solution to react with a chemical reagent coated on a filter paper. After that, the red dye solution (4 mg/ml) was dropped to these bio-cellulose pieces as presented in Figure 3.19. The reproducibility measurement by the color intensity was done (Red: %RSD 1.45, Green: %RSD 5.65, Blue: %RSD 7.66), resulting in the acceptable range, not over 10%RSD. Due to the limitation of cutting membrane in other shapes, a filter paper should be an alternative choice of a reaction zone. Therefore, the research approach was demonstrated by having a newly the prepared membrane as a material as sample preparation and the reaction for detection with reagent solution on filter paper as a detection zone. The preliminary experiment was studied to check the possibility of this sensor; dropping the dye solution to the bio-cellulose sheet was transferred to a filter paper. After 10 min, the product picture was taken (see Figure 3.20). The bio-cellulose membrane can be used together with a filter paper as both have the cellulose structure in providing hydrophilic property.

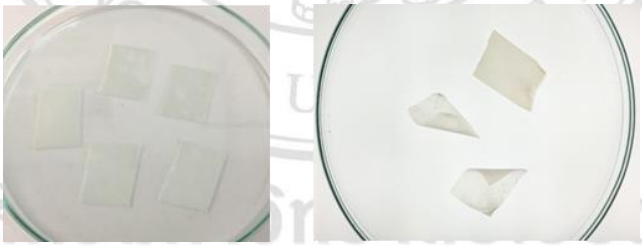

Figure 3.18: The small sheet of bio-cellulose membrane captured in the general environment (left), in the controlling box (right)

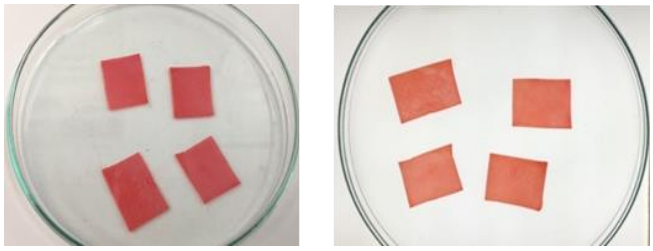

Figure 3.19: The bio-cellulose membrane absorbed with red dye solution

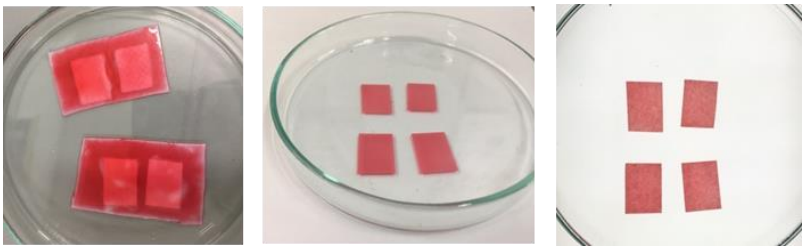

Figure 3.20: The filter paper absorbed with red dye solution via the cellulose membrane

3.3.3 pH determination

3.3.3.1 The possibility of downscaling on pH reaction

The 96 well-plate was chosen for a preliminary study in terms of the possibility of downscaling on pH reaction using universal reagent, reacting with standard buffer solution pH = 4 (measured by a pH meter) as shown in Figure 3.21. The results revealed the suitable ratio based on 200:50 µl because of the clear color and regardless of the excessive use of substances (Figure 3.21).

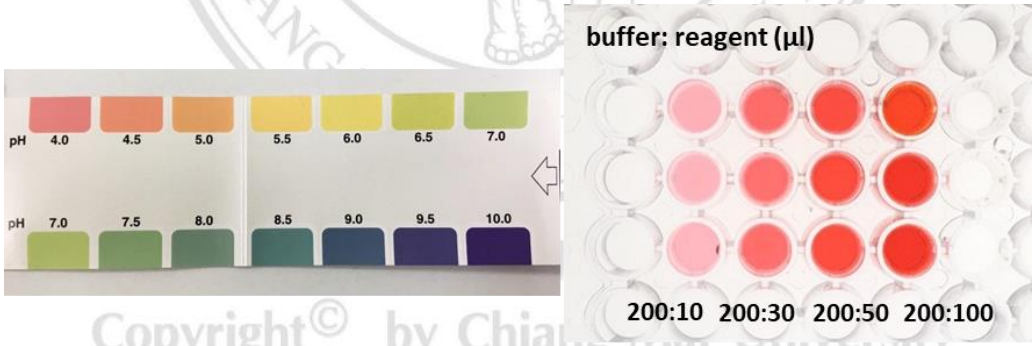

Figure 3.21: The standard color chart of pH determination (left), the ratio of buffer solution and universal indicator (right)

After selecting the suitable condition ratio of a reagent, the different pH buffer solutions were prepared to standardize the unique color for a pH characterization. The color result as shown in Figure 3.22 was properly distinguished based on the different pH buffer similarly with the standard color. It can be concluded that pH assay is probably measured by the downscaling method.

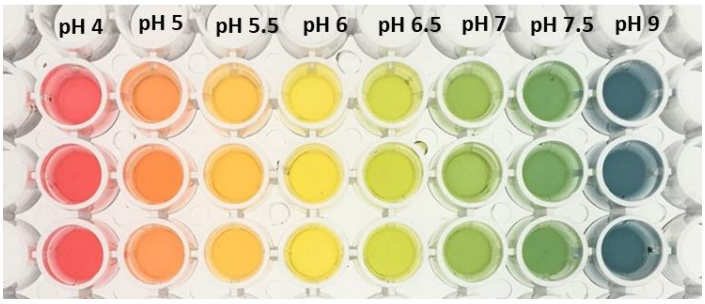

Figure 3.22: The standard color of pH determination using a universal indicator

3.3.3.2 The fabrication of the proposed sensor for pH measurement using a universal indicator

Study the ratio between a standard buffer solution and a universal reagent on a filter paper was done. Several ratios of the buffer solution pH 4 and a universal reagent were performed on a filter paper (8 mm diameter) number 1. It can be concluded that the best ratio was 10:5 µl since the benchmark color was obtained with less reagent quantity (Figure 3.23). Interestingly, when the universal reagent 5 µl was used to react with more buffer volume, the color was remained stable verifying the suitable choice of reagent ratio in terms of the bio-cellulose sensor. The obtained color from buffer solution at different pH values was presented in Figure 3.24.

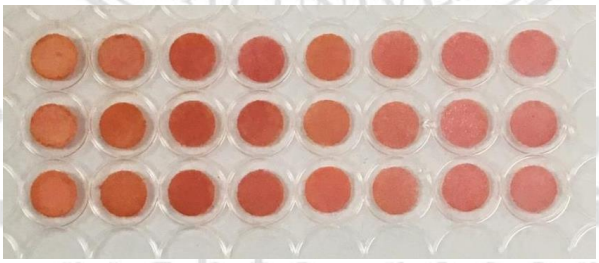

Figure 3.23: The ratio of buffer solution: a universal indicator from left to right: 2:10 µl, 5:10 µl, 10:10 µl, 20:10 µl, 5:5 µl, 10:5 µl**,** 15:5 µl**,** 20:5 µl

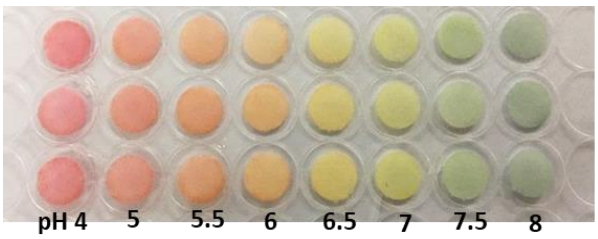

Figure 3.24: The obtained color from the different pH buffer based on a filter paper

The possibility of chemical sensors based on bio-cellulose and filter paper was demonstrated by flowing sample solution pass through the bio-cellulose membrane (sample preparation) and then reacted with the reagent covered on a filter paper (detection zone), occurring the diagram presented as Figure 3.25, more details shown in experimental part (section 3.2.2)

It can be mentioned that the color intensity from the proposed device was weaker than the filter paper, but the trend of the color change following the different pH values of buffer solutions was still the same. This is why the expected sensor can possibly apply to pH determination.

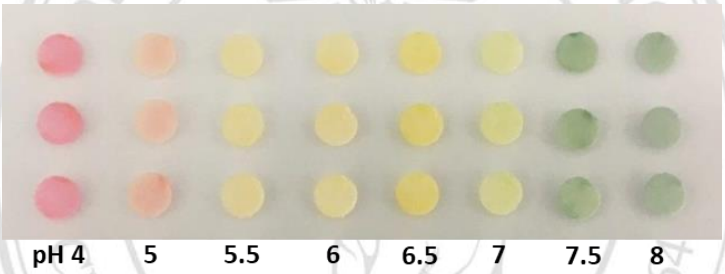

Figure 3.25: pH determination based on the proposed sensor with a universal indicator

3.3.3.3 The fabrication of the proposed sensor for pH measurement using the butterfly pea reagent (BP)

An alternative reagent for pH assay was considered on extracting a butterfly pea flower. The 96 well-plate was chosen for the preliminary study on the possibility of downscaling in terms of pH reaction by BP reagent, reacting with standard buffer solution (evaluated by pH meter) in the ratio of 200:50 µl as shown in Figure 3.26. The color result was fairly distinguished based on the different pH buffer, agreed with the result via dropping solution on a filter paper as shown in Figure 3.27. Therefore, pH assay can be measured by a downscaling method with the natural reagent (BP extraction) as an alternative way.

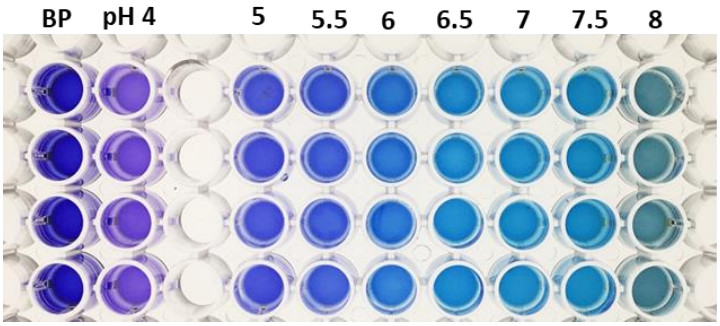

Figure 3.26: The standard color of pH determination using the BP reagent

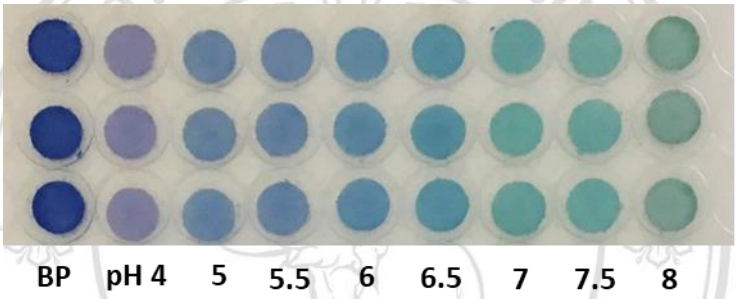

Figure 3.27: The obtained color from the different pH buffer based on a filter paper

After that, the fabrication of chemical membrane sensors based on bio-cellulose and a filter paper was demonstrated by flowing a sample solution pass through the bio-cellulose membrane (sample preparation) and then reacted with the reagent covered on a filter paper (detection zone), as illustrated in Figure 3.28.

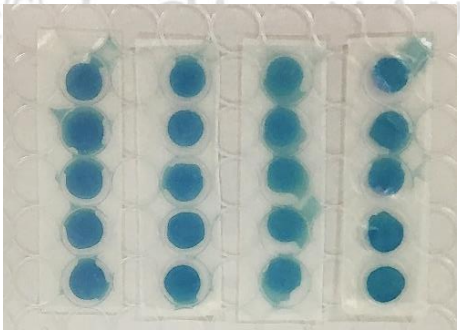

Figure 3.28: The mixture of the buffer and BP reagent based on bio-cellulose membrane

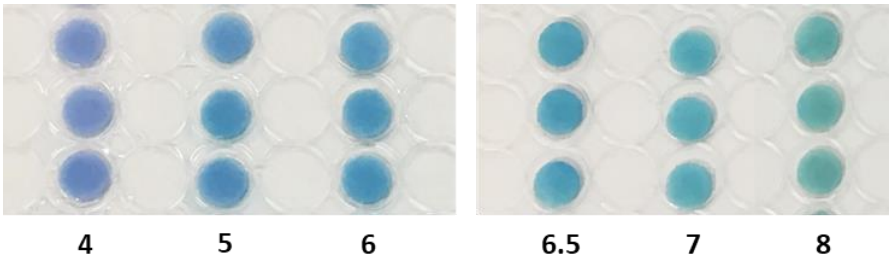

Figure 3.29: pH determination based on the proposed sensor with BP reagent

It can be mentioned (Figure 3.29) that the color intensity from the proposed device was not dramatically different from the well-plate system previously. Although this natural reagent from extracting the butterfly pea can be used for pH measurement, the universal reagent provided a better result, clear separation. Therefore, this natural reagent should be used as an alternative method.

3.3.4 Glucose determination

3.3.4.1 The possibility of downscaling on a glucose reaction

From the proposed sensor which tested with pH detection, another chemical analysis (glucose determination) is also focused on. Numerous mechanisms in the introduction part were concentrated (Figure 3.1); however, one of them did not fit with this cellulose sensor because of the complex color is brown (Figure 3.1B), difficult to evaluate by RGB system. The mechanism that related to form the red product via glucose oxidase and anisidine (substrate) was investigated as below. The chemical reagents were shown in the experimental part in chapter 2 (section 2.2.3, mix reagents 1), which initiated the red complex on a well-plate by the ratio of glucose: GOD: mix reagent 1 = 1:1:5, standard glucose: 0-1 mM (Figure 3.30A-B), 0-20 mM (Figure 3.30C).

It can be seen that this reaction can apply to determine the glucose value based on changing the red color by means of increasing glucose quantity (Figure 3.30). Unfortunately, p-anisidine is quite high toxic and do not be a good candidate for on-site analysis where a safe hood does not include.

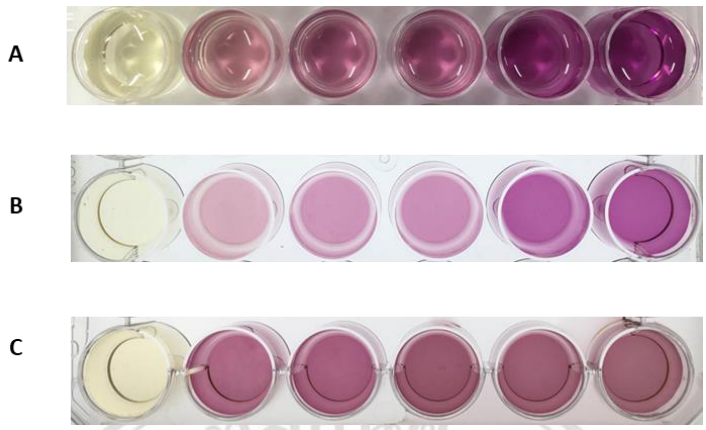

Figure 3.30: Glucose determination on the well-plate: 0-10 mM (outside the controlling box (A), inside the controlling box (B)), 0-20 mM (C)

Another mechanism is based on glucose oxidase, horseradish peroxidase and TMB (substrate). There are some solutions which illustrated in the experimental chapter 2 section 2.2.3 (mix reagents 2). The blue complex was appeared on well-plate by the ratio of glucose: GOD: HRP: buffer: TMB = 80: 10: 10: 40: 250 µl, standard glucose: 0-20 mM. The well-plate platform was chosen for testing a downscaling analysis in glucose assay (figure 3.31). The result revealed the good trend between the color intensity and the sample concentration in the range of 0-10 mM glucose (Figure 3.32). That why this concentration range should be selected for the proposed sensor.

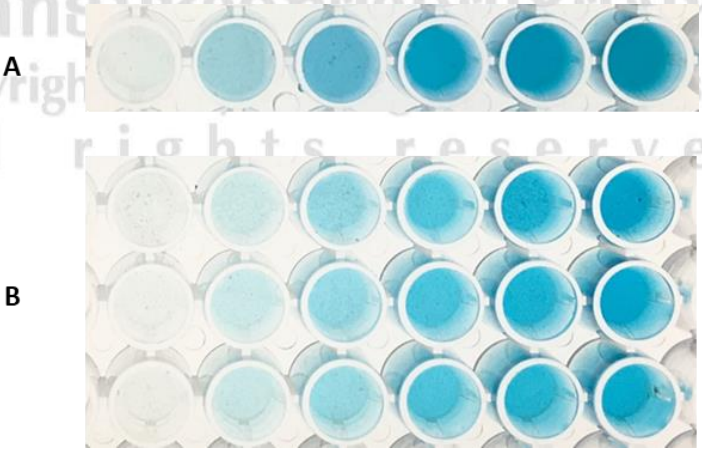

Figure 3.31: Glucose determination using the 96 well-plate: 0-20 mM (A), 0-10 mM (B)

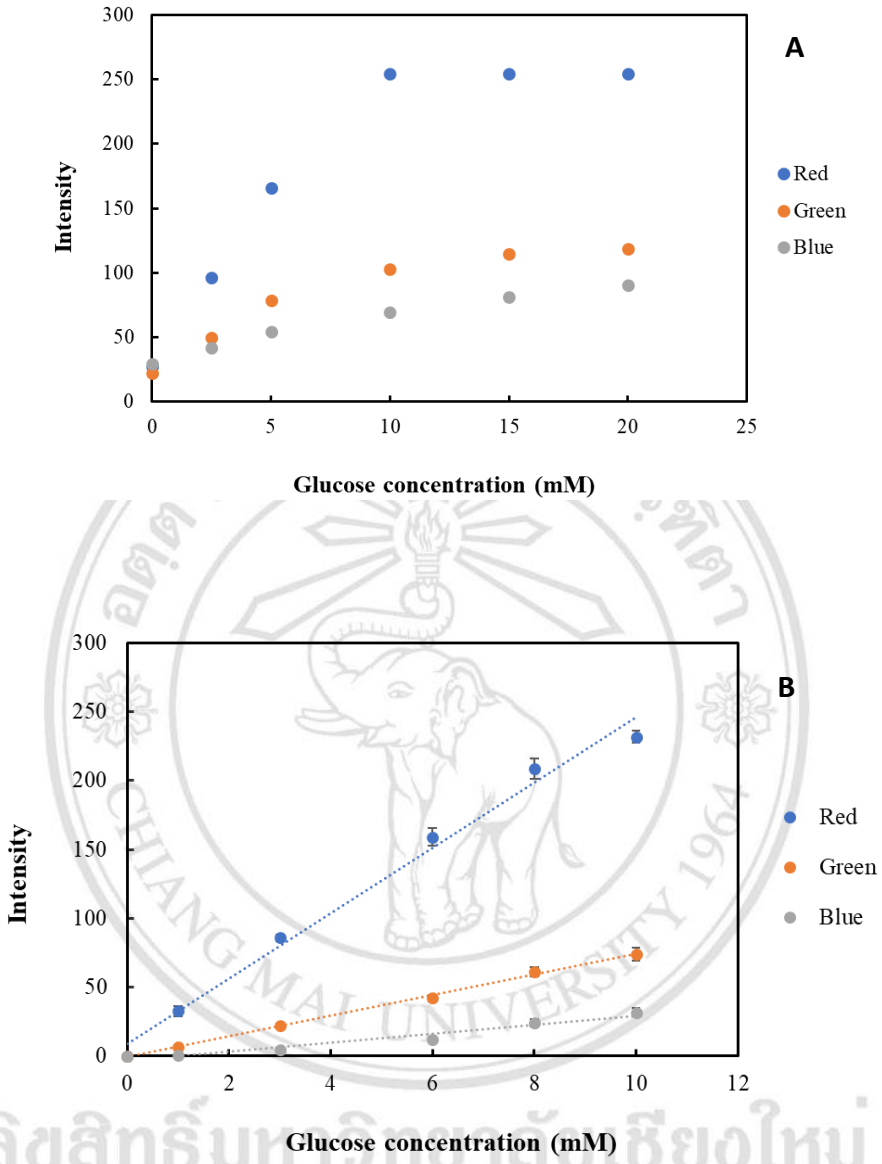

Figure 3.32: A calibration graph of glucose determination using the well plate: 0-20 mM (A), 0-10 mM (B)

3.3.4.2 The fabrication of the tiny sensor for glucose assay

After that, the possibility of chemical sensors based on bio-cellulose and a filter paper was demonstrated, a similar procedure with the previous experiment (pH measurement) as shown in Figure 3.33. In the experimental part, some solutions were required following the experimental part. It can be noticed that glucose measurement (0-10 mM) can be done via the red or gray intensity. A calibration graph between the red

intensity and the standard glucose concentration was plotted providing good linearity and correlation (Figure 3.34-3.35). The limit of detection of this biodegradable sensor was 0.56 mM, 3×SD of the blank solution.

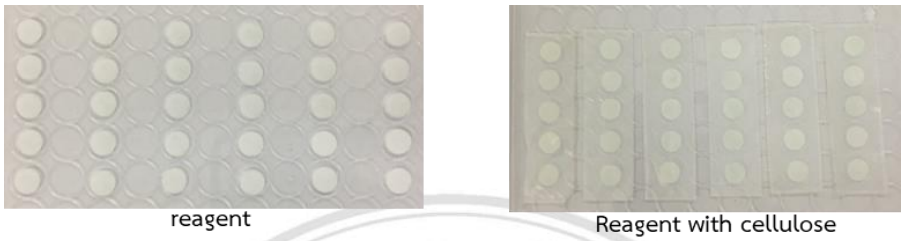

Figure 3.33: The glucose sensor diagram of the bio-cellulose and a filter paper

Figure 3.34: The glucose assay of 0-20 mM glucose based on the cellulose sensor (A), 0-10 mM glucose (B)

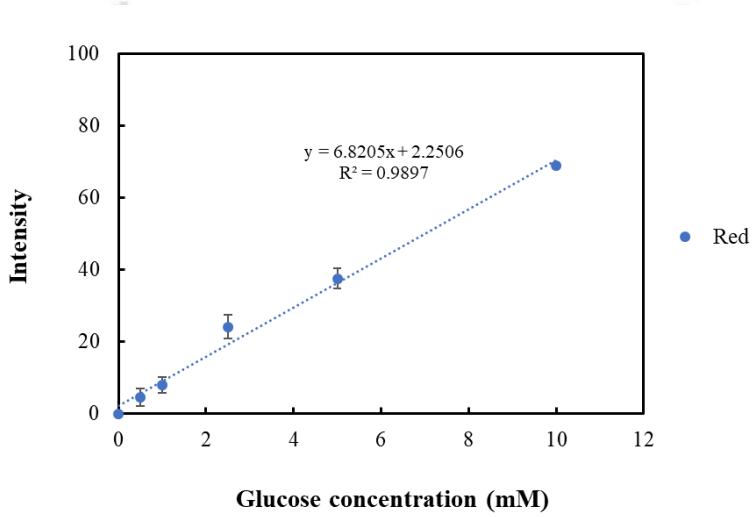

Figure 3.35: A calibration graph for glucose measurement using the bio-cellulose sensor

3.3.5 The health related application

The possibility of this bio-cellulose membrane as a portable sensor in analytical chemistry was an alternative way to apply for health related samples (food and artificial sweat). Some standard methods were selected for pH and glucose analysis as mentioned in the appendix.

3.3.5.1 Glucose analysis of healthy beverages

The calculated value was based on the standard calibration, which used ImageJ program for RGB measurement. It can be found that the glucose values of samples 1-6 were 0 mM, 0 mM, 4.0 ± 1.6 mM (not dilute), < LOD, 1.8 ± 2.0 mM (not dilute), and 0 mM (Figure 3.36).

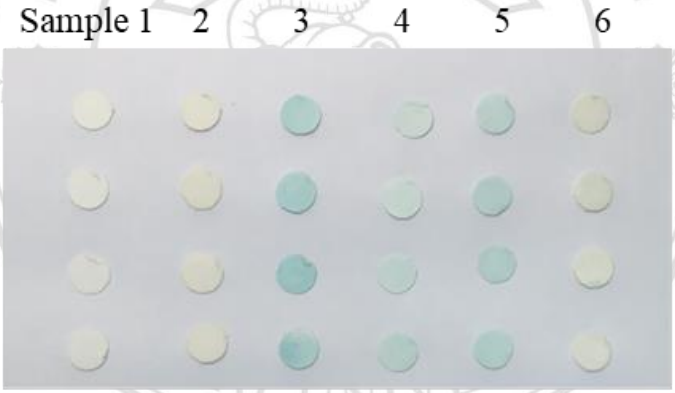

Figure 3.36: Glucose determination of real samples (1-6) via the bio-cellulose sensor

3.3.5.2 pH and glucose analysis of the artificial sweat: sample 7-10

Artificial samples (7-10) were prepared by following the protocol in chapter 2 and then tested of pH value and the glucose content. Comparing to the standard chart of pH via the universal and butterfly pea reagent, the pH values of samples 7-10 were estimated (Figure 3.37) that were 7.0-7.5, 7.0-7.5, 4.0-5.5, 4.0-5.0 (universal reagent), and 7.0-8.0, 7.0-8.0, 4.0-5.0, and 4.0-5.0 (natural reagent).

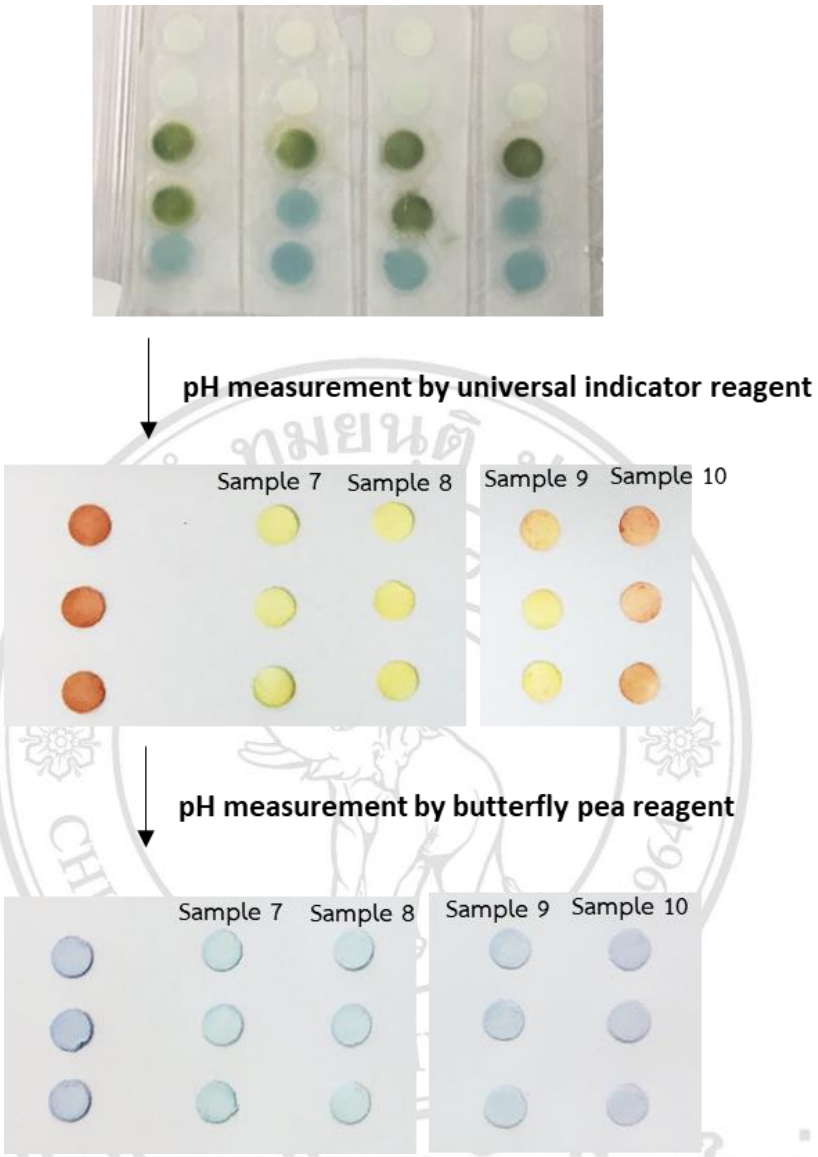

Figure 3.37: pH analysis of real samples (7-10) via the bio-cellulose sensor

After that, the calculated glucose value was based on the standard calibration previously, with ImageJ program for RGB measurement. It can be found that glucose values of samples 7-10 were 4.7 ± 0.8 mM, 7.7 ± 0.1 mM, 4.8 ± 0.9 mM, and 7.4 ± 0.3 mM respectively (Figure 3.38).

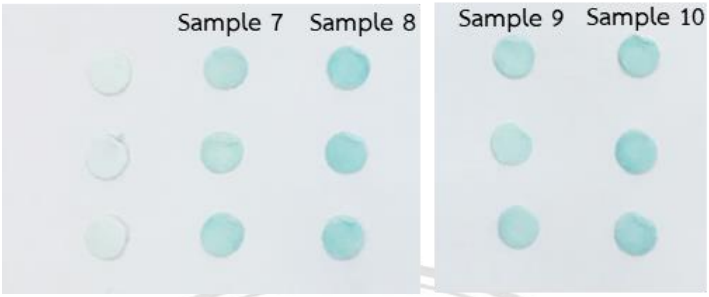

Figure 3.38: Glucose analysis of real samples (7-10) via the bio-cellulose sensor

3.3.5.3 Comparing results between the proposed method and standard techniques

From the experiments (section 3.3.5), the glucose quality in normal and healthy beverages (sample 1-6) were measured by the developed cellulose platform comparing to glucose machine and spectrophotometry. It can be summarized that the proposed sensors provided the glucose concentration almost similarly to all standard methods (Table 3.4). Therefore, this can be a valuable way for diabetic patients or people who concern their obese state. Apart from the food samples, the goal to fabricate wearable sensors is promising. The preliminary step to apply for human biofluid was based on the artificial sweat. Considering some markers in health issue, pH is often considered physiologic health (hydration state) and glucose is also an important marker to diagnose hyperglycemia. It should be noticed that pH and glucose in the artificial sweat via developed sensor compared with all standard methods did not have significant differences. This should be a good guidance to improve this sensor for real- time monitoring in the human body.

Table 3.4: pH and glucose values measured by the proposed sensor compared to standard methods

Samples	pH analysis			Glucose analysis (mM)		
	pH meter	pH strip	This system	Glucose machine	Spectro-photometry	This system
1	ne	ne	ne	ER*	nd	nd
2	ne	ne	ne	nd	nd	nd
3	ne	ne	ne	4.00	4.60±0.01	4.0±1.6
4	ne	ne	ne	nd	nd	nd
5	ne	ne	ne	1.44	1.43±0.01	1.8±2.0
6	ne	ne	ne	ER*	nd	nd
7	7.50	7.5	7.2 / 7.5**	4.88	4.74±0.01	4.7±0.8
8	7.22	7.3	7.0 / 7.0	7.94	8.31±0.02	7.7±0.5
9	4.53	4.5	5.2 / 5.0	5.22	5.01±0.68	4.8±0.9
10	4.05	4.0	5.0 / 4.5	7.50	8.32±0.37	7.4±0.3

ER* = ERROR statement shown (The machine did not show any values)

X/Y** = pH value via universal indicator / natural reagent

ne = no experiment performed

nd = not detection

3.4 Conclusion

The bio-cellulose membrane using bacteria strain has been launched as a chemical sensor with a mobile phone. This membrane purposes for the sample solution flowing whereas the paper immobilized with reagents for a chemical reaction. The performance of the proposed membrane sensor was acceptable and showed no need for sample pretreatment. In our attempt to determine some markers in healthy foods and the artificial sweat, pH and glucose determination were illustrated. The results from real samples have a good agreement with the standard method. The main feature of this approach is a low-cost and quite functional sensor (high adsorption capacity, low toxicity, flexible membrane, small size, and sample solution reduction) apparently for the chemical application. This developed membrane sensors should be promising to behave as a wearable sensor for further monitoring with human skin (the real-time monitoring).

CHAPTER 4

Chemical sensor employing plant-cellulose based membrane

The natural membranes are recently interested in a chemical sensing according to green analysis. These platforms can be demonstrated from plant resources: the cotton thread and paper material. The cellulose structure was deeply described in Chapter3. Thread as a microfluidic behavior without the complicated channels fabrication was chosen for the solution delivery without sample preparation which most researchers had emphasized in low-cost clinical diagnostic.

In this section, the use of these membrane materials combined together into chemical sensor provides separation and detection areas. Several applicable fields are illustrated including heavy metals (Cd, Cu), and antioxidant (polyphenol) determination.

4.1 Introduction

Microfluidic platforms and chemical sensors have recently been of much interest. Several types of materials and their applications have been investigated in various approaches. Apart from paper material, the cotton thread which is another cellulose based material has also gained interest in the purposes as being cost-effective by itself. Their channel fabrication required no sophisticated instrumentation and a clean room. Recently, the concept of cellulose based analytical devices was originated by the Whitesides group in 2007 presenting a type of porous cellulose paper for diagnostics. Glucose and protein assays were measured in a short time [73]. After that, many researchers have developed many types of cellulose-based analytical sensors with excellent performance because of their advantages such as lightness, low-cost, disposable device, and reagent transport. For instance, thread based sensors were applied in environmental science and point-of-care diagnosis. In the most developing countries, laboratory diagnosis was instituted at a center part of the country affected the difficult determination of samples in isolated rural areas. Therefore, the diagnosis application by analyzing the biological measurements including

malaria, HIV, nitrite ion, uric acid was done by thread based sensors [74-76]. Another alternative material was noodle based system which can be a new analytical platform for the copper determination with self-indicator property [77].

Heavy metal ions are considered as the most toxic and carcinogenic pollutants [78]; some of them in drinking water cause vital diseases. As the rapid growth of industrial development, the metal ions are highly contaminated into the water causing to drinking and agriculture purposed water. The recent report explained that the cadmium (Cd^{2+}) quantity is linked to cardiovascular diseases and also involved in prostate, liver, and lung cancers. Other metal ions (Cu^{2+}, Co^{2+}) are also toxic based on receiving the excess dose that why the determination of these heavy metals is important. Colorimetry becomes a choice for metal ions determination, commonly used a chromogenic reagent (4-(pyridyl-2-azo)-resorcinol (PAR)). Complex products between metal ions and PAR absorbed in the range of 410-530 nm [79-80]. There were reported on the determination of metal ions by using 4-(pyridyl-2-azo)-resorcinol (PAR) reagent [81-843].

The phenolic compounds in several plants are vital substances which scavenge and quench free radical reactions, causing oxidative damage (cancer). One of the methods for the total phenolic content assay refers to Folin-Ciocalteu method which involves the reactions of Mo (VI) and Mo (V) compounds via the yellow-blue color change [84, 85]. Various in vitro colorimetric methods are commonly available used for the evaluation of antioxidant capacity including that employing 2,2′-Azino-bis(3-ethylbenzothiazoline-6-sulfonic acid) (ABTS), 2,2-diphenyl-1-picrylhydrazyl (DPPH), and hydroxyl radical scavenging activity [86]. Among those, DPPH is the most popular one for screening. DPPH is a stable free radical that can accept an electron or hydrogen radical to become a stable diamagnetic molecule. The value of IC_{50} defined as the concentration of substrate that causes 50% loss of the DPPH color [87, 88]. The total phenolic content exhibited a strong correlation with DPPH• scavenging activity [89, 90].

4.2 Experimental procedures

4.2.1 The cotton thread combining paper based platform

The cotton thread was obtained from Chom Thong community enterprise, Chiang Mai, Thailand, approximately 0.3 mm diameter using a webcam camera and a ruler. The cotton line is are made up of ~200 fibers, approximately 13±2 µm (n=10) of each fiber's branch-wide. The cotton thread was treated to improve hydrophilic behavior by a modified mercerization method based on soaking this material with 20%NaOH for 5 min. The fibers were then rinsed with DI water and neutralized with hydrochloric acid before putting in a desiccator for drying under the conditions similar in previously reported [91]. For quantitative analysis, cotton thread bunches stuck on a plastic sheet could serve as a channel for a solution to flow due to microfluidic behaviors. The solution migrates along the cotton thread and then reaches a reagent on paper pieces.

4.2.2 Comparing the behavior of cellulose materials

For thread-based device, as shown in Figure 4.4, each cotton line (10 cm per line) was attached on a plastic sheet using transparent tape. Then, SDS solutions, 0 to 5000 mg/L, were added to a container in a volume of 300 µl. To begin, pieces of cotton on plastic material were dipped into a container for 20 minutes. Different concentrations of SDS penetrated on the cotton thread with different distances. Then, a mobile phone camera was used as a detector to take a picture and link the information to a program of distance's evaluation (ImageJ).

4.2.3 Metal ions determination

For three metals assay (Cu^{2+}, Cd^{2+}, Co^{2+}), the rectangular paper (1.5×1.0 cm) has been immobilized with the PAR reagent before the experiment. Then, cotton lines were dipped into the sample container (300 µl) and this solution was reacted with prepared reagent (0.001 M PAR) on paper (Figure 4.1). The reaction can be obtained on the cotton membrane. Mobile phone camera was used as a detector to take a picture and link the information to a program of color evaluation (ImageJ).

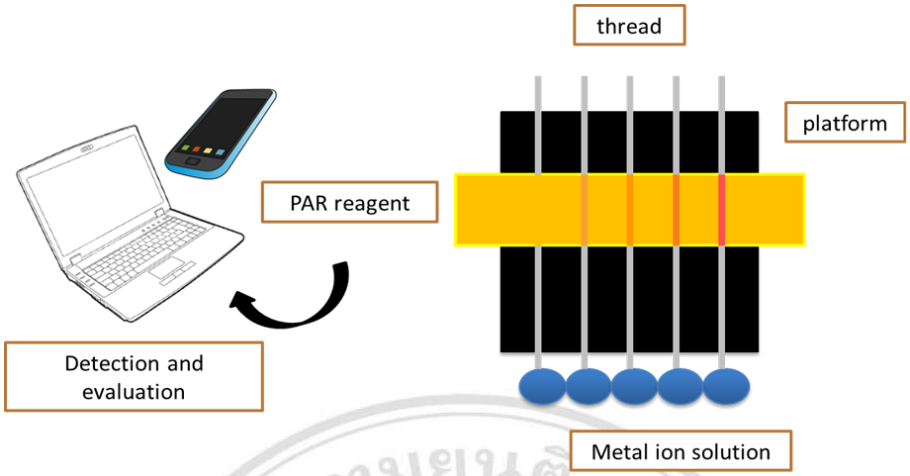

Figure 4.1: Metal ions determination using the thread based platform

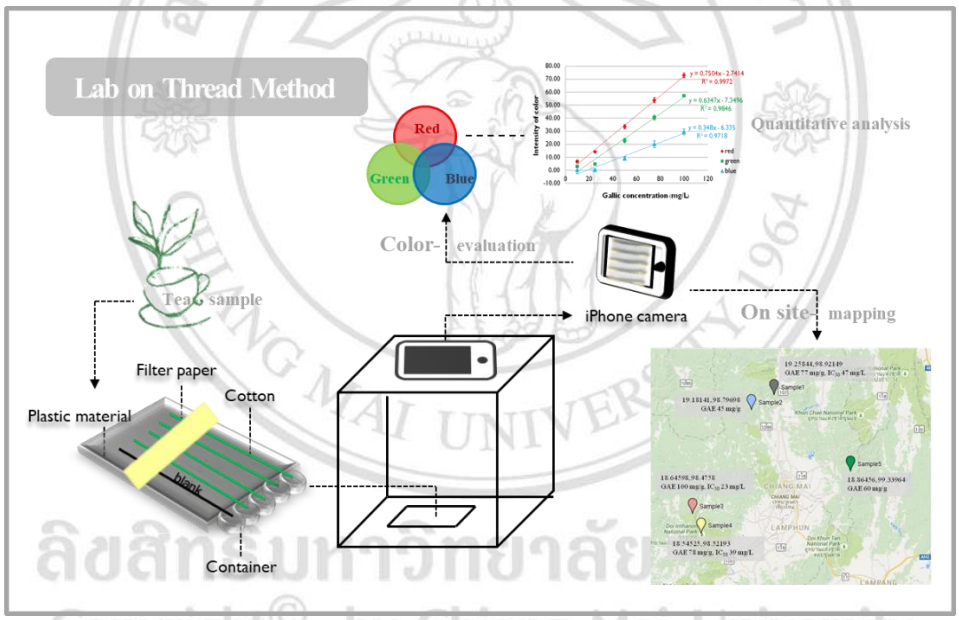

Figure 4.2: Graphical diagram of antioxidant assay via the cellulose based sensor

4.2.4 Antioxidant determination

Similar to the measurement of metals, two platform types were used: one for the total phenolic content and another for antioxidant capacity (Figure 4.2). For the total phenolic content assay, the paper band (1.5×10 cm) has been immobilized with the Folin-Ciocalteu reagent (0.20 M), just before an experiment. Cottons on a plastic sheet were dipped into the sample container (300 µl), then reacted with Folin reagent (0.20 mol/l)

covered on all cotton lines. The reaction can be observed on the cotton thread in 10 minutes. After taking the paper band out of the platform, the cotton thread is placed on a position marked in the light control box for taking photos with mobile phone camera fixed on top of the box. For the DPPH assay, the DPPH reagents (0.06 M) immobilized on the paper strip (1.5×1.0 cm) is fixed at the end of each thread. The cottons on plastic were dipped into the sample container (300 µl). The reaction can be observed on the paper strip after 60 minutes. The paper strip is taken out of the platform and put onto the position marked in the light control box for photos taking. Then this photo was linked to a program of color evaluation (ImageJ).

4.3 Results and discussion

4.3.1 The behavior of cotton thread and paper material

Cellulose materials from plants have been realized and chosen as a membrane platform for microfluidic sensors without external pumping. The behavior of both cellulose materials was quite similar in basic investigation, hydrophilic property, and the main chemical structure. Apart from that chemical property was studies based on several effects. The separation efficiency is one of the important properties in analytical chemistry. The separation behavior on cellulose based platform is significantly focused by some researches [14-15].

According to the preliminary experiment in terms of chromatography manner (Figure 4.3), three types of materials (thread, filter paper, strip filter paper) were chosen to separate the dyes standard and real dyes in drinking product.

From the result, the polarity of mobile phase solvent and cellulose material are an important factor to distinct the dye colors. Some dye colors can be clearly separated due to the separating property of the sample is influenced by the solubility in a mobile phase based on ‘like dissolve like’ theory. However, the suitable mobile phase of thread material differed from the paper filter due to the capillary force, porous and surface tension effect from material confirming by Washburn’s equation [17]. Additionally, the mixed color including blue, light yellow, green and red was divided into three parts involved blue, red and yellow. The behavior of conventional paper was different among a strip paper and cotton thread. Therefore, the separation ability on the conventional filter paper (two

zones) was lower than a strip paper and cotton thread which can separate clearly in three zones. Therefore, cotton thread is also a suitable material for downscaling chromatography similar to strip paper, and better separation in the mixed solution.

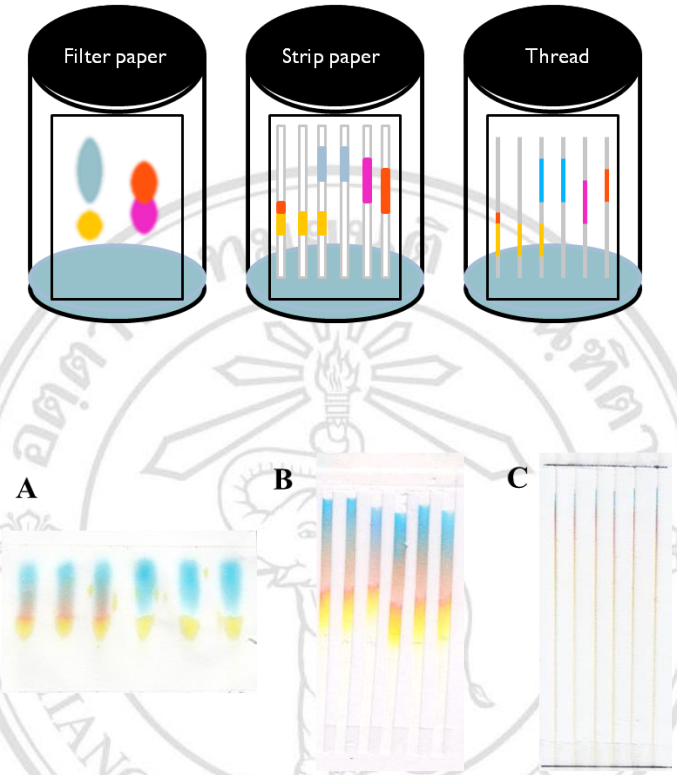

Figure 4.3: Imitated picture of chromatography experiment (above), the separation of mixed dyes solution using a filter paper (A), strip paper (B) and cotton thread (C)

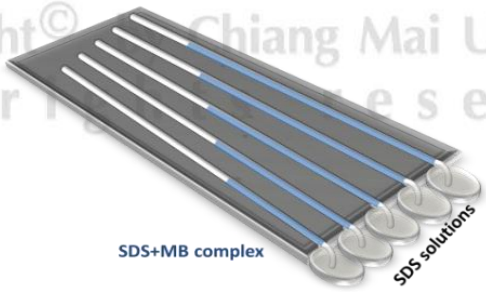

Figure 4.4: Imitated picture of solventless extraction on the thread based system

In addition, these materials (filter paper and cotton thread) were used to clarify the separation of anionic surfactant (SDS: sodium dodecyl sulfate) solution [92]. Thread

based system was able to separate the distances of the different SDS concentration in the range of 1,000-5,000 ppm while filter paper cannot be used to separate different SDS quantity due to the property of the material (Figure 4.4). Basic downscaling of solvent extraction was studied. The part of this cotton thread containing anionic surfactant could be seen blue when threated with methylene blue while the part without anionic surfactant showed no blue color. The results expressed that the increasing of SDS concentrations was directly related to solution flow distances. The calibration curve can be plotted in the range of 0.1-100 ppm. That is why cotton thread based analytical device can be used for the assay of anionic surfactant without using an organic solvent in microliter level.

4.3.2 The chemical reaction: heavy metals determination

According to a preliminary study about the property of natural materials used our membrane sensors (section 4.3.1), they were expected to demonstrate device for the chemical analysis. Metals measurement was fabricated basically which some metal ions (Co^{2+}, Cd^{2+}, and Cu^{2+}) can react with PAR reagent to form a complex generating the color change from a yellow color to others [93].

4.3.2.1 Colorimetric reaction between PAR and metals solution

Preliminary study in well-plate was done in the same concept of down scaling chemical analysis as our proposed sensor. The ratio of PAR and metal was 200 µl: 200 µl, which their concentrations were shown in the experimental chapter 2 (section 2.3.5). From the result, the intensity of color complex increased following by increasing the metal quantity (Figure 4.5). A calibration curve of each metal ion can be plotted; however, the suitable range of metal concentration should be more studied. Moreover, the different metal including Co^{2+}, Cu^{2+}, and Cd^{2+} had their own color shade, although the little different color was found between Co^{2+} and Cd^{2+}.

4.3.2.2 Quantitative analysis using the proposed sensor

The set-up of this cellulose based platform as illustrated in Figure 4.6, was initiated following the step from the experimental procedure 4.2.3. First of all, Co^{2+} was chosen to be a model study for metal ion determination on the cotton material. It was

clearly seen that the intensity of color related to the metal ion concentration (0-100 ppm), noticed similarly to the well-plate system.

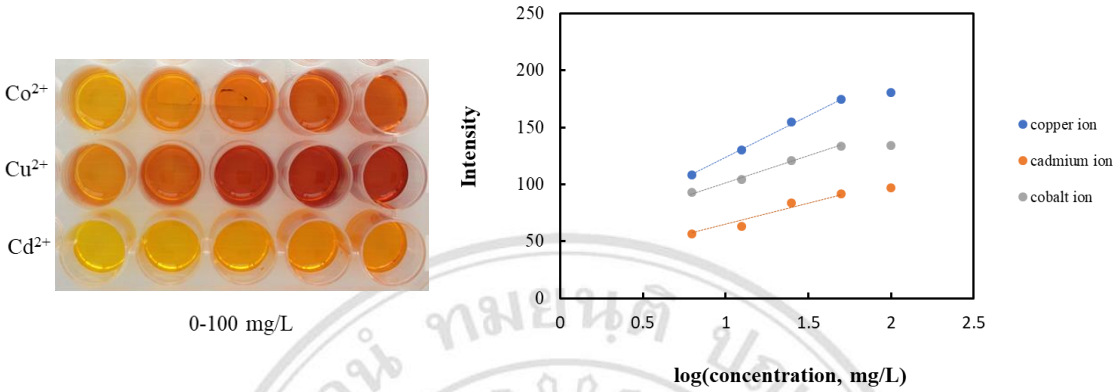

Figure 4.5: The metal ions and PAR reaction

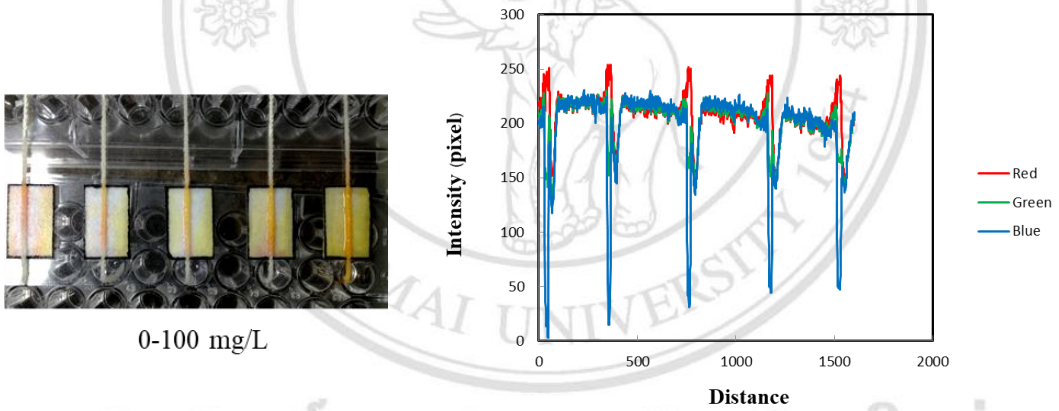

Figure 4.6: The reaction of metal ion (Co^{2+}) and PAR reagent (left), the example of evaluating RGB value (right)

After that, three metal ions involving Co^{2+}, Cd^{2+}, and Cu^{2+} were reacted with PAR reagent and RGB value was used to evaluate the intensity of complex color by ImageJ program. The obtained results are shown in Figure 4.7, which the relation graph between the color intensity and metal concentration of cobalt was $y = 0.48x + 202$, $R^2 = 0.9631$, cadmium was $y = 0.57x + 187$, $R^2 = 0.9832$, and copper was $y = 0.96x + 137$, $R^2 = 0.9846$.

Metal ions determination using this cotton based platform can be available in an individual case of metal ions comparing to the color product with well-plate design. However, the mixed metal ions cannot be applied due to the color shade of complex between Co^{2+} and Cd^{2+} and the proper range of concentration which should be more suitable. Recently, this experiment can be a good model study and useful results for metal ions determination with the natural material platform, already improved by means of the chemometric manner (another project of our group).

Figure 4.7: The reaction of metal ions (Co^{2+}, Cd^{2+}, Cu^{2+}) and PAR reagent

4.3.3 The chemical reaction: antioxidant determination

It has been demonstrated a new thread-based microfluidic device for antioxidant assay [91]. Chemical assays were based on Folin-Ciocalteu and diphenylpicryhydrazyl (DPPH) for total polyphenol and antioxidant capacity, respectively) with some real samples (green tea). This is an approach in terms of cost-effective green chemical analysis. Folin-Ciocalteu reagent method is electron transferring which the yellow color

of Mo (VI) was changed to Mo (V) with blue color measured at 750 nm. Then, the scavenging activity was measured based on DPPH color changing from purple to yellow (517 nm). Inhibition capacity is calculated by the equation: % I = [(Io – Is)/ Io] × 100, where Is is the relative magenta intensity (CMYK mode) of the sample, and Io the relative magenta intensity of DPPH•. A mobile phone camera (iPhone 4S) was used as a simple detection with Image J or Photoshop for evaluation. A reference standard in this experiment is gallic acid, the highest polyphenol structures in numerous plants.

It can be noticed from the previous results, the appropriate platform was a multiple-lines type of the cotton material for using through this experiment since it provides the multiple samples per time assay, relative quantitative analysis, and similar matrix effect.

4.3.3.1 Quantitative analysis using a well-plate system

To more confirm the possibility of downscaling system of antioxidant assay before applying to cellulose based sensor, the well-plate analysis was investigated as shown in Figure 4.8-4.9. The increase of gallic acid concentrations was directly related to the blue color intensity, plotting a calibration curve in the range of 0-100 ppm ($y = 1.0699x – 1.8841$, $R^2 = 0.9961$). Five samples of green tea were determined the total phenolic content (Figure 4.8). This well plate system is also used for the antioxidant scavenging as the result presented in Figure 4.9. Antioxidant capacity determination is an evaluated method of the antioxidant efficiency (often found in phenolic green tea compounds) that is the capacity of inhibiting on free radical DPPH. In the evaluation sector, the color change was measured from the purple of DPPH reagent turned to yellow after reacting with antioxidant samples. Capacity value (IC_{50} value) of Tea samples were measured: the result of tea sample1 ($y = 1.2155x + 1.1487$, $R^2 = 0.9957$), tea sample2 ($y = 1.7677x + 1.0943$, $R^2 = 0.9982$), and tea sample3 ($y = 1.3751x + 1.0858$, $R^2 = 0.9970$). These mean that downscaling chemical analysis can be probable to moderate the antioxidant assay, leading to demonstration on the cellulose based sensor.

4.3.3.2 Quantitative analysis using the proposed sensor

The cotton thread was modified by soaking in a base solution and then neutralized with an acid solution to improve a hydrophilic property. One set of the

experiment included cotton bunches stuck on a plastic sheet (5 × 10 cm). The sample solution flowed along the cotton membrane and then reacted with the reagent on the filter paper, following the protocol in section 4.2.4 to measure the total phenolic and antioxidant capacity. The results were taken by a mobile phone camera via the light control box. The blue color intensity was referred to the total phenolic contents (Figure 4.10A). Also, the decrease of purple color to yellow was expressed as DPPH inhibition (Figure 4.10B), measuring the antioxidant capacity of each sample (IC_{50} value).

Figure 4.8: (A) The reaction of different gallic acid concentrations and Folin reagent (Gallic acid: 0, 10, 25, 50, 75, 100 mg/L, n = 3), (B) the reaction of tea samples 1 to 5 and Folin reagent comparing with a standard gallic acid

Figure 4.9: (A) The reaction of different gallic acid concentrations and DPPH (Gallic acid: 0, 25, 50, 100, 250, 500 mg/L), (B) the reaction of tea samples 1 and DPPH comparing with a standard gallic acid (one set of the experiment)

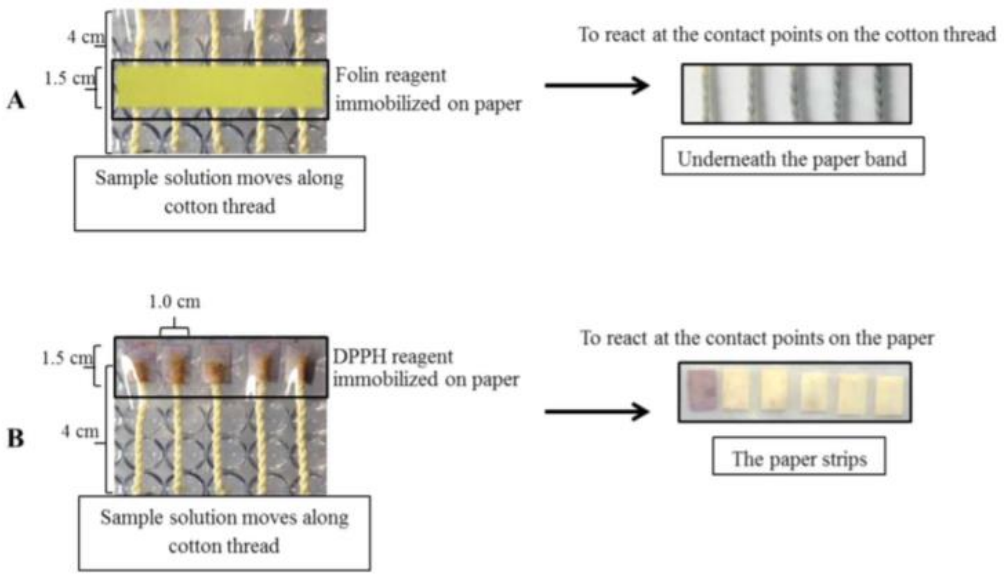

Figure 4.10: The cotton thread combining paper based platforms: (A) total phenolic content assay, (B) antioxidant capacity assay

4.3.3.3 Real sample application using the proposed sensor

The total phenolic contents in the green tea samples via cellulose based sensor were found to be 48–105 mg/g, with % RSD of less than 10 for that of higher 50 GAE mg/g and IC_{50} values of the samples studied were 25–50 mg/L. The results obtained by the developed methods agree with that of the standard methods and downscaling well-plate system Table 4.1-4.2. For mapping evaluation from the original production of tea samples, it can reveal that the total phenol and antioxidant scavenging are depended on the sort of tea, collecting procedure, and environmental characteristics of resources.

Table 4.1: Total phenolic content as GAE obtained by the developed method and that of the conventional spectrophotometric standard method and well-plate system

Tea samples	Total phenolic content (GAE; mg/g)		
	Spectrophotometry	Well-plate	Thread sensor
Tea sample1	75.8±1.5	79±8	77±4
Tea sample2	47.5±2.3	44±7	48±6
Tea sample3	104.6±1.7	100±3	103±3
Tea sample4	74.6±1.6	67±4	82±4
Tea sample5	53.7±1.2	52±3	60±4

Table 4.2: Antioxidant capacity (IC_{50} values) obtained by the proposed method and that by the conventional spectrophotometric method and well-plate system

Samples	IC_{50} of phenol substances (mg/L)		
	Spectrophotometry	Well-plate	Thread sensor
Tea sample1	48.5±0.3	40 ±1	50±2
Tea sample2	24.8±0.2	28±1	26±1
Tea sample3	34.6±0.4	36±1	32±4

The proposed sensors via cellulose based materials (thread and filter paper) have been demonstrated as an alternative method for antioxidant assay. This cost-effective green approach was developed for total phenolic content and antioxidant capacity in real tea samples by means of Folin-Ciocalteu and DPPH reagents, respectively. The bunches of cotton thread served as the sample delivery under microfluidic behaviors while the paper used as a reagent zone.

4.4 Conclusion

The chemical platforms engaging these natural membranes, cotton thread and filter paper, have been demonstrated with mobile phone regardless of complicate instrument. They can deliver the solution via microfluidic flow behavior from the capillary force and surface tension. The cotton thread bunch functions for sample solution delivery whereas the paper immobilized with reagents. These chemical sensors consisted of separation and detection part, not required any sample pretreatments. This work has established a new concept in the possibility of green analytical chemistry such as heavy metals and polyphenol determination (total phenolic content and antioxidant capacity). The developed membrane sensors should be possible for at site assay, especially being useful in some remote areas and locations with limited budget states.

CHAPTER 5

Colorimetric sensor employing ion-exchange based membrane

There is a recent requirement for seawater phosphate determination to better assess eutrophication. Today, most accepted sensing approaches are based on the established colorimetric molybdenum blue assay. It requires one to modify the sample to strongly acidic conditions and to add various reagents, principally molybdate and reducing agent (e.g. ascorbic acid), to form a blue colored phosphate complex that is subsequently detected spectrophotometrically. The associated need for large sample and mobile phase reservoirs and sample preparation, unfortunately, not ideally adapted for the development of in situ sensing instruments. It is here demonstrated for the first time that the key reagents needed to achieve phosphate detection by the molybdate method may be delivered by passive counter transport across ion-exchange membranes. A cation-exchange Donnan exclusion membrane placed in contact with a sample flow (450 μm thick) is shown to provide the strongly acidic conditions (pH~1) necessary for phosphate determination. Proton transport is driven, via cation-exchange, by the high sodium content of the seawater sample. Molybdate was similarly released through an anion-exchange membrane by chloride counter transport. Consequently, an in-line flow system containing the two membrane modules in series was used for delivering both hydrogen and molybdate ions into the sample to form the phosphomolybdate complex for subsequent spectrophotometric detection. A linear calibration graph in the range of 0.1–10 μM phosphate was achieved, which is sufficiently attractive for environmental work. A range of seawater samples was tested and the results from this membrane delivery device showed no significant differences compared to the classical molybdate assay chosen as the reference method.

5.1 Introduction [94]

Phosphate is a vital nutrient for all living organisms as it is needed for almost all essential biomolecules as well as most metabolic processes such as photosynthesis, respiration and energy delivery. It is also an important key parameter of water quality and often the limiting nutrient for the primary production in ecosystems. Excessive concentrations of phosphate are known to be harmful to environmental aquatic systems as they promote eutrophication. The monitoring and control of phosphate is urgently required for these reasons. From the late 1960s to mid 1970s, the measurement of phosphate became an important issue to allow for a better understanding of marine systems. All phosphorus forms in the environment are transformed into their inorganic forms that are transported from terrestrial to aquatic system by natural processes including wind erosion and leaching. Total phosphate arrival into open seawater has been estimated to be in the range from 9.3×10^{10} mol/year to 34×10^{10} mol/year. Phosphate concentration depends on the specific marine environment and depth. Vertical profiling of phosphate concentration in the North-East Atlantic gave concentrations below 2.5 µM. A depth profile of phosphate in the eastern Mediterranean was gave less than 0.25 µM in surface waters, but nutrient sinking increased this to 10 µM at higher depth. In another study in deep seawater (321 m depth) of Toyama Bay, Japan, a significant daily phosphate changes were observed from 0.86 to 1.98 µM.

Established techniques for phosphate determination commonly used in routine analysis include colorimetry, ion chromatography and flow injection analysis. The standard method for the determination of soluble phosphate is colorimetry by the molybdenum blue reaction (MB). By far the most widely-used reduction method for batch and automated analyses is based on the approach described by Murphy and Riley. It asks for ascorbic acid to reduce the phosphomolybdate complex in the presence of potassium antimony tartrate as catalyst in acidic medium. The reaction pH and the molybdate concentration are key parameters for the formation of the phosphomolybdate complex and for controlling its reduction. The best sensitivity for orthophosphate detection occurs at a pH < 1.

In the past few years, increased attention has been given to the molybdenum blue reaction in flow analysis for determining phosphate in aquatic systems. The currently

available flow methods involving flow injection analysis (FIA), segmented flow analysis (SFA), and sequential injection analysis (SIA) often provide the low detection limits for the analysis of natural seawater samples. The FIA methods are typically coupled to UV-VIS spectrophotometry, ICP-AES detection and fluorometric or chemiluminescence detection. However, special care in sample and reagent delivery and stability is required for these performances. Despite the wide acceptance of MB-based spectrophotometric methods, they are still rather unwieldly for field monitoring applications: they involve high cost, operational complexity, high energy consumption, and require sample pre-treatment, reagent additions and storage. For these reasons, the development of systems for in-situ phosphate determination is an important research direction for the advancement of environmental science and conservation. Recent research by the group of *Garçon* suggested a new approach based on the electrochemical generation of molybdate by the oxidation of a molybdenum electrode and electrochemical release of hydrogen ions through a cation-exchange membrane, followed by electrochemical detection of the resulting complex. While this interesting research is still in the early stages, it forms an important step towards achieving a miniaturized and simplified phosphate sensing assay.

Ion-exchange membranes have been established in fuel cells and in a range of analytical instrumentation such as ion suppressors in ion chromatography, electrochemical desalinators, and potentiometric probe materials. They are an attractive means to deliver reagents as they allow to avoid sample dilution and the use of complex mixing valves and pumps, thereby greatly simplifying the instrument. The example of ion-exchange concept was cation-exchange membrane (Nafion). The anionic groups, sulfonic acid ($-SO_3H$), within polymer structure PTFE backbone allow only protons to pass through it. The use of proton-exchange membranes for the acidification of the sample plug has been well-established in the past with ion suppressors in ion chromatography. A few new approaches based on ion-exchange membranes have been recently suggested.

New report here on the use of cation- and anion-exchange membranes for realizing a well-designed and simplified approach to phosphate determination in seawater samples. The key reagents (molybdate anions and hydrogen ions) are delivered separately into the sample by diffusional counter transport across ion-exchange membranes (Figure 5.1). The phosphomolybdate complex formed in this method is spectrophotometrically detectable, as done here, but in principle also be measured electrochemically (chapter 6).

The proposed setup is based on a flow configuration and is compatible with integration in a membrane module for in-situ determinations, similar to other systems described recently [95, 96]. The suggested approach is therefore less complex than those based on classical mixing of reagent streams and likely easier to accomplish compared to the concept suggested by *Garçon et al.*, as the reagent delivery is being achieved under zero-current conditions, by passive diffusion.

5.2 Experimental procedures

5.2.1 Acidification and molybdate-releasing modules

Cation-exchange membrane (FKL-PK-130) and anion-exchange membranes (FAPQ-375-PP) were cut in pieces of 6×110 mm (for the acidification/molybdate module). The FKL membranes were pre-conditioned in deionized water for at least 6 h at room temperature and then at least 1 day in 1 M HNO_3 to ensure complete saturation of the membrane with hydrogen ions. The anion-exchange membranes were pretreated as per supplier recommendations: the FAB, FAS and FAD membranes were pre-conditioned in 100 mM NaCl (overnight), the FAPQ membranes need no pre-conditioning and were mounted dry in the module directly after cutting.

The design of the acidification and molybdate-releasing modules is illustrated in Figure 5.2. The cell consists of a sheet of cation- or anion-exchange membrane placed between two rubber channels (rubber: 10 × 119 × 0.45 mm, channel: 1.7 × 100 × 0.45 mm). One rubber was prepared for the sample and the other for the acid solution (acidification module, H-module) or molybdate solution (molybdate module, Mo-module). These elements are in turn placed between two acrylic blocks (30 × 120 × 14 mm) and tightly closed by screws. The ends of the channels connect with the inlet and outlet of each block. The inlets and outlets of the two blocks of each module are placed in reverse order to provide counter flow in the two channels.

5.2.2 Membrane selectivity of molybdate-releasing module

Aqueous solutions were prepared by dissolving the appropriate salts in deionized water. FAPQ membrane was cut in the size of 7 mm diameter and mounted in OSTEC bodies (Oesch Sensor Technology AG, Sargans, Switzerland). A membrane disk was conditioned in 0.6 M NaCl overnight. The inner compartment of the Ostec electrode

bodies was also filled with 10 mM NaCl. Solutions of Cl^- (NaCl), $H_2PO_4^-$ (NaH_2PO_4) and MoO_4^{2-} (Na_2MoO_4) were used to evaluate the selectivity of membrane. Potentiometric experiments were performed against a double-juncion Ag/AgCl/sat. KCl/1 M LiOAc reference electrode. Membrane selectivity was evaluated by adding aliquots of salts into water and the selectivity coefficients were calculated using the separate solution method [45]. To do this, the obtained separate calibration curves were extrapolated to 1 M and the selectivity coefficient was calculated from this potential difference dividing by the theoretical slope (59.2 or 29.6 mV for singly- and doubly-charged anions, respectively). The activity of the ion was calculated with a two-parameter Debye-Huckel approximation and the speciation of phosphate and molybdate was calculated for each concentration from the experimental pH value.

5.2.3 In-line phosphate detection

The experimental setup for phosphate determination is shown in Figure 5.3. The solution was delivered by peristaltic pumps (ISMATEC, Model ISM935c, Clattbrug, Switzerland) equipped with tygon tubings (ISMATEC, inner diameter 1.42 mm). Two pumps were used to allow for the delivery of solution streams at identical flow rates (90 μL min^{-1}). The solutions were pumped through at four different positions (A-D). The tygon tubings installed on the pumps were connected to the flow path using PTFE tubings (BOLA, inner diameter 0.8 mm). The used reagents (hydrochloric acid and sodium molybdate from the ion-exchange modules) and the analyzed solutions from the system were collected in waste bottles.

To obtain the calibration traces, sample solutions with different phosphate concentrations were introduced by a peristaltic pump (flow rate 90 μL min^{-1}). The solution at the inlet of the system was changed every 10 min by switching from the sample to the calibrant solution and the baseline (artificial seawater). These sequential solutions were passed through the in-line configuration containing the molydate module and acidification module, respectively. An acid concentration of 5-6 M and 6 mM of molybdate were fed into the H-module and Mo-module, respectively. The stream of the resulting solution containg the phosphomolydate complex was merged and mixed with an excess of reducing reagent (mixed solution $Reagent^{(R)}$ of S_{ascorb} and $S_{antimony}$ at the same ratio as colorimetry by standard spectrophotometry [97], chapter 2, section 2.3.8) via

a mixing coil. The resulting absorbance was recorded as a function of time by spectrophotometry at a 1-s time interval. After each experiment (involving three repetitions), the baseline solution was flushed through the system for 20 (or 15) min after every phosphate-containing solution, in order to eliminate any baseline drift.

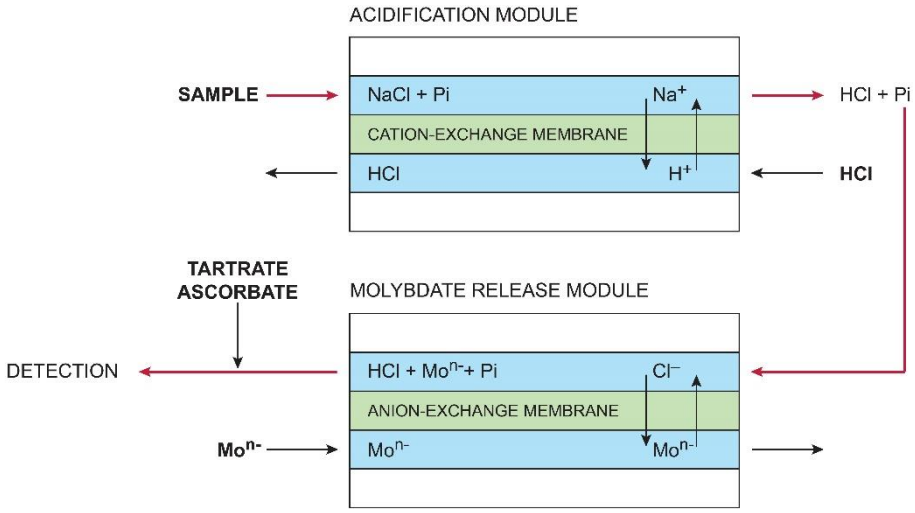

Figure 5.1: The main concept of this in-line membrane sensor

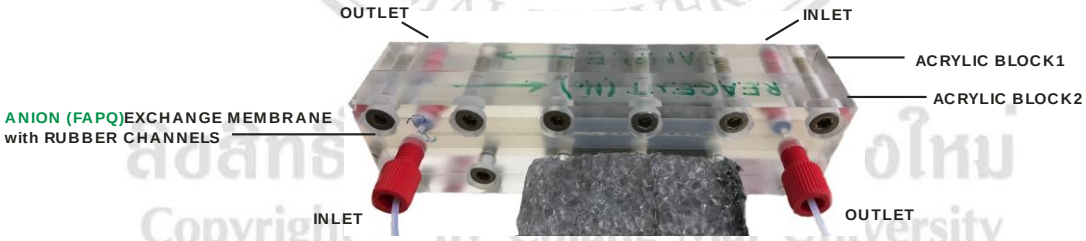

Figure 5.2: Schematic illustration of the custom-made module for membrane delivery: inlet, outlet, acrylic block, rubber channel. Anion-exchange membrane (FAPQ) are used for acidification- and molybdate-module respectively.

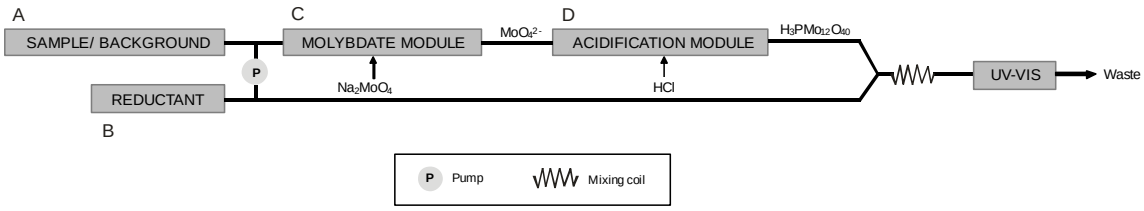

Figure 5.3: Schematic diagram of in-line configuration with spectrophotometric detection. The solution is delivered by peristaltic pumps at a flow rate of 90 μL min^{-1}.

5.3 Results and discussion

5.3.1 Acidification and molybdate-releasing modules

5.3.1.1 Membrane-releasing module (molybdate reagent delivery)

This work explores the use of ion-exchange membranes to deliver hydrogen and molybdate ions to seawater samples with the goal to achieve a simpler phosphate measurement. While sample acidification by ion-exchange has been established in the past, the release of molybdate anions into the sample by chloride counter transport across an anion-exchange membrane has not yet been reported. A previous study has explored a range of anion-exchange membranes as anion-responsive membranes in potentiometry, and similar materials were explored here: FAB-PK-130, FAS-PET-130, FAD-PET-75, and FAPQ-375-PP. After having the comparative studies of these membranes [98], the FAPQ anion-exchange membrane was chosen for an ion-exchange module of in-line configuration because the efficiency of molybdate transport can pass through the FAPQ membrane evaluated by a colorimetric molybdate assay, allowing to calculate the molybdate delivery efficiency as 70-75 %.

The anion-exchange membrane used for molybdate delivery allows for some passage of other anions such as phosphate. The potential loss of phosphate in the anion-exchange module was therefore evaluated. The anion selectivity of the FAPQ membrane was assessed by potentiometry. The membrane responded to Cl^- with a Nernstian slope of 59.12 mV, similar as traditional ion-selective electrode membrane, see Figure 5.4b. No significant membrane selectivity was observed for chloride over

phosphate, with log KCl, $H_2PO_4^-$ ^{pot} = -1.12 ± 0.25 (Figure 5.4a). However, the concentration of NaCl in seawater (~0.6 M) is significantly higher than that of phosphate (sub-µM range). This suggests that the exchange of molybdate anions from the feed solution will be mainly accompanied by chloride counter transport, thereby suppressing loss of phosphate from the sample.

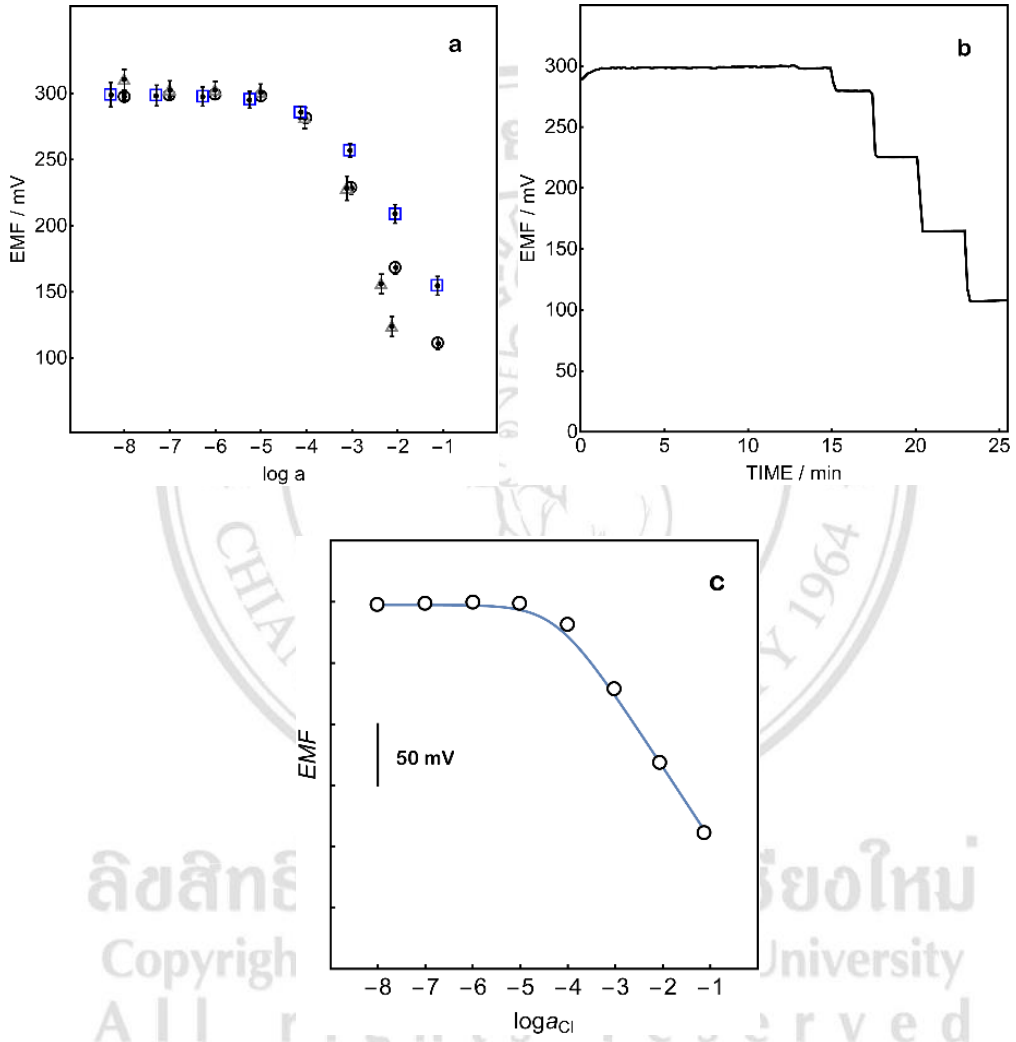

Figure 5.4: (a) Experimental data points (error bars are standard deviations) for the EMF responses of FAPQ-based electrodes for different anions: Cl^- (black circle), MoO_4^{2-} (gray triangle), and $H_2PO_4^-$ (blue square), (b) Associated EMF time-trace upon NaCl addition, obtained with a FAPQ-based electrode. (c) Potentiometric calibration curve upon NaCl addition, obtained with a FAPQ-based electrode.

5.3.1.2 Membrane-releasing module (acid reagent delivery)

An in-line acidification approach based on passive hydrogen ion transfer through a cation-exchange FKL membrane has been recently proposed in our group to adjust the pH of freshwater samples for nitrite detection [99]. Previous studies with such cation-exchange membranes showed that they are sufficiently impermeable to anions and therefore should allow one to maintain the same phosphate concentration in the sample plug after passing through the acidification module. This custom-built module was adapted for the assay of phosphate, see Figure 5.2. The anion-exchange (molybdate-releasing) and the cation-exchange (acidifying) modules were coupled in series (see Figure 5.2).

5.3.2 The performance of both membrane modules

To study the performance of ion exchange membranes in term of phosphate loss while passing the sample through the acidification module and molybdate module. Injection sample by standard condition (without membrane module) was used to compared with flow system with ion exchange module.

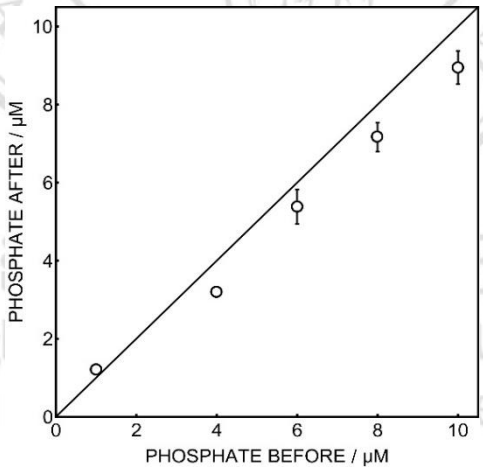

Figure 5.5: Correlation graph between phosphate concentrations after passing through membrane modules, including molybdate module and acidification module, and in sample initially (n=3).

The extent of phosphate loss was studied by a standard colorimetric phosphate assay for varying levels of phosphate in a 0.6 M NaCl background before and after passage through the combined acidification and molybdate modules. Figure 5.5 shows the resulting correlation of phosphate concentration obtained from the two experiments. The loss of phosphate was indeed not dramatic, on the order of 10%, and might also be caused by processes other than membrane transport.

5.3.3 Effect of the flow system parameters

Optimization of the experimental conditions was performed before turning to seawater measurements. Phosphate calibration curves (0-100 µM) were recorded at different flow rates, see Figure 5.6. phosphate concentration 0-100 µM. 5-6 M HCl and 3 mM molybdate solutions were fed into the H-module and Mo-module respectively.

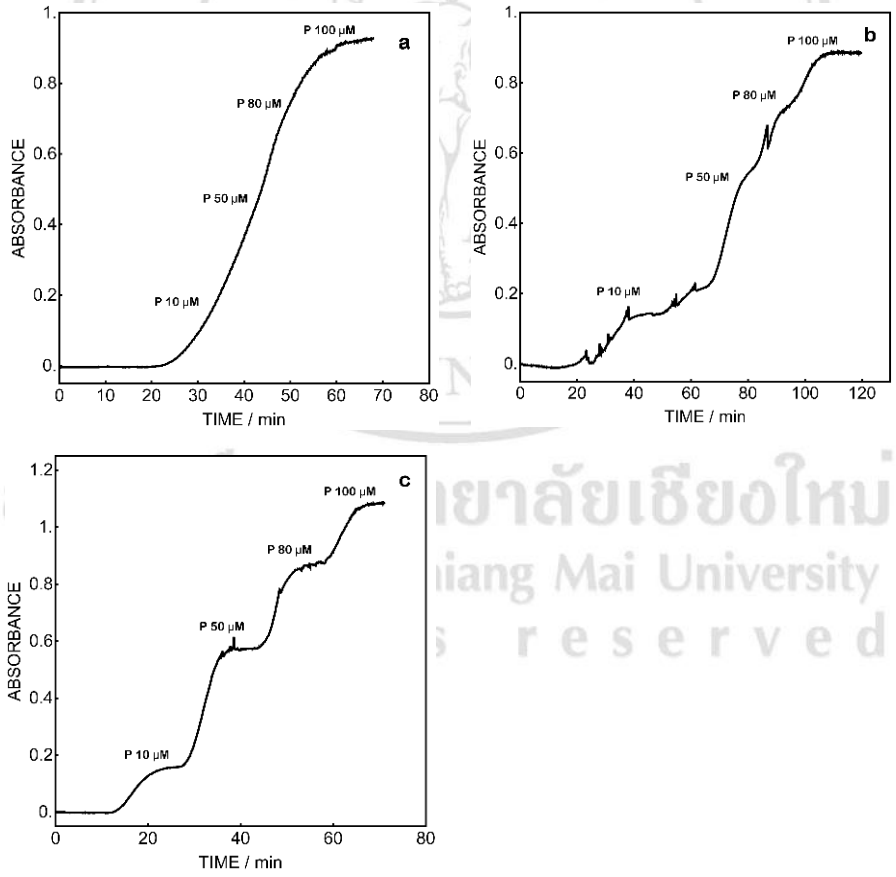

Figure 5.6: Absorbance vs time response for different flow rates: (a) 20 µL min^{-1}, (b) 45 µL min^{-1} and (c) 90 µL min^{-1}

A higher flow rate is known to decrease the residence time and therefore the dispersion of mixed solution zone, providing a narrower peak signal [100]. However, the expense of a decreased sensitivity was owed to incomplete ion exchange by the membrane module and insufficient reaction time. From the data shown in Figure 5.6, a flow rate of 90 µL min^{-1} was selected as each solution gave good separation.

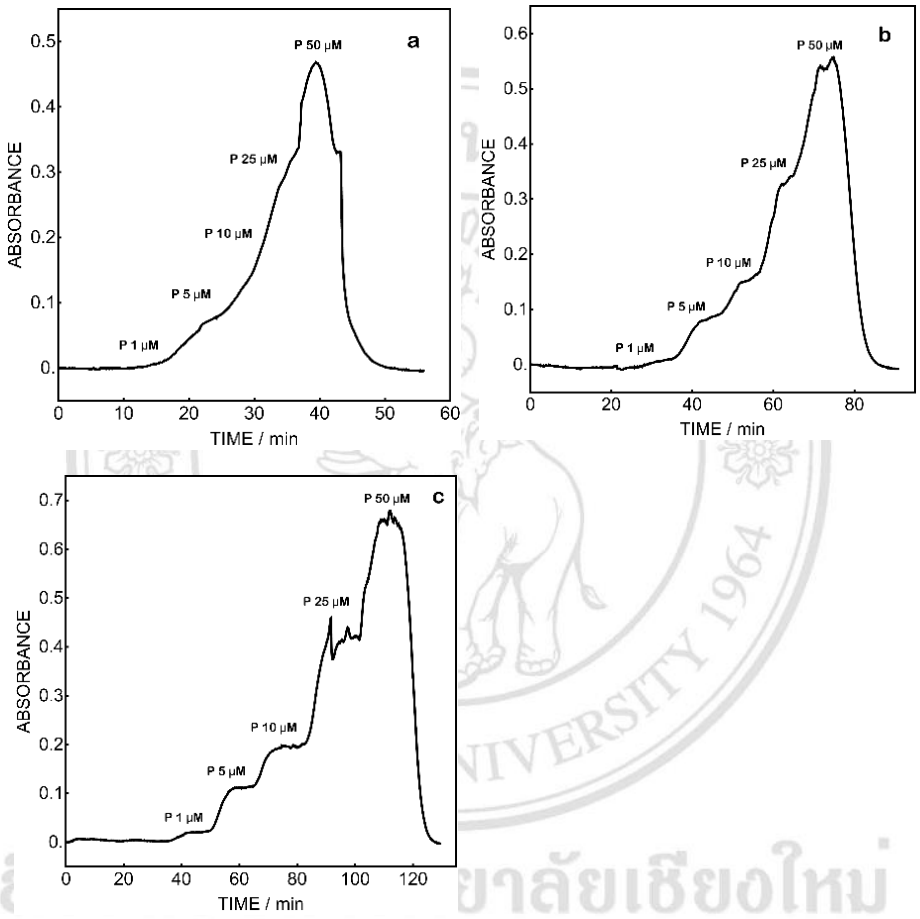

Figure 5.7: Absorbance vs time response for different solution volumes: (a) 0.45 mL, (b) 1 mL and (c) 1.35 mL

The volume of the sample plug also affects the separation. It is controlled by the injection time via the preselected flow rate. Here, 5, 10- and 15-min injection times gave 0.45, 1.00- and 1.35-mL sample volumes. Figure 5.7 shows the corresponding results for a range of phosphate concentrations (0–50 µM), suggesting that 1 mL is suitable as each phosphate concentration can be clearly separated.

5.3.4 The optimization of reagent concentrations

The current study refers to phosphate detection in seawater, which contains a high concentration of sodium chloride (0.6 M). This high concentration forms a strong diffusional driving force for membrane exchange with hydrogen ions. In order to enable the detection of phosphomolybdate complex, a final pH of <1 is required after acidification. The suitable acid concentration in the acidification module was determined by passing 100 µM phosphate solution in 0.6 M NaCl background through the molybdate module (3 mM Na_2MoO_4) and the acidification module with different acid concentrations (HCl 1-8 M). The color intensity of blue product was analysed colorimetrically after spiking reducing reagent. The correlation graph is shown in Figure 5.8 and suggests that optimal performance is observed with 5-6 M HCl, giving a final pH in the sample plug of ca. 0.85-1.00. The same membrane was used for at least three weeks without significant deterioration of the analytical performance.

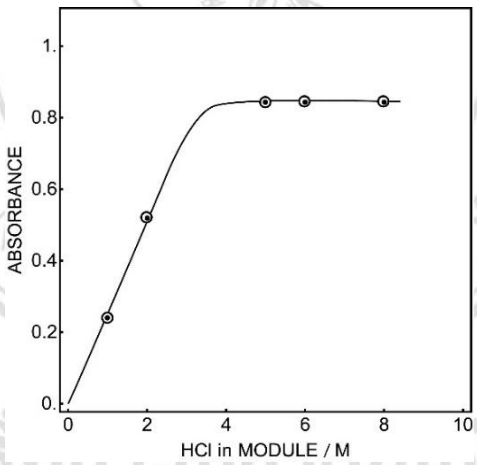

Figure 5.8: Effect of acidity on color intensity (n=3) for a sample containing 100 µM phosphate. Explored HCl concentrations were in the range of 1-8 M.

The concentration of molybdate in the Mo-module was varied to study the influence on system performance. Most literature ask for a molybdate concentration in the millimolar range. Consequently, the range of explored concentrations in the reagent solution was 0-20 mM, see Figure 5.9 for results. The absorbance of the blue product was analysed colorimetrically after spiking reducing reagent. Two phosphate standards, with 100 µM (blue line) and 10 µM (black line) phosphate concentrations, were analyzed in the suggested setup with different molybdate concentrations and a 5 M HCl acid

concentration in the feed streams. The sensitivity of the method was found to increase with increasing molybdate concentration up to 6 mM, after which it was constant. For this reason, a 6 mM molybdate reagent concentration was chosen in the reagent stream of the Mo-module.

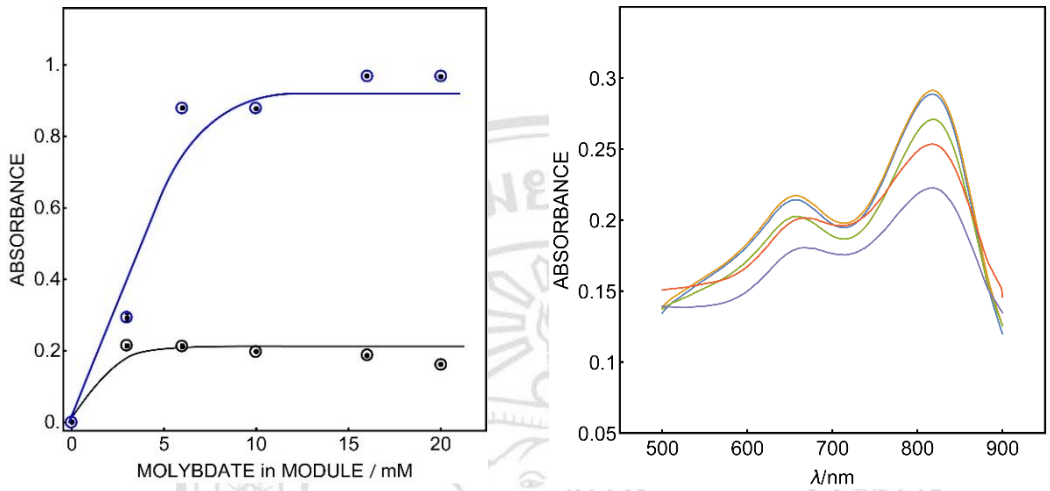

Figure 5.9: Effect of molybdate reagent on color intensity for phosphate assay: standards containing 100 µM (blue circles) and 10 µM (black circles) phosphate. The explored molybdenum concentrations were in the range of 0-20 mM (right).

5.3.5 In-line phosphate detection via spectrophotometry

Seawater samples were analyzed for phosphate by guiding the sample plug first through the acidification module and subsequently through the molybdate-releasing module. While the final goal of the work is to achieve an electrochemical detection of the resulting phosphomolybdate complex, the more established spectrophotometric detection was chosen here to best assess the performance of the membrane modules. The associated time profiles for samples containing varying levels of phosphate in a 0.6 M NaCl are presented in Figure 5.10 (left). Linearity was obtained in the range of 0.1-10 µM phosphate, see Figure 5.10 (right).

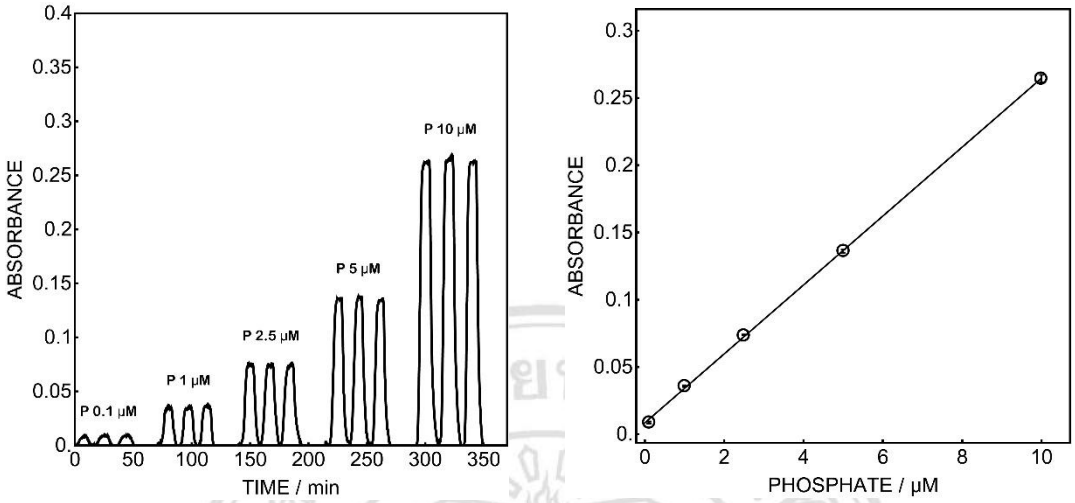

Figure 5.10: Time-dependent signals for different phosphate concentrations (0.1-10 µM: left), corresponding calibration graph from the time-based data (right), volume of sample plug ca. 1 ml.

Silicate is known to be the principal interferent in the molybdenum blue method as it also forms heteropoly acids (12-MSA/12-molybdosilicic acid, $H_4SiMo_{12}O_{40}$), thereby reducing available molybdenum blue concentration. Generally, silicate concentration in aquatic systems is in the submicromolar range. Silicate concentration required for siliceous phytoplankton such as diatoms is <0.1-0.6 µM in the euphotic zone. From the liturature, it is suggested that silicate interference can be suppressed with high acidity or using antimonyl tartrate as the source of Sb(III) [94]. Here, organic acid was used in the combined reductant reagent (potassium antimonyl tartrate), as tartaric acid may help to minimise silicate interference. From the result shown in Figure 5.11, adding 10 µM silicate solution to a 1 µM phosphate solution does not significantly interfere. Only excessive silicate concentrations not common for most seawater environments give interference.

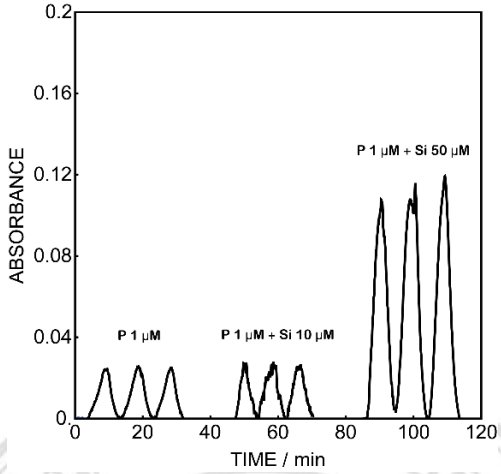

Figure 5.11. Absorbance and time response illustrating silicate interference in phosphate determination, volume of sample plug ca. 0.45 ml.

5.3.6 Seawater samples application

The in-line membrane system was applied to the determination of phosphate concentration in a range of unmodified seawater samples as shown in Figure 5.12a. Phosphate concentrations of (0.794 ± 0.018), (0.871 ± 0.051), and (0.513 ± 0.061) µM were detected in the samples, see Table 5.1. The phosphate concentrations in the same samples were also determined by the traditional molybdate assay chosen as reference method. The resulting cross-correlation is shown in Figure 5.12b. The data from the two methods are in a good agreement, although we note that the phosphate level in seawater sample 3 was too low to be detectable with either method.

Table 5.1. Phosphate analysis in seawater samples (n=3)

Sample	Developed method (µM Phosphate)	Spectrophotometry (µM Phosphate)
SW1	0.794 ± 0.018	0.800 ± 0.027
SW2	0.871 ± 0.051	0.877 ± 0.035
SW3	ND*	ND*
SW4	0.513 ± 0.061	0.531 ± 0.043
SW4 + spike P 5 µM	5.701 ± 0.094	5.615 ± 0.039

P 3.5 µM**	-	3.553 ± 0.080
P 1 µM**	-	1.185 ± 0.044

* ND: not detected, ** For checking the performance of spectrophotometric method using known concentration of phosphate

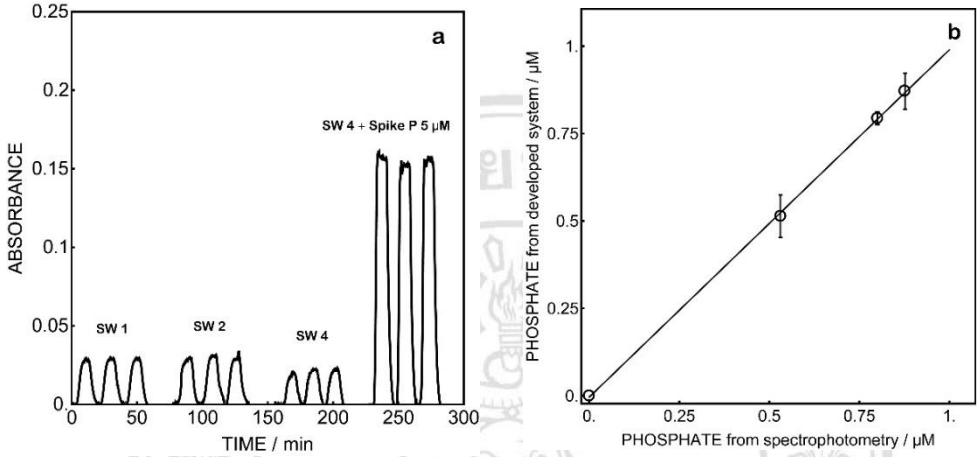

Figure 5.12: (a) Time-based responses for seawater samples containing different phosphate levels, (b) Correlation graph between phosphate concentration obtained using developed system and phosphate determined by standard spectrophotometry, volume of sample plug ca. 1 ml.

5.4 Conclusion

An in-line flow system employing ion-exchange membrane-based reagent delivery was successfully developed for the determination of inorganic phosphate in seawater. The performance of the ion-exchange membranes was acceptable and showed no dramatic loss of phosphate via the membrane modules. The device was coupled to spectrophotometric detection for seawater measurement, demonstrating the detection of phosphate levels as low as 0.1 µM. The key advantage of this approach is a simpler, more integrated membrane-based reagent delivery principle, compared to established approaches that rely on mixing. While the long-term goal of this research is to develop a miniaturized sensing device with integrated electrochemical detection, the spectrophotometric detection chosen here is an intermediate goal that lends itself well to the validation of the membrane-based delivery principle.

CHAPTER 6

Electrochemical sensor employing ion-exchange based membrane

Here, a novel in-situ electrochemical sensor was studied with ion-exchange membranes. The necessary reagents (molybdate anions, hydrogen ions) for the formation of electroactive phosphomolybdate complex are delivered into the microfluidic flow system. The recently reported experiment on the cation-exchange process (Donnan exclusion membrane) was adapted for the sample acidification achieving a highly acidic condition. Then, the possibility of molybdate anion transported through an anion-exchange membrane was chosen for the successful phosphate measurement (chapter 5). The proposed membrane system in this section was focused on connecting with electrochemical measurement using square wave voltammetry. The previous work from our group reporting on these ion-exchange membranes was well suited for phosphate determination. Therefore, the next challenging for this membrane sensor has studied on electrochemical detection (electrode part) instead of a spectrophotometer to receive the minimized sample volume and demonstrate a piece of small, portable equipment and receiving low power consumption interfaced with the microfluidic module that is suitable to be used directly on-site monitoring.

6.1 Introduction

Phosphate is an essential nutrient for growth and energy transfer used by all living organisms [101]. The current approaches for phosphate monitoring are normally related to the conventional method, which the molybdate and phosphate solution are reacted in a suitable quantity under acidic medium, providing the phosphomolybdate complex. It is reduced with ascorbic acid, in the existence of antimony and subsequently measured by colorimetry [97].

Electroanalytical technique based on the form of phosphomolybdic complex is also chosen for phosphate determination which does not suffer from the interferences and the

refractive index effect [102,103]. The non-zero current techniques were selected to determine this electroactive complex such as amperometry, linear or cyclic voltammetry, pulse method and square wave voltammetry [104-110]. However, these techniques had to the addition of reagents or using modified screen-printed electrodes with precoated reagents. Also, the reports of potentiometric sensors based on phosphate receptors were rarely known to reveal insufficient performance (lower detection limit, selectivity) for successful phosphate assay in environmental fields [111].

There are only a few in-line methods for molybdate production via electrochemical techniques reported previously. The new research for electrochemical phosphate determination had been newly submitted by *V. Garçon et al.* based on the production of both molybdate and protons into the sample solution simultaneously [112]. In this study, protons were electrochemically passed through a cation-exchange membrane into the sample partition, using the oxidation of molybdenum electrode section behind this membrane. Also, the molybdate species were transported into this sample by oxidizing the secondary molybdenum electrode (achieving the protons excess over molybdate). The interference from silicate was avoided under the ratio of proton over molybdates close to 70 at pH 1, confirmed by previous reviews.

Previous work from our group reported on the use of membrane-based reagent delivery for phosphate colorimetric determination which was well suited for the seawater application [94]. The next challenging for this membrane system has focused on miniaturized electrode detection (detection part) instead of a spectrophotometer to improve sensitivity, minimized sample volume and demonstrate a piece of small, portable equipment interfaced with microfluidic membrane module.

Herein, an in-line electrochemical system was fabricated for phosphate assay in the real seawater by transporting both hydrogen ions and molybdate species into the sample, subsequently detected by mini-electrochemical electrode using an electrochemical technique (square wave voltammetry). The proposed setup is simple to incorporate to the in-situ determination with the fluidic system in a submersible element. Additionally, ascorbic acid which unstable reagent has not required for reduction of complex occurring at the electrode surface. This system is suitable to be used directly for in-situ monitoring.

6.2 Experimental procedures

In-line construction for electrochemical measurement

The proposed scheme of a experimental set-up for phosphate determination is shown in Figure 6.1. The solution was delivered by a peristaltic equipped with tygon tubings (inner diameter 0.76 mm). Two pumps were used for the delivery of flow solutions at the flow rate 40 μL min^{-1}. Importantly, the sample and background flows should be delivered on the same pump in order to receive precisely the same flow rate and thus avoid the bubbles formation in the channel. The tygon tubings were connected to the PTFE tubings (ID 0.8 mm) of the flow path, installed on the pumps. Valve 1 has been installed before the pump, in order to select one of the two solutions (sample/calibrant or background). Then, valve 2 was connected after the pumps delivering the flow to the detection part, in order to switch between analyte and washing reagent. The electrochemical detection (electrode part) was connected at the end of membrane delivery. An acid cleaning was an additional option for eliminating the problem of baseline drift.

The phosphate reaction is based on Keggin anion formation by molybdate reagent in acidic medium. This phosphomolybdate complex can be detected by electrochemical measurement. To obtain the calibration graph, solutions with different phosphate concentrations and 0.6 M NaCl background were passed through the in-line sensor by peristaltic pump shown in Figure 6.1. These sequential solutions were passed through the in-line configuration including molybdate module and acidification module respectively. The stream of the phosphomolybdate complex was detected by electrochemical part (radial cross-flow electrode in Figure 6.2). The sample solutions at the inlet of this system were changed every 20 (or 10) minutes by switching the valve 1 between the calibrant and NaCl baseline.

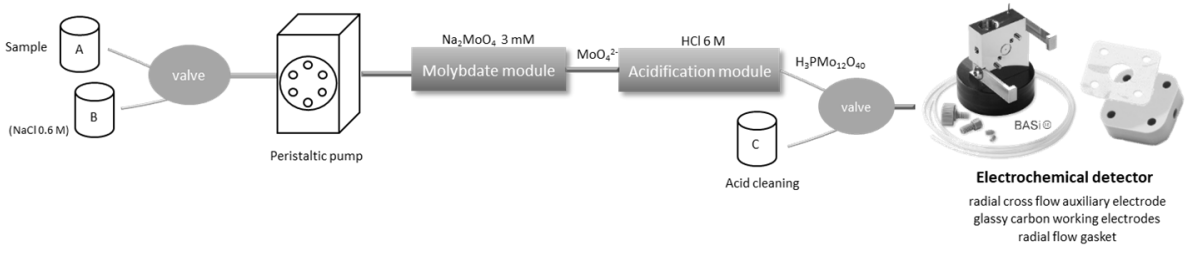

$$PO_4^{3-} + 12MoO_4^{2-} + 27H^+ \rightarrow H_3PMo_{12}O_{40}\,(electroactive\ complex) + 12H_2O$$

Figure 6.1. A schematic diagram of in-line configuration with electrochemical detection, the solution is delivered by peristaltic pumps at a flow rate of 40 µL min^{-1}.

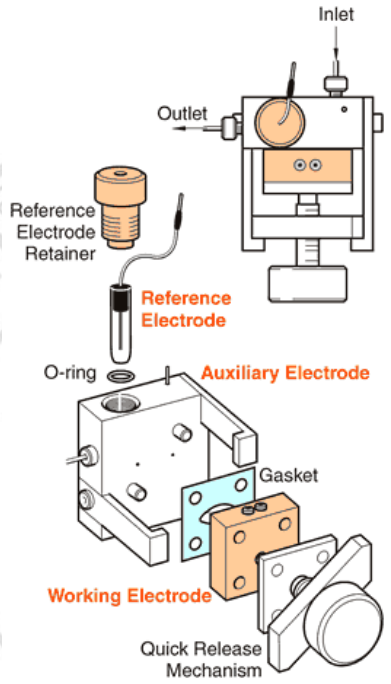

Figure 6.2. The structural component of the radial electrode (https://www.basinc.com)

6.3 Results and discussion

6.3.1 The effect of flow system parameters

Microfluidic flow system via the membrane delivery (acidification- and molybdenum- module) was previously studied in terms of spectrophotometric detection [94]. Apart from that measurement, the electrochemical detection of phosphate by the form of the phosphomolybdic complex has been demonstrated on this report.

Firstly, considering the flow system section, some parameters were investigated. Compared to the previous studies (chapter 5), the flow rate should be decreased which was preferred around 40 µL min^{-1}. This is due to the small size of the radial-cross electrode which the leaking of solution was occured at higher flow rates. According to the result in the reproducibility, sample volume (0.4 ml) of P 1 µM was chosen. Each plug of these

solution was passed through both membrane modules for five repetitions separating by switching to a background solution. From the result, the peak current of 2 – 5 plugs did not change dramatically and %RSD can acceptable (Table 6.1). This is because every sequence of each plug is the same (same solution and same matrix dispersion). Moreover, the volume of sample solution also affects a dispersion. From the results in Figure 6.3, the different volumes of solution based on fixing time injection were studies (1 min = 0.04 ml, 3 min = 0.12 ml, 5 min = 0.2 ml). Phosphate 1 µM (n=3) was flowed into the system and switching between background solution (NaCl). Peak separation of three repetitions of the solution was clearly seen with 0.2 ml volume (gray line) comparing with lower volume. So, more than 0.2 ml should be suitable for further experiment.

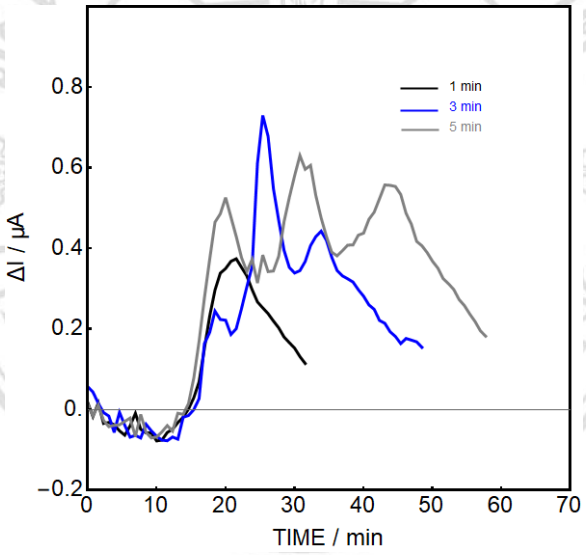

Figure 6.3. Time-based diagram of phosphate 1 µM solution passed through both modules in terms of different sample volumes

Table 6.1. The average peak current of phosphate 1 µM which each plug solution (0.4 ml) passed through both modules (subtracting by background solution)

Peak current (ΔI, µA)						
Peak 2	Peak 3	Peak 4	Peak 5	AVE	SD	%RSD
0.63	0.57	0.67	0.66	0.63	0.05	7.11

6.3.2 The peak potential of molybdate complex by cyclic voltammetry

Electrochemical mini-electrode was studied as its general configuration shown in Figure 6.2. From the preliminary studies, it can be mentioned that some types of working electrodes (gold and glassy carbon) were performed in the bulk and the flow system. The results revealed that the gold electrode requested the special control and the surface regeneration after contacting to the phosphomolybdate complex even as low concentration. Therefore, glassy carbon electrode was selected as a more suitable material that is easier-to-treat, and having the similar sensitivity with gold electrode (the co-worker's data).

An electrochemical signal from reducing phosphomolybdate complex was obtained in Figure 6.4, generating by phosphate in the acid and molybdate medium. The stability of this electro-signal from the developed flow system was studied by injecting the phosphomolybdate solution through tubing for 30 minutes (Figure 6.5). Cyclic voltammetry has been commonly used for confirming the complex qualitative. As our attempt to vary scan rate from 50 to 1000 mV/s, 4 times repetition per each scan rate were recorded (Figure 6.5). From a voltammogram, the reproducibility of this solution in a flow tube is good. All graphs were plotted from the result of voltammogram based on a relationship between peak current ($I_{p1} - I_{p4}$) and scan rate or a square root of scan rate. It seems to be a linear trend in both types of graph.

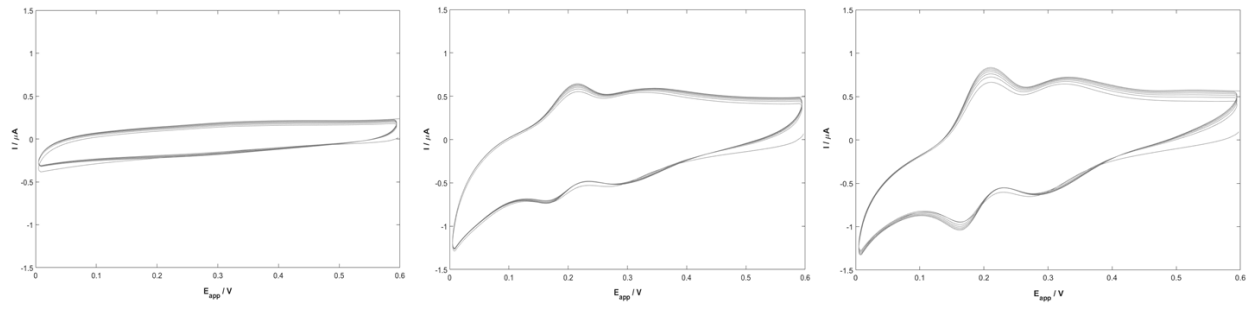

Figure 6.4: Cyclic voltammogram of different solutions (NaCl, NaCl + acid + molybdate, phosphomolybdate complex) scanning from 0.6 to 0 V, number of crossing = 14

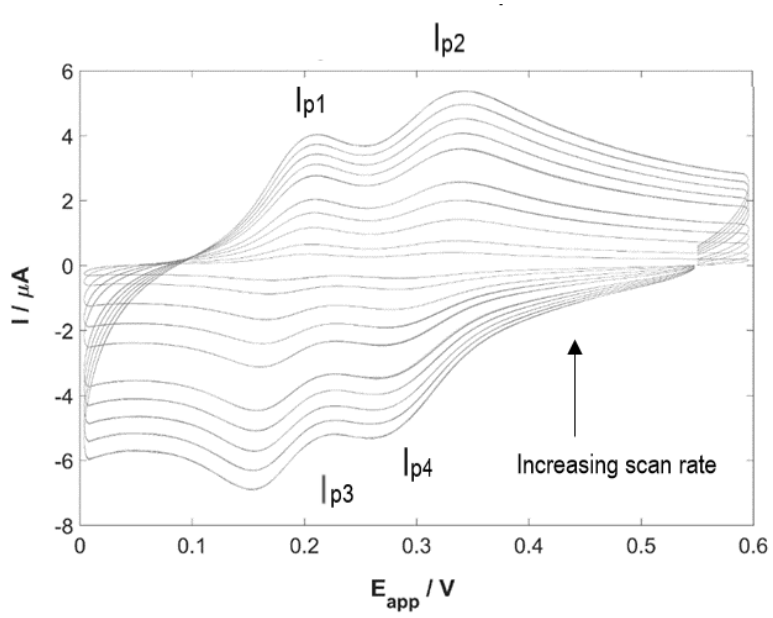

Figure 6.5: Cyclic voltammogram of phosphomolybdate complex, scan rate 50, 100, 200, 300, 400, 600, 700, 800, 900, 1000 mV/s

6.3.3 Different electrochemical techniques

The main propose of this electrochemical readout is focused on reducing a phosphomolybdate complex. There are two techniques including cyclic voltammetry and square wave voltammetry that are chosen for electrochemical detection part. In addition, the condition of both voltammetric methods was expressed in Figure 6.6-6.7. A baseline of background did not drift extensively in the range of low concentration of phosphate. However, the peak current from the phosphate concentration between 0.1-10 μM did not clearly distinguish by a basic flow set-up with cyclic voltammetry comparing to the better result by square wave voltammetry. Additionally, an electrochemical method (SWV) should be chosen as it has been one of the most sensitive methods because of the significant reduction of charging current effects based on the phosphomolybdate determination, reported previously.

6.3.4 The different scan rate, scan direction, and reproducibility

The phosphate determination via phosphomolybdic complex was done in the forward potential (0 to 0.6 V) of SWV, two peaks were obtained around 0.2 V and a higher than 0.3 V as shown in Figure 6.8-6.9. These peaks related to the reduction of

phosphomolybdate complex. According to the literature review, two steps of the complex reduction provided two peaks potential is similar with these results. These two peaks were also referred to the chemical reduction of Mo(VI) to Mo(IV) and Mo(IV) to Mo(II) respectively, reported by some authors [106]. However, these observed two peaks can be interpreted by the Mo(VI) reduction into two complexes including the ratios of combined oxidation states (Mo(V) and Mo(VI)) [110,112]. For instance, *Garçon et al.* described these two peaks by the chemical mechanisms via two and three electron-transfer reductions.

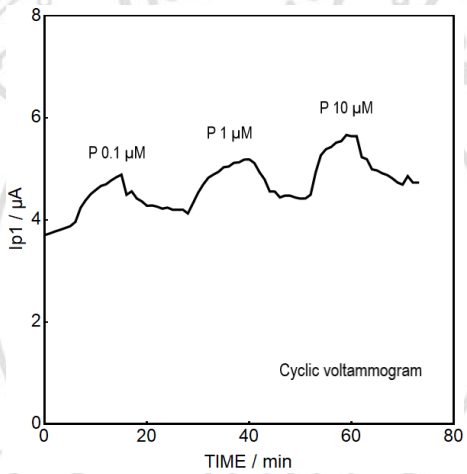

Figure 6.6: Time-based diagram of the peak current from cyclic voltammetry (CV), scan direction from 0.6 to 0 V, scan rate 700 mV/s

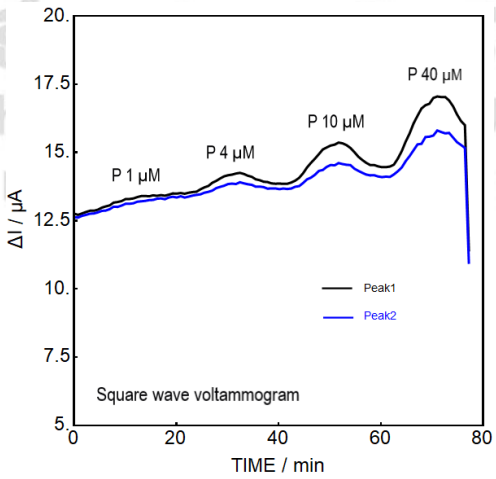

Figure 6.7: Time-based diagram of the peak current from square wave voltammetry (SWV), scan direction from 0.6 to 0 V, amplitude 25 mV

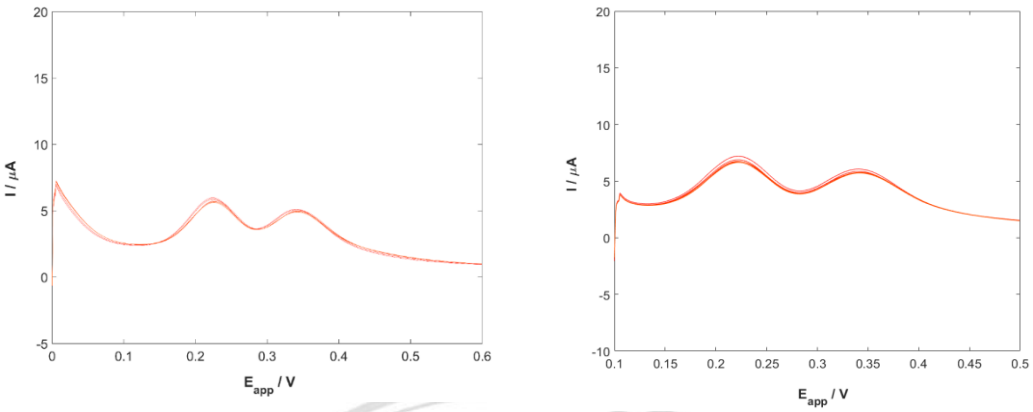

Figure 6.8: Square wave voltammogram of phosphomolybdic complex

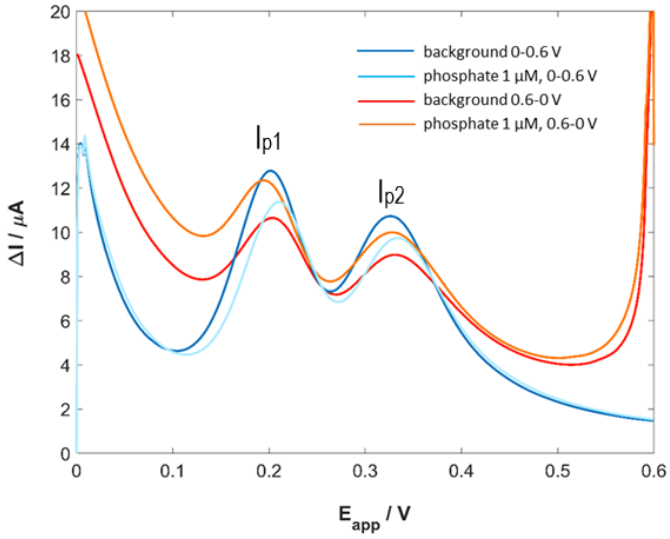

Figure 6.9: Square wave voltammogram of different direction potentials

Considering the effect of the different direction of the scanning potential is interested. There are two scan directions including 0-0.6 V and 0.6-0 V that is a range of expected peak position of the phosphomolybdate complex based on the literature review. The difference of scan directions has a similar peak position as shown in Figure 6.9. However, the different peak height of both directions is can be depended on an adsorption of the complex from the previous experiment. Importantly, the dominant peak at E~0.2 V (indicated as Peak 1 in Figure 6.9 and Figure 6.10) was chosen for further experiment due to higher currents and the stability of current signals.

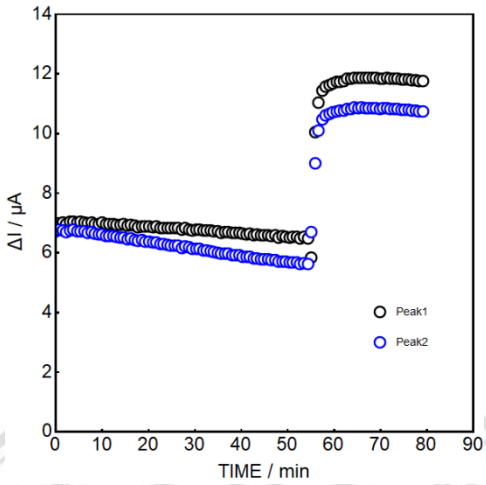

Figure 6.10: The peak currents (peak1, peak2) of phosphate from square wave voltammetry (SWV) scan from 0.6 to 0 V, amplitude 25 mV

Due to the peak current from the previous result by square wave voltammogram, studying the effect of different frequency should be done. Switching valve was used to change the direction of this flow solution between the background reagent (NaCl+acid+molybdate) and the different phosphate concentrations (0-100 µM). The current signal of peak1 at 50 Hz would be chosen because of the lower background drift and a significant difference of phosphate concentration (Figure 6.11).

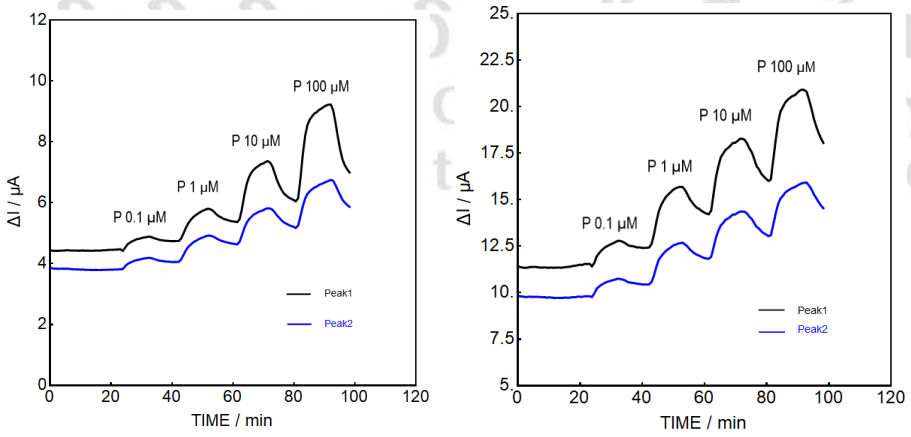

Figure 6.11: A diagram of peak currents from SWV (I_{p1}, I_{p2}) with a time of different phosphate solutions, scan direction 0-0.6 V, frequency 50 Hz (left), 250 Hz (right)

6.3.5 The optimization of reagent concentrations

The suitable acid concentration in the acidification module was obtained from Figure 6.12. The acid concentration around 5-6 M was chosen because a peak current position did not shift significantly. In order to study the influence of molybdate in Mo-module, the different molybdate was varied in the range of mM. The peak current was increased corresponding to the molybdate quantity. The molybdate around 3 mM was an optimum condition (Figure 6.13) because of high sensitivity and the same peak position comparing to electrochemical protocols.

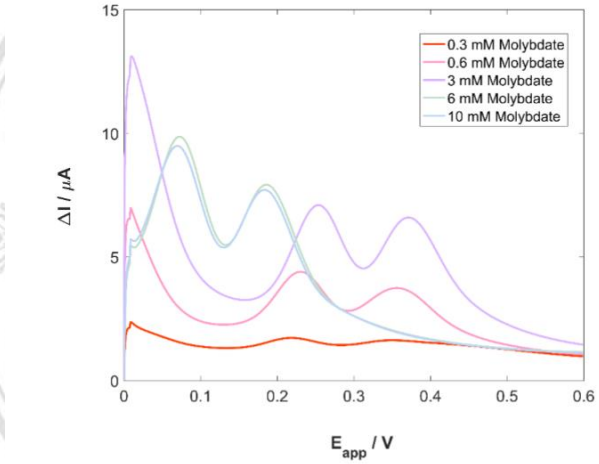

Figure 6.12: Square wave voltammogram of the different molybdate concentration from 0-10 mM

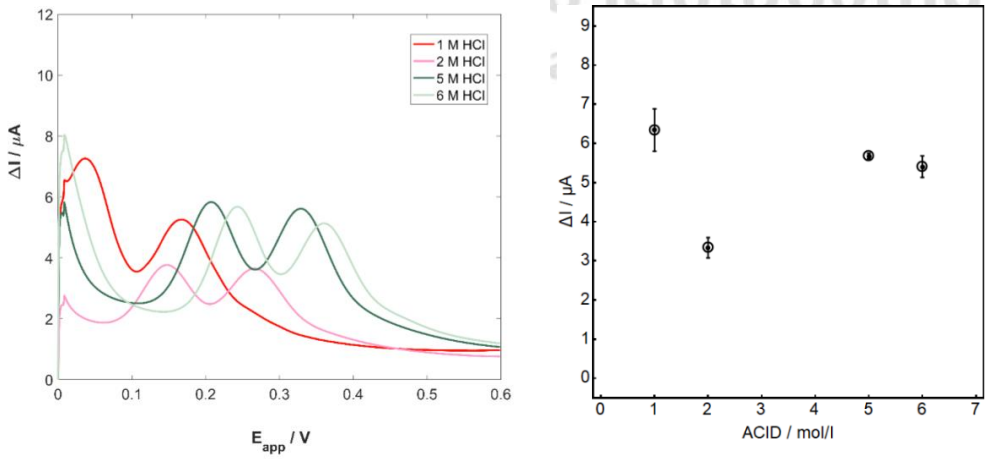

Figure 6.13: Square wave voltammogram of the different acid concentration from 0-6 M (left), the correlation profile between the acid concentration and the peak current (right)

6.3.6 In-line phosphate detection via the cleaning process

To illustrate the phosphate determination in artificial seawater, the baseline drift from the previous result should be eliminated. The attempt to tackle this problem was studied by adding a washing-step between measurements, using cyclic voltammetry of sulfuric acid ~0.5 M (Figure 6.14). This method was selected due to the results that cyclic voltammetry has an acceptable performance to clean the electrode surface both in the bulk and in the flow system (preliminary experiment). According to several scan rate conditions, the protocol of 100 mV/s or 200 mV/s from -0.7 to 1 V should be used because of shorter time cleaning (Figure 6.15). Moreover, in order to eliminate this background-peaks, it was exposed that the surface of GC working electrode should be regenerated by polishing or running CV cycles of sulfuric acid solution continuously for 10 min or less. After cleaning system, some unexpected peaks were disappeared as shown in Figure 6.16 and Figure 6.17. As the polishing process has been done in this flow configuration, another valve was chosen for switching between the solution (calibrant or background) and the washing reagent (sulfuric acid). After running this in-line membrane sensor with cleaning step, the voltammogram result of the experiment was presented in Figure 6.18-6.19. From the time-based diagram, each baseline of the different phosphate concentrations had a similar peak height (especially of lower concentration, figure 6.18). Then, the peak current form peak 1 known as the reduction peak (E~0.2V) was plotted with time, by increasing the phosphate concentration passed through an in-line structure as shown in Figure 6.19.

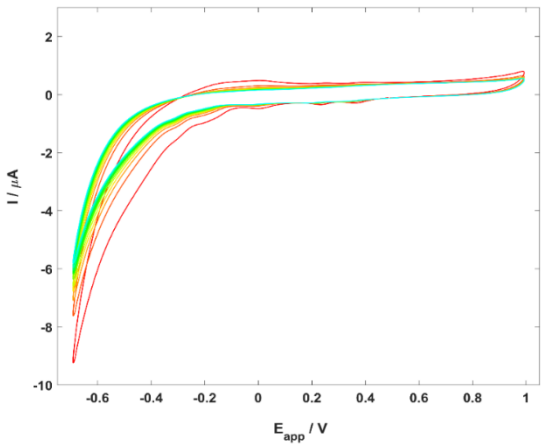

Figure 6.14: The voltammogram of the cleaning process (H_2SO_4 scanning in the range of potential from -0.7 to 1 V, scan rate 50 mV/s)

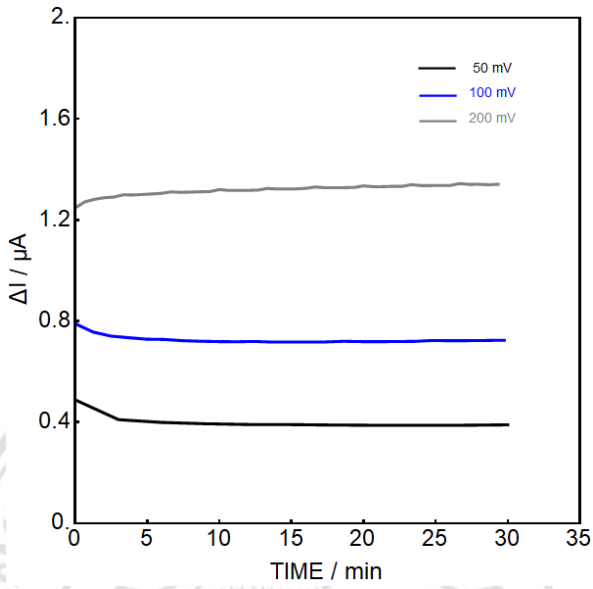

Figure 6.15: A diagram of peak currents with time in terms of several scan rate in the cleaning process (H_2SO_4 scanning in the range of potential from -0.7 to 1 V)

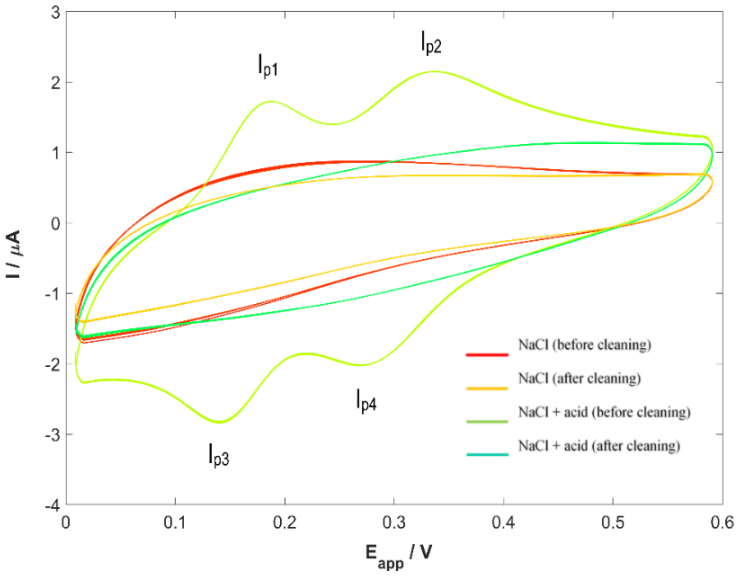

Figure 6.16: Cyclic voltammogram comparing between before- and after- cleaning process

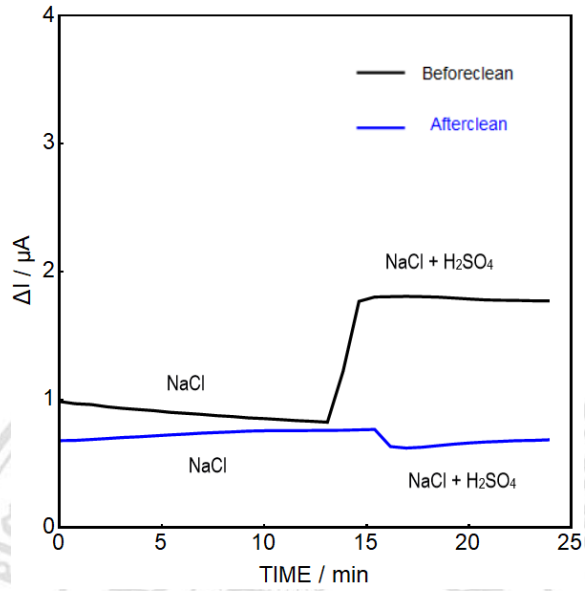

Figure 6.17: Time-based diagram of the peak current influenced by the cleaning process (before- clean and after- clean expressing as the black line and the blue line)

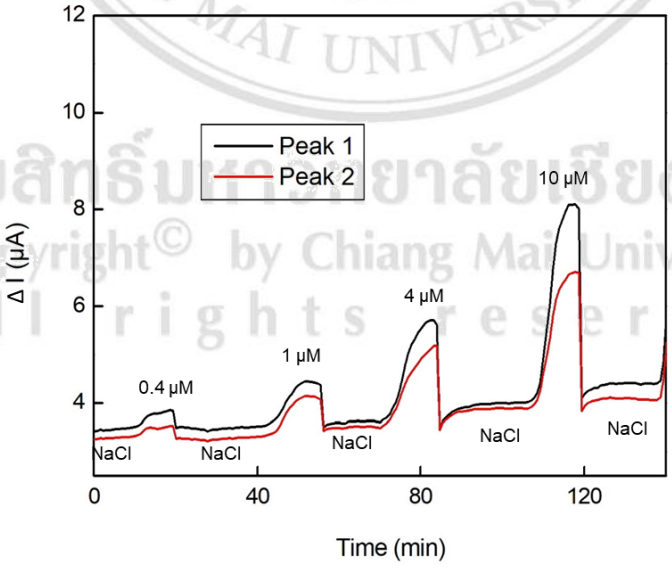

Figure 6.18: A diagram of peak currents from SWV with time (phosphate concentration 0-10 μM)

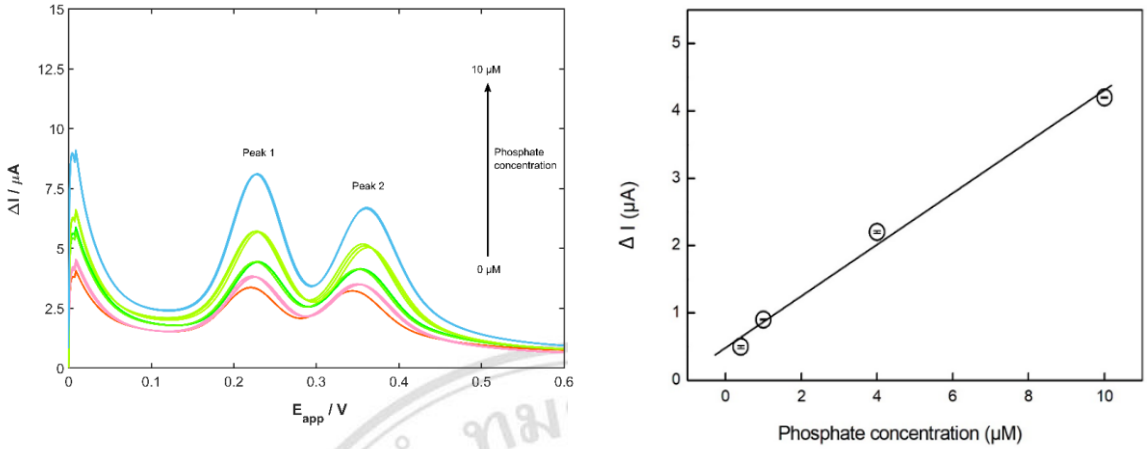

Figure 6.19: A square wave voltammogram of the different phosphate contents in the range of 0-10 μM (left), a calibration graph of the different phosphate quantity (right)

6.3.7 Application to seawater samples

According to the real sample application, seawater matrix was demonsrated. It can be seen that this developed sensor was possible for the phosphate determination. Although this method is promising to measure the micromolar phosphate, some factors should be improved such as a precise range of phosphate addition, and the repetition of each solution (Figure 6.20). In addition, using concentrated acid for cleaning process should be replaced due to the electrode demage during long time analysis.

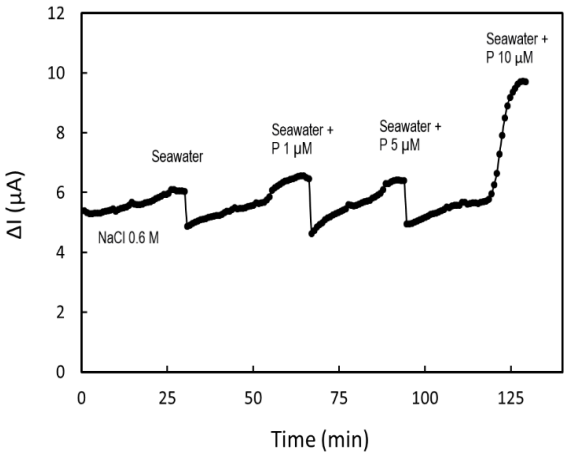

Figure 6.20: A diagram of peak currents from SWV with time (the seawater solution added by the phosphate concentration 0-10 μM)

6.4 Conclusion

A microfluidic flow system with electrochemical detector has been developed allowing for the phosphate determination in the seawater sample. In-line flow sensor for reagent delivery was occurred, which protons and molybdate anions were passed into the seawater sample. The phosphate detection in seawater was possible measured in the terms of the formation of electroactive phosphomolybdate. The developed sensor has been effectively coupled with the electrochemical phosphate detection in artificial seawater, allowing for the detection limits of micromolar. The potential in forward ramp has been shown a suitable option in this proposed membrane sensor for calculating submicromolar phosphate concentrations in the seawater sample. Comparing to other instruments, this system did not require the addition of reagents which is less complex and easily established for a further monitoring system in environmental science. Importantly, this proposed electrochemical system do not require the ascorbic acid reductant which is an unstable reagent. Considering the long-time measurement, the cleaning process by an electrochemical method with acidic washing for eliminating the notable signal drift should be replaced with the new protocol, leading to less electrode damage.

CHAPTER 7

Conclusion

The chemical sensors employing polymeric membranes for separation and detection within one system were successfully developed for colorimetric and electrochemical detections. The novel possibilities of various membrane platforms based on bacteria cellulose, plant cellulose, and synthetic polymers were fabricated.

Assembling of these systems for downscaling in the chemical analysis were explored. The bacteria-produced cellulose membrane was introduced (Chapter3) for the determination of important markers such as pH and glucose measurement in the food and health related samples. The pH assay was based on colorimetric technique using the synthesized universal and natural reagent extracted from butterfly pea flower, providing the standard color (visible range) for the different pH value from pH 4 to 8. The glucose determination was based on enzymatic method, illustrating a linear calibration: $y = 6.8205x + 2.2506$. This approach is the low-cost and quite functional sensor (high adsorption capacity, low toxicity, flexible membrane, small size, and sample solution reduction), promising to behave as a wearable sensor with human skin.

Plant cellulose materials, established as a chemical sensor, was easily fabricated due to its self-microfluidic behavior for chemical analysis (Chapter4) employing a mobile phone. This platform was used for heavy metals (Cd, Cu), and antioxidant (polyphenol) assay. The heavy metal was investigated by PAR reagent to produce the color intensity from the complex product, relating to their concentration. The antioxidant measurement was also based on the colorimetric method of the polyphenol content and DPPH capacity, plotting a calibration graph in a range of 0-100 mg/L. Applications to the real green tea samples were demonstrated. This work has established a new concept in the possibility of green analytical chemistry and possible for on-site assay, especially being useful in some remote areas.

Ion-exchange membrane (chemical synthetic polymer) in terms of an in-line flow system for the determination of phosphate in seawater was developed. The reaction was based on molybdate mechanism via a colorimetric method, as shown in Chapter 4. Apart from that, phosphomolybdate was electrochemically measured by mini-electrode (Chapter5). The seawater samples were used to measure the phosphate concentration in the range of 0-10 µM. The key advantage of this approach is the simpler, more integrated membrane-based reagent delivery, compared to the older approaches that rely on mixing of the reagent addition.

The results obtained from the proposed membrane sensors illustrated a good agreement with their related standard methods. These chemical systems include a separation and detection zone, without the sample pretreatment. They are the alternative ways for the on-site analysis engaging with easy operation, sample and reagent reduction, cost-effectiveness, and multi-functional work.

REFERENCES

[1] M. Cheryan, Ultrafiltration and Microfiltration Handbook, Techonomic Publishing Co., Inc., Florida, USA (1998) 1-8.

[2] M. G. Afshar, G. A. Crespo, E. Bakker, Biosens. Bioelectron., 61 (2014) 64−69.

[3] E. Grygolowicz-Pawlak, G. A. Crespo, M. G. Afshar, G. Mistlberger, E. Bakker, Anal. Chem., 85 (2013) 6208−6212.

[4] E. Bakker, Trends Analyt. Chem., 53 (2014) 98-105.

[5] W. Pusch, A. Walch, Angew. Chem. Int. Ed. Engl., 21 (1982) 660-685.

[6] A. Hulanicki, S. Glab, F. Ingman, Pure&Appl. Chem., 63 (1991) 1247-1250.

[7] C. McDonagh, C. S. Burke, B. D. MacCraith, Chem. Rev., 108 (2008) 400−422.

[8] G. M. Whitesides, Nature, 442 (2006) 368-373.

[9] K. Ren, J. Zhou, H. Wu, Acc. Chem. Res., 46 (2013) 2396–2406.

[10] R. Schafrik, Expanding the vision of sensor materials, National Academy Press, Washington, D.C., (1995) 1-146.

[11] A. W. Martinez, S. T. Phillips, G. M. Whitesides, Anal. Chem., 82 (2010) 3–10.

[12] K. Grudpan, S. Lapanantnoppakhun, S. K. Hartwell, K. Watla-iad, W. Wongwilai W. Siriangkhawut, W. Jangbai, W. Kumutanat, P. Nuntaboon, S. Tontrong, Talanta, 79 (2009) 990-994.

[13] D. R. Reyes, D. Iossifidis, P. A. Auroux, A. Manz, Anal. Chem., 74 (2002) 2623– 2636.

[14] D. R. Ballerini, X. Li, W. Shen, Anal. Bioanal. Chem, 399 (2011) 1869–1875.

[15] T. Songjaroen, W. Dungchai, O. Chailapakul, C. S. Henry, W. Laiwattanapaisal, Lab Chip, 12 (2012) 3392-3398.

[16] W. Dungchai, O. Chailapakul, C. S. Henry, Anal. Chem. Acta, 674 (2010) 227-233.

[17] G.Z. Zhou, R. Safaviah, X. Mao, and D. Juncker, Biomed. Eng., 1 (2010) 25-27.

[18] A. Nilghaz, D. R. Ballerini, X. Y. Fang, W. Shen, Sens. Actuators B Chem., 191 (2014) 586–594.

[19] A. Apilux, W. Dungchai, W. Siangproh, N. Praphairaksit, C. S. Henry, O. Chailapakul, Anal. Chem., 82 (2010) 1727-1732.

[20] D. Dorokhin, G. A. Crespo, M. G. Afshar, E. Bakker, Analyst, 139 (2014) 48–51.

[21] J. Ding, W. Qin, J. Am. Chem. Soc., 131 (2009) 14640–14641.

[22] M. Sohail, R. D. Marco, K. Lamb, E. Bakker, Anal. Chim. Acta, 744 (2012) 39–44.

[23] K. Grudpan, S. K. Hartwell, S. Lapanantnoppakhun, and I. McKelvie, Anal. Methods, 2 (2010), 1651-1661.

[24] J. Ruzicka, G.D. Marshall, Anal. Chim. Acta, 237 (1990) 329-343.

[25] P. Abgrall, A. Gue, J. Micromech. Microeng., 17 (2007) 15-22.

[26] K. Grudpan, S. Khonyoung, S. K. Hartwell, S. Lapanantnoppakhun, J. Jakmunee, J. Flow Injection Anal., 23 (2006), 94-101.

[27] D. A. Bruzewicz, M. Reches, and G. M. Whitesides, Anal. Chem., 80 (2008), 3387–3392.

[28] E. M. Fenton, M. R. Mascarenas, G.l P. López, S. S. Sibbett, ACS Appl. Mater. Interfaces, 1 (2009) 124-129.

[29] B. Weigl, G. Domingo, P. LaBarre, J. Gerlach, Lab Chip, 8 (2008) 1999–2014.

[30] X. Li, J. Tian, W. Shen, ACS Appl. Mater. Interfaces, 2 (2010) 1-6.

[31] M. Reches, K. Mirica, R. Dasgupta, M. Dickey, M. Butte, G. M.Whitesides, ACS Appl. Mater. Interface, 6 (2010) 1722-1728.

[32] D.R. Ballerini, X. Li, W. Shen, Biomicrofluidics, 5 (2011) 1-13.

[33] A. J. Ninfa, D. P. Ballou, M. Benore, Fundamental Laboratory Approaches for Biochemistry and Biotechnology, Wiley & Sons., Hoboken (2010) 1-479.

[34] G. Schwedt, The essential guide to analytical chemistry, John Wiley, Michigan (1997) 1-256.

[35] A. Choodum, K. Parabun, N. Klawach, N. N. Daeid, P. Kanatharana, W. Wongniramaikul, Forensic. Sci. Int., 235 (2014) 8-13.

[36] M. L. Firdausa, W. Alwi, F. Trinoveldi, I. Rahayu, L. Rahmidar, K. Warsito, Procedia Environ. Sci., 20 (2014) 298-304.

[37] M. Granica, Ł. Tymecki, Talanta, 197 (2019) 319-325.

[38] A. F. João, A. L. Squissato, G. M. Fernandes, R. M. Cardoso, A. D. Batista, R. A. A. Muñoz, Microchem. J., 146 (2019) 1134-1139.

[39] S. Soares, K. G. Torres, E. L. Pimentel, P. B. Martelli, F. R. P. Rocha, Talanta, 195 (2019) 229-235.

[40] A. A. Mohamed, A. A. Shalaby, Food Chem., 274 (2019) 360-367.

[41] A. Soni, S.K. Jha, Anal. Chim. Acta, 996 (2017) 54-63.

[42] P. Martinkova, M. Brtnicky, J. Kynicky, M. Pohanka, Chem. Pap., 72 (2018) 2719-2728.

[43] D. A. Skoog, F. J. Holler, S. R. Crouch, Principles of instrumental analysis, Cengage learning, Cengage learning, Boston, USA (2017) 23-113.

[44] E. Bakker, Fundamentals of Electroanalysis: Electrochemistry of Ion and Electron Transfer Processes, University of Geneva, Switzerland (2014) 58-342.

[45] E. Bakker, Anal. Chem., 69 (1997) 1061−1069.

[46] J. F. Fauvarque, P. Simon, In Carbons for Electrochemical Energy Storage and Conversion Systems, CRC Press: Boca Raton (2010) 1-36.

[47] J. Wang, Analytical electrochemistry, John Wiley & Sons, Hoboken (2006) 250.

[48] F. A. Santos, G. C. V. Iulianelli, M. I. B. Tavares, Mater. Sci. Appl., 7 (2016) 257-294.

[49] W. W. Y. Voon, Y. Rukayadi, A. S. M. Hussin, Lett. Appl. Microbiol., 62 (2016) 428-433.

[50] A. Suwanposri, P. Yukphan, Y. Yamada, D. Ochaikul, Maejo Int. J. Sci. Technol., 7 (2013) 70-82.

[51] D. Raghunathan, Int. J. Curr. Microbiol. App. Sci, 2 (2013) 275-290.

[52] P. Lestari, N. Elfrida, A. Suryani, Y. Suryadi, Jordan J. Biol. Sci., 7 (2014) 75-80.

[53] S. M. Mohammad, N. A. Rahman, M. S. Khalil, S. R. S. Abdullah, Advan. Biol. Res., 8 (2014) 307-313.

[54] K. Wongravee, H. Gatemala, C. Thammacharoen, S. Ekgasit, S. Vantasin, I. Tanabe, Y. Ozaki, RSC Adv., 5 (2015) 1391-1397.

[55] A. Martín, J. Kim, J. F. Kurniawan, J. R. Sempionatto, J. R. Moreto, G. Tang, A. S. Campbell, A. Shin, M. Y. Lee, X. Liu, J. Wang, ACS Sens., 2 (2017) 1860-1868.

[56] A. Koh, D. Kang, Y. Xue, S. Lee, R. M. Pielak, J. Kim, T. Hwang, S. Min, A. Banks, P. Bastien, M. C. Manco, L. Wang, K. R. Ammann, K. Jang, P.

Won, S. Han, R. Ghaffari, U. Paik, M. J. Slepian, G. Balooch, Y. Huang, J. A. Rogers, Sci. Transl. Med., 8 (2016) 1-13.

[57] D. Morrisa, S. Coylea, Y. Wua, K. T. Laua, G. Wallaceb, D. Diamond, Sens. Actuators B Chem., 139 (2009) 231-236.

[58] M. M. Pribil, G. U. Laptev, E. E. Karyakina, A. A. Karyakin, Anal. Chem., 86 (2014) 5215-5219.

[59] W. Jia, A. J. Bandodkar, G. Valdés-Ramírez, J. R. Windmiller, Z. Yang, J. Ramírez, G. Chan, J. Wang, Anal. Chem., 85 (2013) 6553-6560.

[60] H. Y. Y. Nyein, L. Tai, Q. P. Ngo, M. Chao, G. B. Zhang, W. Gao, M. Bariya, J. Bullock, H. Kim, H. M. Fahad, A. Javey, ACS Sens., 3 (2018) 944-952.

[61] J. Morris, Genet. Resour. Crop Evol., 56 (2009) 421-427.

[62] K. Grudpan, S.K. Hartwell, W. Wongwilai, S. Grudpan, S. Lapanantnoppakhun, Talanta, 84 (2011) 1396-1400.

[63] D.L.P. Macuvele, G.Z.S. Sithole, K. Cesca, S.L.P. Macuvele, J.V. Matsinhe, Environ. Sci. Pollut. R., 23 (2016) 11639-11644.

[64] K. Watla-iad, T. Sakai, N. Teshima, S. Katoh, K. Grudpan, Anal. Chim. Acta, 604 (2007) 139-146.

[65] S. A. Klasner, A. K. Price, K. W. Hoeman, R. S. Wilson, K. J. Bell, C. T. Culbertson, Anal. Bioanal. Chem., 397 (2010) 1821-1829.

[66] I. O. Gómez, A. S. Castillo, A. G. García, J. A. Á. Bermejo, I. de O. Payá, A. R. Diéguez, L. F. C. Vallvey, Microchim. Acta, 185 (2018) 1-8.

[67] K. Ponhong, S. Kradtap Hartwell, K. Grudpan, Talanta, 85 (2011) 804-808.

[68] W. C. Lin, C. C. Lien, H. J. Yeh, C. M. Yu, S. H. Hsu, Carbohydr. Polym., 94 (2013) 603–611.

[69] E. F. M. Gabriel, P. T. Garcia, F. M. Lopes, W. K. T. Coltro, Micromachines, 8 (2017) 1-9.

[70] M. Phisalaphong, T. Suwanmajo, P. Tammarate, J. Appl. Polym. Sci., 107 (2008) 3419–3424.

[71] H. S. Barud, A. Tercjak, J. Gutierrez, W. R. Viali, E. S. Nunes, S. J. L. Ribeiro, M. Jafellici, M. Nalin, R. F. C. Marques, J. Appl. Phys. 117 (2015) 17B734.

[72] P. Aramwit, N. Bang, BMC Biotechnol., 14 (2014) 1-11.

[73] A. W. Martinez, S. T. Phillips, M. J. Butte, G. M. Whitesides, Angew. Chem. Int. Ed., 46 (2007) 1318–1320.

[74] K. Talalak, J. Noiphung, T. Songjaroen, O. Chailapakul, W. Laiwattanapaisal, Talanta, 144 (2015) 915–921.

[75] X. Mu, L. Zhang, S. Chang, W. Cui, Z. Zheng, Anal. Chem., 86 (2014) 5338−5344.

[76] A. Nilghaz, L. Zhang, M. Li, D. R. Ballerini, W. Shen, ACS Appl. Mater. Interfaces, 6 (2014) 22209−22215.

[77] K. Kiwfo, W. Wongwilai, P. Paengnakorn, S. Boonmapa, S. Sateanchok, K. Grudpan, Talanta, 181 (2018) 1-5.

[78] L. Zhao, S. Zhong, K. Fang, Z. Qian, J. Chen, Food Chem., 166 (2015) 568-575.

[79] E. Engstrom, I. Jonebring, B. Karlberg, Anal. Chim. Acta, 371 (1998) 224-227.

[80] J. Karpinka, M. Kulikowska, J. Pharm. Biomed. Anal., 29 (2002) 153-158.

[81] J. R. Jezorek, H. Freiser, Anal. Chem., 51 (1979) 373-376.

[82] G. Chakrapani, D. S. R. Murty, P. L. Mohanta, R. Rangsawamy, J. Geochem. Explor., 63 (1998) 145-152.

[83] S. Srijaranai, S. Chanpaka, C. Kukusamude, K. Grudpan, Talanta, 68 (2006), 1720-1725.

[84] D.H. Kodama, A.E.S.S. Goncalves, F.M. Lajolo, M.I. Genovese, Cienc. Tecnol. Aliment. 30 (2010) 1077–1082.

[85] R.L. Prior, X. Wu, K. Schaich, J. Agric. Food Chem., 53 (2005) 4290–4302.

[86] M. Carocho, I.C.F.R. Ferreira, Food Chem. Toxicol., 51 (2013) 15–25.

[87] J. Moon, T. Shibamoto, J. Agric. Food Chem., 57 (2009) 1655–1666.

[88] P. Molyneux, Songklanakarin J. Sci.Technol., 26 (2004) 211–219.

[89] E. Buyuktuncel, E. Porgali, C. Colak, Food Nutr. Sci., 5 (2014) 1660–1667.

[90] X. Li, X. Wu, L. Huang, Molecules, 14 (2009) 5349–5361.

[91] S. Sateanchok, S. Wangkarn, C. Saenjum, K. Grudpan, Talanta, 177 (2018) 171-175.

[92] S. Sateanchok, W. Wongwilai, K. Kiwfo, K. Grudpan, J. Flow Injection Anal., 33 (2016) 5-7.

[93] J. Ghasemi, A. Niazib, M. Maeder, J. Braz. Chem. Soc., 18 (2007) 267-272.

[94] S. Sateanchok, N. Pankratova, M. Cuartero, T. Cherubini, K. Grudpan, E. Bakker, ACS Sens., 3 (2018) 2455-2462.

[95] M. Cuartero, N. Pankratova, T. Cherubini, G. A. Crespo, F. Massa, F. Confalonieri, E. Bakker, Environ. Sci. Technol. Lett., 4 (2017) 410−415.

[96] M. Cuartero, G. A. Crespo, E. Bakker, Anal. Chem., 87 (2015) 8084−8089.

[97] J. D. H. Strickland, T. R. A. Parsons, Practical handbook of seawater analysis, Fisheries research, Ottawa, Canada (1972) 45-65.

[98] N. Pankratova, Development of Sensing Principles for Electrochemical Detection of Nutrients and Species Relevant to the Carbon Cycle, University of Geneva, Switzerland (2018) 112-140.

[99] N. Pankratova, M. Cuartero, T. Cherubini, G. A. Crespo, E. Bakker, Anal. Chem., 89 (2017) 571−575.

[100] J. Ruzicka, E. H. Hansen, Flow Injection Analysis, Wiley Interscience, USA (1988) 15−36.

[101] J. M. Estela, V. Cerda, Talanta, 66 (2005) 307-331.

[102] I. D. McKelvie, D. M. W. Peat, G. P. Matthews, P. J. Worsfold, Anal. Chim. Acta, 351 (1997) 265-271.

[103] Y. Udnan, I. D. McKelvie, M.R. Grace, J. Jakmunee, K. Grudpan, Talanta, 66 (2005) 461-466.

[104] S. M. Harden, W. K. Nonidez, Anal. Chem., 56 (1984) 2218-2223.

[105] N. G. Carpenter, A. W. E. Hodgson, D. Pletcher, Electroanal., 9 (1997) 1311-1317.

[106] A. V. Kolliopoulos, D. K. Kampouris, C. E. Banks, Anal. Chem., 87 (2015) 4269-4274.

[107] A. G. Fogg, N. K. Bsebsu, Analyst, 107 (1982) 566-570.

[108] D. Talarico, F. Arduini, A. Amine, D. Moscone, G. Palleschi, Talanta, 141 (2015) 267-272.

[109] J. Jonca, W. Giraud, C. Barus, M. Comtat, N. Striebig, D. Thouron, V. Garcon, Electrochim. Acta, 88 (2013) 165-169.

[110] D. Talarico, S. Cinti, F. Arduini, A. Amine, D. Moscone, G. Palleschi, Environ. Sci. Technol., 49 (2015) 7934-7939.

[111] L. M. L. Nollet, Handbook of Water Analysis, CRC Press, Boca Raton (2007) 219-252.

[112] C. Barus, I. Romanytsia, N. Striebig, V. Garçon, Talanta, 160 (2016) 417-424.

APPENDIX

The standard method for glucose and pH determination

1. pH analysis by the strip test

According to pH and glucose determination (chapter 2), the proposed bio-cellulose sensor was compared with the standard techniques in order to test the possibility based on real samples (more details in chapter 2). The color results from strip paper were illustrated to identify the pH values of samples 7-10, which were pH~7.5, pH~7.3, pH~4.5, and pH~4.0 respectively (Figure A1).

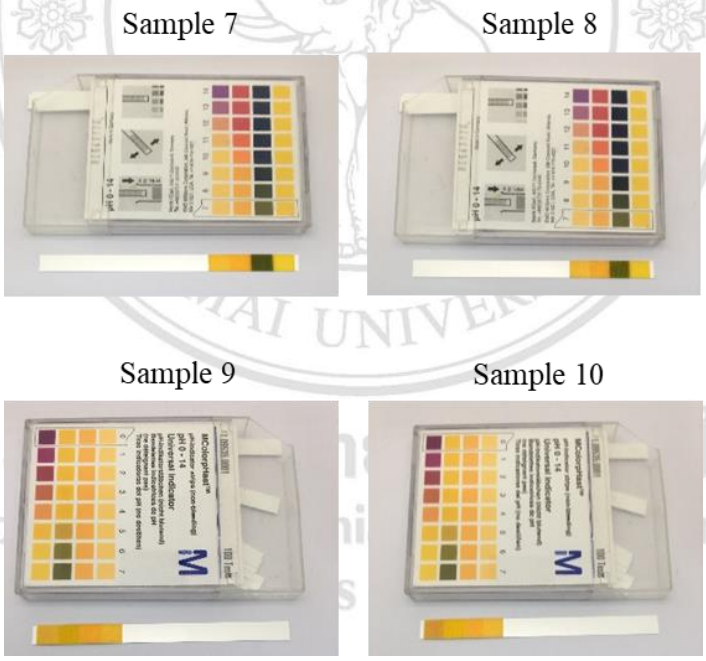

Figure A1: pH analysis of samples 7-10 using the standard strip test

2. pH analysis by pH probe

Another method (pH probe) for checking the pH value of real samples was shown in Figure A2. The digital numbers on screen expressed the pH value of sample 7-10, which were pH~7.50, pH~7.22, pH~4.53, and pH~4.05 respectively.

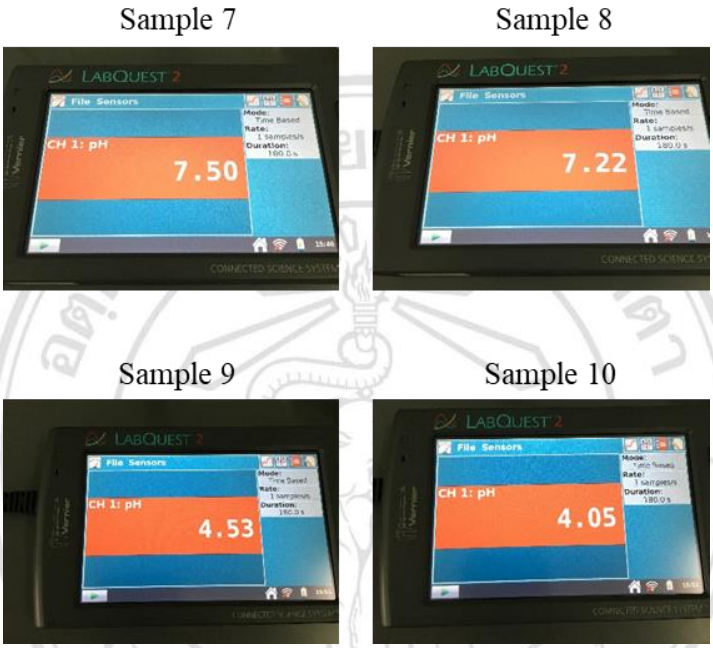

Figure A2: pH analysis of samples 7-10 using pH probe

3. Glucose analysis by ACCU machine: converting the unit mg/dL to mM (m×mg/L)

ACCU-CHEK Performa, Roche was chosen as electroanalysis for glucose assay. The results were obtained in Figure A3, which glucose values of samples 1-10 were *ERROR, 0, 2.00 mM (dilute), 0, 0.72 mM (dilute), *ERROR, 4.88 mM, 7.94 mM, 5.22 mM, and 7.50 mM (*ERROR = The machine did not show any data)

4. Glucose analysis by spectrophotometry

Another glucose determination was studied via spectrophotometry measuring at 645 nm wavelength. The glucose enzyme reaction is related to the experimental part of chapter 2. The blue products were appeared responsible for standard glucose and real

samples in Figure A4. The glucose values were then received by spectrophotometry and the calibration graph was illustrated in Figure A5.

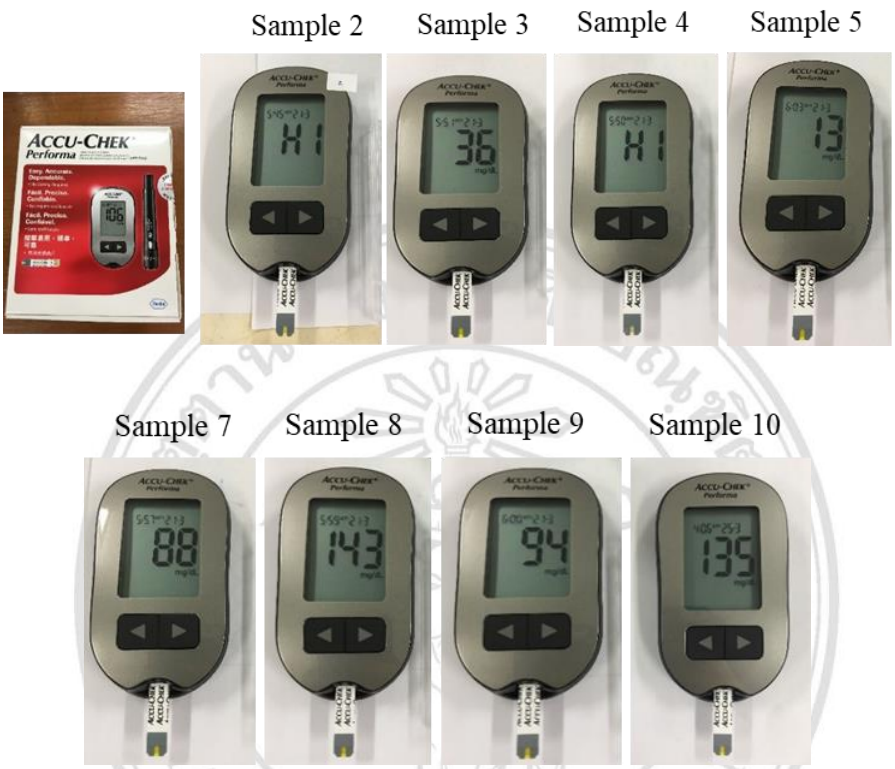

Figure A3: Glucose analysis of samples 2-10 using ACCU machine

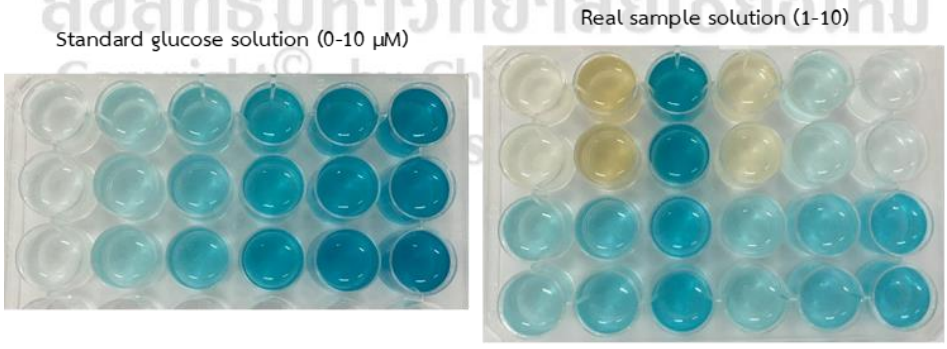

Figure A4: Glucose analysis of samples 1-10 using colorimetric method

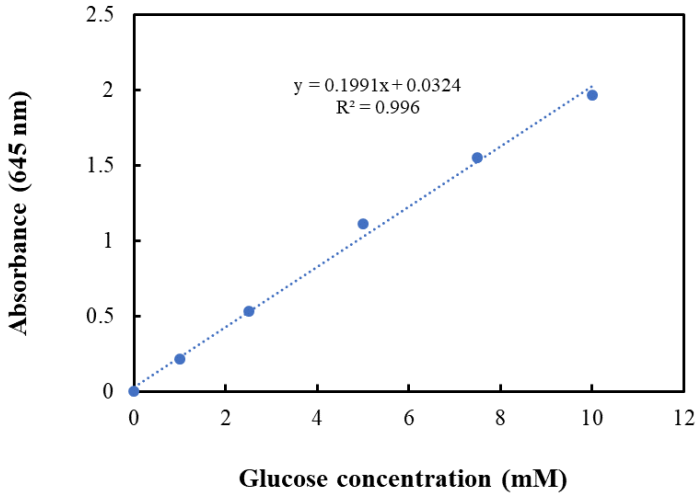

Figure A5: Calibration graph of glucose determination by spectrophotometry

Table A1: Absorbance of the blue complex from different samples and the glucose values by spectrophotometry

Sample	Absorbance (645 nm)					Glucose (mM)
	1	2	3	Average	SD	
Blank	0.473	0.477	0.476	0.475	0.002	0
1	0.319	0.321	0.528	0.389	0.120	-
2	0.350	0.352	0.356	0.353	0.003	-
3	0.992	0.989	0.990	0.990	0.001	2.30±0.01 (dilute)
4	0.166	0.164	0.167	0.166	0.001	-
5	0.675	0.672	0.676	0.674	0.002	0.71±0.01 (dilute)
6	0.199	0.206	0.201	0.202	0.003	-
7	1.474	1.477	1.475	1.475	0.002	4.74±0.01
8	2.187	2.190	2.182	2.186	0.004	8.31±0.02
9	1.452	1.686	1.451	1.530	0.135	5.01±0.68
10	2.230	2.233	2.105	2.189	0.073	8.32±0.37

CURRICULUM VITAE

Author's Name Miss Suphasinee Sateanchok

Date of Birth June 8, 1991

Education

Academic year	
2016–2018	Ph.D. (Chemistry) Chiang Mai University
2013–2015	M.S. (Chemistry), GPAX = 4.00 Chiang Mai University
2009–2012	B.Sc. (Chemistry), 1st class honour, GPAX = 3.84 Chiang Mai University

Scholarship Science Achievement Scholarship of Thailand (SAST)

Experiences

Presentations

1. Oral presentation which the title is "In-line Thin Layer Sensors for Phosphate Determination in Seawater", *CH*analysis 2018, the Division Analytical Sciences of the Swiss Chemical Society, Dorint Hotel Beatenberg, Switzerland, 2018

2. Poster presentations which the titles are "Novel sensor: Ion-exchange membrane reagent delivery for phosphate detection" and "Thread based chemical analysis platforms", International Symposia on Research toward Green Innovation, The empress international convention center, Chiang Mai, Thailand, 2018

3. Oral presentation which the title is “Miniaturization of chemical analysis for aspirin determination via PiCOEXPLORER”, the 2nd Workshop on PiCOANALYSIS, Faculty of Science, Chiang Mai University, Thailand, 2017

4. Poster presentation which the title is “Antioxidant assay using simple thread based device”, 13th Asian Conference on Analytical Sciences (Asianalysis XIII), The empress international convention center, Chiang Mai, Thailand, 2016

5. Poster presentation which the title is “Solventless and microextraction for anionic surfactant assay via microfluidic platforms employing cotton thread”, TRF Seminar Series in Basic Research, Chiang Mai University, Thailand, 2015 (Certificate of Best Poster)

6. Poster presentation which the title is “Determination of anionic surfactant using solventless and micro solvent extraction”, TRF Seminar in Basic Research CVIII (Analytical Science: Past, Present and Future), Faculty of Science, Chiang Mai University, 2015

7. Poster presentation which the title is “Down Scaling for micro solvent extraction with flow and non-flow based approaches”, 19th International Conference on Flow Injection Analysis (ICFIA), Across Fukuoka, Fukuoka, Japan, 2014

8. Poster presentation which the title is “Green analytical chemistry”, “Lab on chip”, International symposia on research towards Green innovation conference, Chiang Mai, Thailand, 2014

9. Poster presentation which the title is “Simple lab on thread for down scaling in chemical analysis”, 12th Asian Conference on Analytical Sciences (ASIANALYSIS XII), Kyushu University, Fukuoka, Japan, 2013

10. Poster presentation which the title is “Simple lab on thread”, 50th Annual Meeting of Japan Association for Flow Injection Analysis (JAFIA), Tokushima University, Japan, 2012 (Certificate of Young Best Poster)

Staff member in organizing Conferences/ Meetings and other academic activities

1. Staff in "International Symposia on Research towards Green Innovation", The empress international convention center, Chiang Mai, Thailand, 2018

2. Teacher Assistant of the bachelor student project based on "comparative study of the chemical composition of various natural waters", University of Geneva, Spring Semester 2018

3. Teacher Assistant of Analytical Chemistry laboratory (Bachelor student), University of Geneva, Autumn Semester 2017

4. Staff in "13th Asian Conference on Analytical Sciences (Asianalysis XIII)", Chiang Mai, Thailand, 2016

5. Staff in "TRF Seminar Series in Basic Reseach CVIII", Faculty of Science Chiang Mai University, 2015

6. Coworker Staff in "CHEINNO Congress III conference", Rajamangala University of Technology Suvarnabhumi, Ayutthaya, Thailand, 2016

7. Coworker Staff in "CHEINNO Congress II conference", Buriram Rajabhat University, Buriram, Thailand, 2014

8. Staff in "2nd UPPER Greater Mekong Sub-region (Youth Camp) in local wisdom connection with science and technology", MAE HIA Agricultural Research Station and Training Center, Chiang Mai University, Thailand, September 2014.

9. Staff in "Chemical Analysis and Its Applications (agricultural, environmental and food safety labs: Workshop)", Souphanouvong University, Luang Prabang, Lao, March 2014

10. Staff in "Local wisdom based innovation exhibition, Regional Research Expo 2014", Chiang Mai University Chiang Mai, Thailand, March, 2014

11. Staff in “International symposia on research towards Green innovation”, Chiang Mai orchid hotel, Chiang Mai, Thailand, January 2014

12. Staff in “1st UPPER Greater Mekong Sub-region (Youth Camp)”, Haripunchai Lamphun Campus of Chiang Mai University, Lamphun, Thailand, June 2013